



Graz University of Technology



Production of synthetic proteins in the bioreactor

New prospects for protein engineering

Master's Thesis in Biochemistry and Molecular Biomedicine

by Patrik Fladischer, BSc

Graz, 2013

Supervisor

Dr. Birgit Wiltschi

Junior group Synthetic Biology

**ACIB-Austrian Centre of Industrial Biotechnology,
Graz, Austria**

Examiner

Ao.Univ.-Prof. Mag.rer.nat. Dr.rer.nat. Anton Glieder

**ACIB-Austrian Centre of Industrial Biotechnology,
Graz, Austria**

**TU Graz Institute of Molecular Biotechnology,
Graz, Austria**

Statutory Declaration

Acknowledgment

I am indebted to Prof. Glieder, who gave me the opportunity to do my master thesis on this topic, as well as for being the examiner of this work. Without him this work would not have been possible.

I would also like to thank my supervisor Dr. Birgit Wiltschi for her valuable support and helpful assistance throughout my work. I am very grateful for her continues support and encouragement. I am also thankful for her expertise and advices which proved to be essential in accomplishing my work, as well as for critical reading of the thesis.

Special thanks go to Niklaus Anderhuber, who had not merely been a college, but rather a good friend. Only his assistance and ideas made parts of this work possible.

Furthermore, I would like to extend my gratefulness to all lab members for their advices and support.

I would also like to thank the Austrian Centre of Industrial Biotechnology for the funding of this project.

Last but not least, I would like to pay tribute to the constant support of my family during the 5 years of my studying.

Graz, April 2013

Fladischer Patrik

Abstract

It was shown previously that the incorporation of non-canonical amino acids (ncAAs) can have positive effects on enzyme activity and stability. The ultimate goal of ncAA incorporation into proteins would be to create new protein functions. To make the technique attractive for industrial protein engineering, it is important to develop a method for the inexpensive production of ncAAs as well as synthetic proteins in large scale. Existing protocols for global ncAA incorporation use auxotrophic *E. coli* strains supplemented with limiting amounts of the canonical amino acid (cAA) to support growth. Upon depletion of the cAA, the cultures are supplemented with the ncAA and target protein production is induced. The aim of this study was to tackle the question whether this method could be adapted for increased cell density fermentations (ICDF) by re-formulating the medium. Screening of synthetic protein variants with changed properties should highlight the potential of ncAA incorporation for protein engineering approaches. The ultimate goal was to prove in principle that the biosynthesis of an ncAA and its incorporation into an enzyme could be performed in one step. The amino acid focused on in this work was the methionine (Met) analog norleucine (Nle). We developed a shake flask protocol for supplementation based incorporation (SPI) of Nle as well as other ncAAs into proteins. The protocol was up-scaled to the bioreactor and evaluated by the production of synthetic variants of TTL, a lipase of a thermophile bacterium, as the model enzyme. Based on previous publications on the beneficial effect of Nle incorporation on TTL, the protocols were employed to incorporate Nle into members of the alpha/beta hydrolase family. The enzymes were screened for their activity on biotechnologically relevant polyester poly-ethylene-terephthalate (PET). The observed effects of Nle incorporation reached from improved activity in case of the lipase TTL to different pattern of release products for the known polyesterase cutinase 1. Finally, Nle was biosynthesized by a metabolically engineered strain and incorporated into TTL in one step in a bioreactor.

In summary, we established ICDF protocols for SPI of ncAAs in shake flask cultures, as well as the bioreactor. The incorporation of Nle into biotechnologically relevant enzymes of the alpha/beta hydrolase family for protein engineering is feasible and yields enzymes with altered properties. We were also successful in combining Nle biosynthesis and incorporation in the same fermentation process.

Kurzzinhalt

Nicht-kanonische Aminosäuren (nkAS) können die Eigenschaften von Proteinen positiv beeinflussen. Aufgrund der chemischen Eigenschaften der nkAS könnte diese Technik ein Meilenstein zur Verwirklichung neuer Enzymfunktionen sein. Die aktuellen Methoden zum globalen Einbau von nicht kanonischen Aminosäuren in Zielproteine nutzen die promiskuitiven Eigenschaften der tRNA Synthetasen aus, welche in der Abwesenheit der kanonischen Aminosäure ein nicht-kanonisches Analog als Substrat akzeptieren können. Eine Limitation dieser Technik ergibt sich aus den sehr geringen Ausbeuten an synthetischen Proteinen, da bestehende Protokolle bei sehr geringen Zelldichten arbeiten. Aus diesem Grund zielte diese Studie darauf ab, Protokolle zur Produktion von synthetischen Proteinen bei erhöhten Zelldichten zu entwickeln. Des Weiteren wurden diese Protokolle dazu benutzt, neue synthetische Proteinvarianten herzustellen und diese auf veränderte Eigenschaften zu testen. Schließlich sollte noch überprüft werden, ob die Biosynthese einer nkAS mit ihrem direkten Einbau in ein Zielprotein in einem Bioreaktor gekoppelt werden kann.

Der Fokus dieser Arbeit lag auf dem Methionin-Analog Norleucin (Nle), für dessen globalen Einbau in Zielproteine Protokolle zur Hochzelldichtefermentation entwickelt wurden. Aus früheren Publikationen war bekannt, dass der Einbau von Nle die Eigenschaften von Lipasen positiv beeinflussen kann. Deswegen wurden in dieser Arbeit Nle-Varianten von alpha/beta-Hydrolasen hergestellt. Diese wurden anhand des Abbaus eines biotechnologisch relevanten Polymers (PET) auf ihre veränderten Eigenschaften getestet. Abhängig vom getesteten Enzym konnten unterschiedliche Effekte beobachtet werden. Im Falle des Modellenzym TTL war die Aktivität der Nle-Variante im Vergleich mit dem kanonischen Enzym etwa um das Doppelte erhöht. Bei der bekannten Polyesterase Cutinase 1 wurde das Spektrum der Abbauprodukte verändert. Zum Abschluss wurde im Bioreaktor die Kombination der Nle Biosynthese mit dem direkten Einbau in das Enzym TTL realisiert.

Zusammenfassend ist festzustellen, dass alle Ziele der Diplomarbeit erreicht wurden. Neben der Entwicklung und Etablierung von Protokollen für den globalen Einbau von nkAS in Proteine bei hohen Zelldichten konnte auch das Potential von Nle als Kandidat zur Proteinmodifikation an zwei Hydrolasen gezeigt werden. Biosynthetisch hergestelltes Nle wurde in einem Bioreaktor in einem metabolisch veränderten Stamm biosynthetisiert in im gleichen Prozess in ein Zielprotein eingebaut.

Table of contents

Acknowledgment.....	3
Abstract.....	4
Kurzinhalt	5
Table of contents.....	6
1. Introduction.....	9
1.1. Non-canonical amino acids.....	9
1.1.1. Norleucine.....	10
1.2. Global incorporation of ncAAs.....	11
1.3. Synthetic proteins containing ncAAs.....	13
1.4. Polyesterases	15
1.5. High cell density fermentation.....	15
1.6. Main thesis objectives	17
2. Material & Methods	18
2.1. Materials	18
2.1.1. Strains	18
2.1.2. Plasmids	18
2.1.3. Primers.....	20
2.1.4. Instruments and Devices	22
2.1.5. Chemicals and enzymes.....	23
2.1.6. Media and buffers	25
2.2. Methods.....	29
2.2.1. Preparation of electrocompetent <i>E. coli</i> cells	29
2.2.2. Electroporation of <i>E. coli</i>	29
2.2.3. PCR.....	30
2.2.4. Gel electrophoresis	30

2.2.5.	Gibson assembly	31
2.2.6.	Preparation of plasmids, PCR products and DNA fragments	33
2.2.7.	Restriction enzymes	33
2.2.8.	Sequencing.....	33
2.2.9.	Titration of the optimal yeast extract concentration as Met limiting growth source	33
2.2.10.	High cell density SPI in <i>E. coli</i>	34
2.2.11.	SDS-PAGE.....	38
2.2.12.	Protein purification.....	39
2.2.13.	Protein concentration	41
2.2.14.	PET, PLA & 3PET degradation assay.....	41
2.2.15.	Esterase activity assay.....	42
2.2.16.	PET adhesion assay (HisProbe HRP)	42
2.2.17.	Thin layer chromatography (TLC)	43
2.2.18.	HPLC-UV for amino acid analysis.....	43
2.2.19.	Mass analysis.....	44
3.	Results.....	45
3.1.	Synthetic protein production by external non-canonical amino acid supplementation	45
3.1.1.	High cell density fermentation.....	45
3.1.2.	Applications	49
3.1.3.	Production of synthetic proteins in a bioreactor	65
3.2.	Norleucine biosynthesis	76
3.3.	Synthetic protein production by incorporation of biosynthesized Nle.....	79
3.3.1.	Nle biosynthesis in growing cells	80
3.3.2.	Nle biosynthesis in resting cells	84
4.	Discussion.....	91

4.1.	Increased cell density fermentation.....	91
4.2.	Synthetic proteins	92
4.2.1.	Production in high cell density shake flask cultures	92
4.2.2.	Production in the bioreactor	93
4.3.	Applications.....	95
4.4.	Nle production and amino acid analysis.....	97
4.5.	Nle biosynthesis and direct incorporation	97
5.	Conclusions.....	99
6.	References.....	100
7.	Appendix	107

1. Introduction

Naturally occurring proteins and enzymes display highly diverse functionalities that are perfectly adapted to operate in their natural environment. Wild-type enzymes, though, do not always exhibit the properties needed to make them useful biocatalysts for industrial application. Nevertheless, there is growing interest in biotransformations as “greener alternatives” to organo-chemical synthesis. This interest has been reflected by flourishing protein engineering approaches during the last decade [1].

The 20 canonical amino acids (cAA) encoded by the genetic code furnish proteins with a limited variety of chemical groups being responsible for limitations of these approaches [2]. Nature compensates these limitations by introducing chemical diversity via post-translational modifications [3]. As post-translational modifications are difficult to control, they are usually avoided as a means of modification of heterologous proteins [4]. In contrast, non-canonical amino acids (ncAAs) are not encoded by the genetic code [5]. Yet, they are very abundant in nature and display much more diverse side chain chemistries than the cAAs. Permitting ncAAs for ribosomal translation into proteins vastly expands the panoply of chemical protein modifications [6].

To date, two main approaches for the introduction of ncAAs into proteins are available [7, 8]. The extraordinary traits of synthetic proteins containing non-canonical building blocks make them attractive for academic as well as biotechnological applications. However, a reliable process for the large-scale production of synthetic proteins has not yet been described.

In order to fill this gap, the current study focuses on the development of increased cell density fermentation (ICDF; OD₆₀₀ 3 (shake flask); OD₆₀₀ 30 (bioreactor)) protocols for global ncAA incorporation into target proteins.

1.1. Non-canonical amino acids

NcAAs are a diverse group of compounds beyond the standard set prescribed by the genetic code. While the genetic code was evolutionarily established with only 20 cAAs, ncAAs are widespread in nature. More than 700 ncAAs are produced as secondary metabolites in fungi and plants [9]. As well, ncAAs can be used as building blocks in non-ribosomal peptide synthesis, e.g., for the antibiotics micrococcin P1 [10] and ramoplanin [11].

Selenocysteine (Sec) and pyrrolysine (Pyl) have only recently been discovered as building blocks of naturally occurring proteins [12]. Often, these compounds are termed the 21st and 22nd cAAs. However, as their occurrence is limited to certain proteins [13] & [14] or particular organisms [15], respectively, they more likely represent natural supplements to the standard genetic code. Selenoproteins and selenoenzymes play important roles in fundamental cellular processes and metabolic regulation [16] and Pyl is involved in methylamine metabolism [15]. Sec insertion at in-frame TGA codons is controlled by SelB and the SECIS element while decoding of in-frame amber codons with Pyl requires an orthogonal pyrrolysyl-tRNA synthetase/suppressor tRNA pair [17].

Due to their occurrence in nature [18], their biological properties [19] and their amenability to ribosomal translation into proteins [20], ncAAs are interesting compounds for biotechnological applications. Many commercial ncAAs are very expensive and can be procured only in small amounts. For the production of synthetic proteins in the bioreactor, they must be available in sufficient amounts at a reasonable price. Recent progress in the transfer of whole metabolic pathways from one host to another [21] as well as efficient techniques to genetically modify host organisms, e.g., by gene deletions [22], open up new opportunities for the heterologous production of ncAAs by synthetic biology approaches.

1.1.1. Norleucine

Incorporation of structurally related amino acids during protein expression was first reported almost 55 years ago [20]. Norleucine (Nle) is very active in this respect. Acting as a methionine (Met) analog, the isosteric Nle exerts a higher hydrophobicity by the exchange of the sulfur with a CH₂ group [23] (structures see in Figure 1).

Nle is a useful ncAA for biotechnological purposes. The fact that Nle can be formylated and act as translation start is essential for its utility in protein engineering [24]. Substitution of Met by Nle in acylation of *E. coli* tRNA^{Met} has also been shown [25]. However, Nle acts as a DNA methylation inhibitor and, therefore, can be toxic for *E. coli* cells. Nle is tolerated by host cells to a certain amount, even though it is incorporated into host proteins [19]. Baker and co-workers showed that cell growth of Met auxotrophic strains is reduced under Met depletion. Linear growth can be obtained on Nle, as well the cells keep viable over Nle support and depleted Met [26].

Nle labeled proteins show extraordinary properties: Fully labeled Nle variants of extracellular nucleases produced in *Staphylococcus aureus* showed resistance to CNBr treatment [27]. Further examples were published in [6, 7, 28, 29]. How Nle incorporation can affect target proteins is described in section 1.3.

Almost 20 years ago, Bogosian et al. reported the biosynthesis of Nle and its direct incorporation if a leucine-rich protein was over-expressed [30]. Further studies confirmed that Nle is a side product of the branched chain amino acid biosynthesis (see Figure 2) [31].

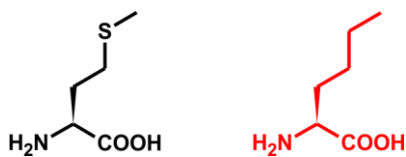


Figure 1 Structures of methionine (Met, black) and its non-canonical analog norleucine (Nle, red)

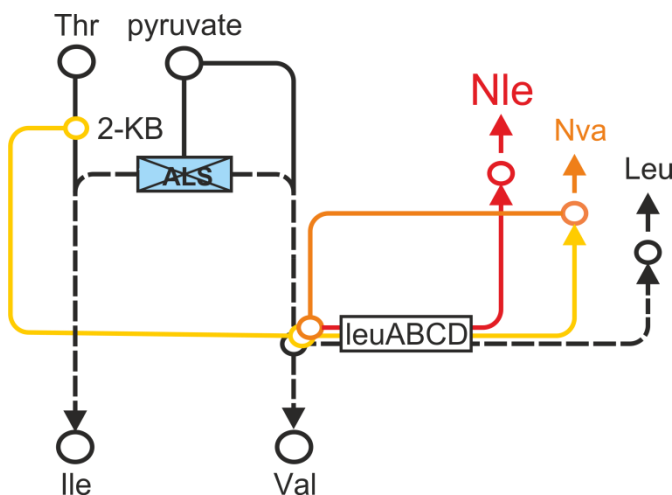


Figure 2 Branched chain amino acid biosynthesis

Thr, threonine; 2-KB, 2-ketobutyrate; Ile, isoleucine; Leu, leucine; Val, valine; Nle, norleucine; Nva, norvaline; ALS, acetolactate synthase; leuABCD, *leuA*BCD* operon [79]

1.2. Global incorporation of ncAAs

Cohen and Cowie [32] already described the basic concept of supplementation incorporation technique (SPI) 20 years ago. Budisa and co-workers adopted the concept and introduced the terminus of SPI. [33]. Although ncAAs are not encoded by the genetic code they can participate in ribosomal translation under tightly controlled conditions. The currently available technique for global substitution of cAA by their non-canonical analogs exploits the natural substrate tolerance of the tRNA charging enzymes, the aminoacyl-tRNA synthetases

(aaRSs). Though guarding translational fidelity, these enzymes accept chemically and/or structurally closely related derivatives of the cAA as substrates [34]. However, as the cAAs are the preferred substrates of the aaRSs, an ncAA is charged onto a tRNA by an aaRS in the presence of a cAA, only if provided in excess [35]. Therefore, it is very important to thoroughly control the intracellular availability of the ncAA, as well as the cAA. The group of Budisa and co-workers really showed that the presence of excess of ncAA and almost depletion of cAA is essential to express fully labeled proteins. [33]. Concepts have also been expanded to other organisms [27]. It was very early ascribed that up-take of the ncAA must be resort to same basic mechanism than for the cAA. Adequate cell transport is essential for the ncAA to be incorporated [35]. If the ncAA is intracellularly abundant during target protein expression while the availability of its canonical counterpart is low, residue specific incorporation of the ncAA at the canonical positions will occur. The global substitution of a cAA by the ncAA can elicit global effects in the target protein, such as improved stability [36], folding [37], activity [38] or resistance to harsh conditions [28].

Currently, two complementary techniques are available for the global and site-specific incorporation of ncAAs into target proteins. On the one hand, the residue-specific ncAA incorporation described above facilitates chemical modifications at multiple sites [39]. It provides a tool to substantially change the physico-chemical properties of proteins [7]. On the other hand, site-specific incorporation of ncAAs at in-frame stop codons is feasible by employing specific orthogonal aaRS/suppressor tRNA pairs [40]. The present study focuses exclusively on global ncAA incorporation.

Experimentally, this is achieved by using a host strain that is auxotrophic for the cAA whose analog is to be incorporated into a target protein. In a two-step procedure, the cells are first supplemented with a limiting amount of the cAA and will grow until its depletion. After depletion, the ncAA is added to the medium and the expression of the target protein is turned on [33] & [32].

The requirement of auxotrophic strains faces one major drawback of the SPI technique. A lot of strains for applicable ncAAs are already available, i.e. *Coli* Genetic Stock center [6] or can be self-produced by well established genetic engineering techniques, i.e. gene deletions in *E. coli* [22].

1.3. Synthetic proteins containing ncAAs

In the last decades, protein engineering has been intensively performed by directed evolution [41], rational [42] or computational [43] design. Usually, ncAAs feature unusual side chain chemistries which expand the possibilities for protein engineering [44] beyond the 20 cAAs. A review article recently published by Zheng [6] provides a comprehensive overview of enzyme engineering with ncAAs.

The choice of the cAA/ncAA pair can influence the activity and stability in a large part. For an enzyme to remain active, only a minimal perturbation of the structure is expectable. That is one reason why fluorinated amino acid analogs [45], as well as Met [33] and tryptophan [46] analogs are widely used for the biosynthesis of synthetic proteins. Figure 3 provides an overview of those ncAAs that are commonly used for global protein labeling.

Presumably, the more similar the physico-chemical properties of cAA and ncAA are, a positive effect is more likely [35]. Nonetheless, it has repeatedly been observed that fluorinated prolines tend to improve the stability and folding of proteins [47-50], and substitution of Met by Nle positively affects the activity of lipases [38]. Especially for fluorinated amino acids the physico-chemical properties are totally changed compared to the cAA counterparts. Therefore, the global effects of ncAAs are not yet predictable. Until now there is no existing rule of thumb for prediction of the influence of ncAA incorporation [6]. It has to be explored for any ncAA in a specific protein. In order to make the effects of global ncAA incorporation on proteins more predictable, they will have to be included into future software tools for structural modeling [51].

It has been shown that ncAA incorporation can change spectral properties of proteins [52], incorporation of selenium and tellurium can help to solve the phase problem in x-ray crystallography [33] and ncAA can also be used for isotopic labeling for NMR spectroscopy [53].

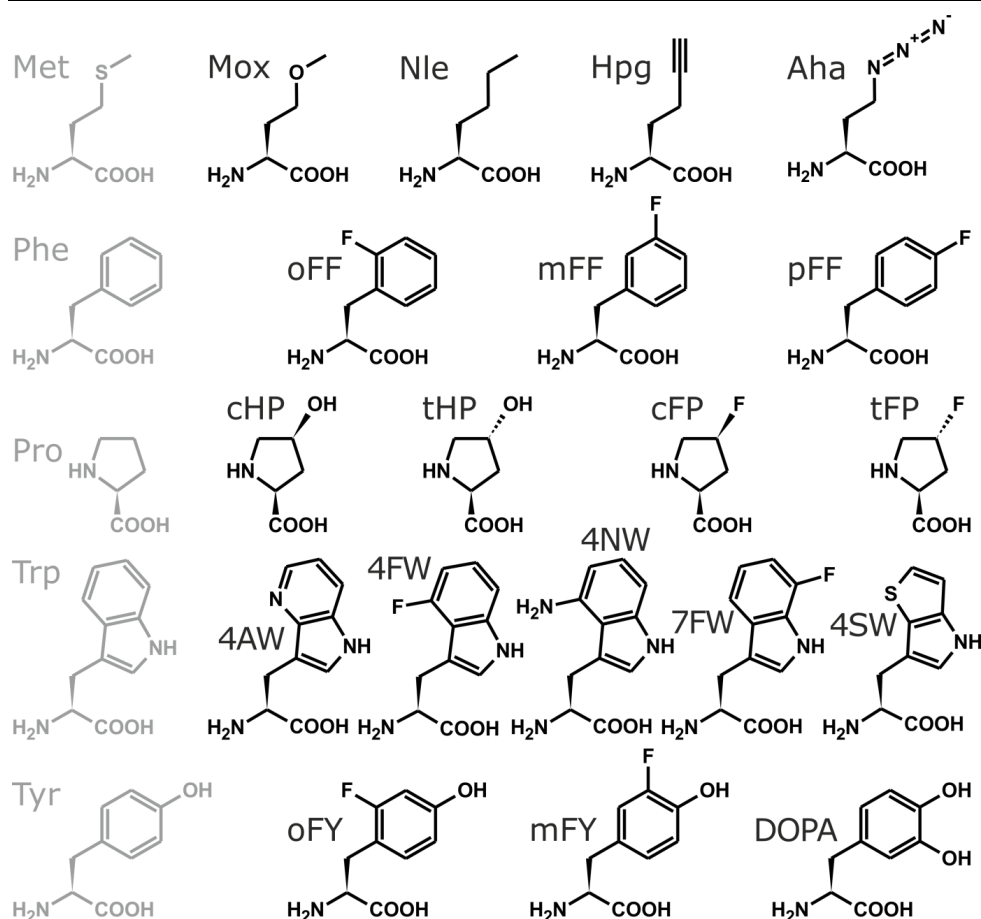


Figure 3 Commonly used ncAAs for global modification of proteins

The structures of the ncAAs (black) and their corresponding CAA (grey) are shown. .Mox, methoxinine; Nle, norleucine; Hpg, homopropargylglycine; mFF, *meta*-fluoro-phenylalanine, oFF, *ortho*-fluoro-phenylalanine, pFF, *para*-fluoro-phenylalanine; CHP; *cis*-hydroxy-proline; tHP, *trans*-hydroxy-proline; cFP, *cis*-fluoro-proline; tFP, *trans*-fluoro-proline; 4AW, 4-aza-tryptophane; 4FW, 4-fluoro-tryptophane; 7FW, 7-fluoro-tryptophane; 4NW, 4-amino-tryptophane; 4SW, 4-thiofuran-tryptophane; mFY, *meta*-fluoro-tyrosine; oFY, *ortho*-fluorotyrosine; DOPA, dopamine (*meta*-hydroxy-tyrosine)

There are also a lot of examples where enzyme activity [36, 54] and stability [50, 55] could be improved by residue-specific incorporation. A lot of other examples are nicely reviewed by Zheng [6], the ones with focus on Met analogs are given. The exchange of the Met by Nle in BM-3 heme domain variant of a bacterial CYP450 enzyme noticeably increased the stability and resistance to H₂O₂ treatment. Most probably, this is due to the fact that Nle cannot be oxidized because it contains a CH₂ group instead of the oxidation-sensitive sulfur of Met [28].

Global replacement of Met in *Gaussia* luciferase by azidohomoalanine or homopropargylglycine extended the emission half-life of the enzyme [36].

Due to their broad substrate specificity and stability, lipases are versatile biocatalysts [56]. The group of Budisa *et al* studied the influence of different ncAAs on a lipase from *Thermoanaerobacter thermohydrosulfuricus* (TTL). Different analogs yielded specific effects. The Nle variant of TTL, TTL [Nle], showed profoundly increased activity on *para*-nitrophenyl palmitate Due to the different effects obtained with different CAA analogs,

this study really shows the potential of ncAA incorporation as a useful tool for protein engineering. The ultimate goal for protein engineers would be the creation of enzymes with totally new enzyme functions, not found in nature yet.

A really illustrative example of synergism was the work of Tirell and co-workers by combining directed evolution with ncAA incorporation. The incorporation of the leucine analog 5',5',5'-trifluoroleucine into chloramphenicol acetyltransferase lead to a synthetic variant with a substantially lowered enzyme activity. Two rounds of directed evolution of the chloramphenicol acetyltransferase gene could restore wild-type activity after 5',5',5'-trifluoroleucine incorporation. This indicates that the negative effects of ncAA incorporation can be restored by directed evolution approaches [57].

All in all the examples above show that ncAA incorporation can be used as a powerful tool for extend the panoply of protein engineering methods. Even tough, the challenge of missing tools and knowledge for prediction of ncAA effects on target protein has still to be full field.

1.4. Polyesterases

Enzymatic degradation of polymers, especially plastics degradation [58-60] and surface modification [58-63] is a growing and important field as described in literature. Polyesterases for polymer degradation have the potential to revolutionize waste treatment [64]. The cutinases Cut1 and Cut2 from *Thermobifida cellulositica* as well as an esterase from *Thermobifida halotolerans* are used for polyethylene terephthalate (PET) surface modification and degradation [65]. The degradation is supposed to occur in two steps: First, the polyester PET is degraded in smaller fragments, e.g. mono(2-hydroxyethyl)terephthalate (MHET). In a second step, the soluble MHET molecules can be further degraded to terephthalic acid (TA) and ethylene glycol [65].

PET degradation is catalyzed by alpha/beta hydrolases, enzymes that are similar to lipases. The question was if the concept that was successful with lipases on soluble hydrophobic substrates [38] would be transferable to solid hydrophobic and synthetic substrates?

1.5. High cell density fermentation

To customize the production of synthetic proteins for future biotechnology applications, high yield and low cost processes are desirable. Basically, two strategies can be followed to enhance protein production by an existing expression system. On the one hand, engineering the expression strain can increase protein production efficiency. On the other hand

increased cell productivity realized by high cell density fermentation (HCDF) can raise total productivity of the desired end product. Major advantages of HCDF can be seen in reduced culture volumes, enhanced downstream processing, reduced wastewater lower production cost and last but not least, reduced investment in equipment. The main critical issues of HCDF of *E. coli* have been comprehensively reviewed by Lee and coworkers [66] and [67]), and the most important ones should be shortly highlighted here.

Aerobic cultivations under excess-glucose conditions can lead to an overflow metabolism [68] during *E. coli* cultivations. This phenomenon triggers acetate formation at high growth rates [69] and can have a major influence during HCDF. Therefore, process design plays an important role. The choice of carbon source, as well as feeding strategies for nutrients may play an essential role for the productivity (i.e. $\text{amount}_{\text{product}}/(\text{V}_{\text{unit}} \cdot \text{time})$). The usage of high amounts of glucose especially in batch fermentations can trigger acetate formation also under aerobic conditions independent of pO_2 . Acetate can have negative effects on transcription and translation in *E. coli* [70]. Lowering the growth rate by C-source limitation in fed-batch processes can overcome the problem of excess acetate formation [71]. Glycerol instead of glucose as C-source may have positive effects according to lower acetate formation and positive effect protein production [71]. Also genetically engineering of expression host by influencing the TCA cycle and reducing flux into acetate formation can be useful. A major drawback of this technique is that the modifications have to be done for every new expression host. In same perspective, a well balanced redox potential can prevent acetate formation. High levels of NAD are required for glycolysis and can trigger acetate formation via the TCA cycle [70]. The strain background can have major influence on the metabolic flux through the glyoxylate shunt and the TCA cycle. This fact was observed from Schiloach and coworkers for *E. coli* strains BL21 (B strain) and JM109 (K12 descendant). They supposed that the glyoxylate shunt is active in BL21, but inactive in JM109 resulting in the different acetate accumulation patterns. Therefore, K strain descendants are more likely to produce higher yields of acetate than B strains [72]. Further on, it has been shown that the feeding of Met or Gly can prevent negative effects of acetate [73]. This may be considered for processes that involve Met depletion for Met analog incorporation.

Lee *et al.* reported another aspect according to medium design. All nutrients necessary for *E. coli* growth are provided from the beginning in a batch fermentation process [74]. As mentioned above, cultivations at high growth rates can force acetate formation in *E. coli*

during HCDF. During fed-batch fermentations the constant feeding of limiting amounts of one nutrient, i.e. the carbon source, can be used to control the growth rates [74, 75]. Overall, fed-batch processes seem to be more likely to yield higher productivities [66]. It has also been shown that post-induction feeding can dramatically increase protein yields. Insufficient feeding (constant feeding), as well as overfeeding (exponential feeding) of nutrients, resulted in less protein production. This observation is highly depended on the strain background [76].

In general, the productivity of HCDF processes with regard to the protein level is lower than in shake flask cultures [77]. Jeong et al. showed that highest specific productivity (the amount of product formed per unit cell mass per unit time) can be obtained with cultures induced at low cell densities and highest volumetric productivity (the amount of product formed per unit volume per unit time) has been found in cultures induced at moderate cell densities [78].

The separation of the growth and the production phase as well as the right promoter system can increase productivity.

1.6. Main thesis objectives

The recent study deals with the development of ICDF protocols that can be used for global incorporation of Met analogs. Reasonable up-scaling from shake flask cultures to a bioreactor should be proved. The developed protocols are assessed for the production of Nle variants of proteins of the esterase and lipase family. Screening of new variants with changed properties is used to highlight the potential of ncAAs incorporation for protein engineering approaches. At the interface of synthetic biology and process engineering the final goal is to biosynthesis the nAA Nle in a bioreactor using a metabolically engineered *E. coli* strain. The produced Nle should be directly incorporated into a target enzyme.

2. Material & Methods

2.1. Materials

2.1.1. Strains

Cloning work was performed in *E. coli* DH5 α (Invitrogen, BT1582) with the following genotype: F⁻ Φ 80*lacZ_M15_(lacZYA-argF)* U169 *recA1 endA1 hsdR17* (rK⁻, mK⁺) *phoA supE44* λ ⁻ *thi-1 gyrA96 relA1*. All expressions and incorporation experiments were performed in B834(DE3) (Novagen, Kit Nr. 69041-3) with the following genotype: F⁻ *ompT hsdSB*(rB⁻, mB⁻) *gal dcm met*(DE3).

BWEC10 (BT 6900) is a descendant of BL21(DE3)Gold (Agilent, Cat. No. 230130) carrying the genetic knockouts: Δ *ilvBN::0*, Δ *ilvIH::0* and Δ *ilvGM::0*. BWEC14 (BT 6899) carries the same genetic knockouts, but is a descendant of B834(DE3). BWEC10 was used for Nle production and the incorporation of biosynthesized Nle was done with BWEC14 with and without the p*LeuA*BCD* over-expression plasmid p*Leu**). The * indicates that this variant of the operon is feedback intensive. BWEC10 and BWEC14 were produced and kindly provided by N. Anderhuber (ACIB Graz, for further strain information see [79]).

Table 1 Strains produced and used in this work

strain (BT number)	background	mutation/plasmid	reference	plasmid file name
BWEC10 (6900)	BL21(DE3)Gold	Δ <i>ilvBN::0</i> Δ <i>ilvIH::0</i> Δ <i>ilvGM::0</i>	[79]	
BWEC14 (6899)	B834(DE3)	Δ <i>ilvBN::0</i> Δ <i>ilvIH::0</i> Δ <i>ilvGM::0 metE</i>	[79]	
BWEC14{pTTL}	BWEC14	pQE80L-TTL-h ₆	[79]	pQE80L-TTL-h ₆
BWEC14{pTTL + pleu*}	BWEC14	pQE80L-TTL-h ₆ + p <i>LeuA*BCD</i>	[79]	pQE80L-TTL-h ₆ + pBP226-leu_A_BCD

2.1.2. Plasmids

Two vectors, pMS470 (BT 3046) and pQE80L (Qiagen, Cat.No. 32923) were used for recombinant plasmid construction. Heterologous protein expression was performed either

under the control of the *trc* promoter, or the *T5lac* promoter, respectively. The TTL gene from *Thermoanaerobacter thermohydrosulfuricus* was kindly provided by N. Budisa (TU Berlin) cloned in the pQE80L vector carrying a SVP2 signal peptide secretion sequence and a C-terminal hexahistidine-tag (h_6 -tag). The fragment of TTL without the secretion signal was PCR-amplified using primers shown in Table 3. Same strategy was used for subcloning of the TTL gene into the pET26b(+) vector (Novagen, Cat. No. 69862-3) (primers see in Table 3). The produced pET26b(+) expression plasmid was not further used in this work. The cutinases Cut1 and Cut2 from *Thermobifida cellulositytica* (Thc_Cut1 and Thc_Cut2), as well as an esterase from *Thermobifida halotolerans* (Thh_est) were a gift from Doris Ribitsch (ACIB-Graz). The provided constructs were cloned into the chosen expression vectors. All expression constructs carried a C-terminal h_6 -tag. All expression constructs used in this work were generated by Gibson Assembly.

Table 2 Plasmids produced or used in this work

h_6 , hexahistidine-tag

name	insert/property	resistance	abbreviation	plasmid file name	reference
pQE80L-TTL	TTL- h_6	Amp	pTTL	pQE80L-TTL- h_6	this work
pET26b(+)-TTL	TTL- h_6	Kan	-	pET26b(+)-TTL- h_6	this work
pMS470-Thc_Cut1	Cut1- h_6	Amp	-	pMS470-Thc_cut1	this work
pMS470-Thc_Cut2	Cut2- h_6	Amp	-	pMS470-Thc_cut2	this work
pMS470-Thh_Est	Est- h_6	Amp	-	pMS470-Thh_est	this work
pQE80L-Thc_Cut1	Cut1- h_6	Amp	-	pQE80L-Thc_cut1	this work
pQE80L-Thc_Cut2	Cut2- h_6	Amp	-	pQE80L-Thc_cut2	this work
pQE80L-Thh_Est	Est- h_6	Amp	-	pQE80L-Thh_est	this work
pLeuA*BCD	LeuA*BCD	Kan	pLeu*	pBP226-leu_A_BCD	[79]

2.1.3. Primers

Table 3 Primers for subcloning of TTL into pQE80L and pET26b(+)

The colors highlight features like restriction sites (*EcoRI* (magenta), *HindIII* (orange), *NdeI* (blue), *PstI* (cyan)), start codon (red), stop codon (red), RBS (ribosomal binding side, grey) and h₆-tag (green) introduced into the expression construct via the designed primer.

primer name	sequence (from 5' to 3')	T _m [°C]
pQE80L_TTL_up (BPp244)	45 nt hom gcgataacaatttcacacagaattcattaaagaggagaaattaagcATGCAAAGGCTGTTGAAATTAC	61.5
pQE80L_TTL_down (BPp245)	45 nt hom tctatcaacaggagtccaagctcagctaattaagcttggctgcagttatcagtgatggatggatggatggatggatggatcc TCCCTTTAACAATTCCTTTTTG	59.0
pET_TTL_up (BPp246)	45 nt hom ccctctagaataattttgtttaactttaagaaggagatatacatATGCAAAGGCTGTTGAAATTAC	61.5
pET_TTL_down (BPp247)	45 nt hom agccgatctcagtggtggtggtggtggtgctcgagtgcggccgcAAGCTTTATCAGTGATGGTGATGGTG	59.2

Table 4 Primers for subcloning of Thc_cut1, Thc_cut2 into pMS470

primer name	sequence (from 5' to 3')	T _m [°C]
pMS470_up (BPp241)	33 nt hom cctctagaataattttgtttaactttaagaag	60.9
pMS470_down (BPp242)	45 nt hom aatctgtatcaggctgaaaatcttctctcatccgcaaacagccAAGCTTCAAGTGGTGGTGG	60

Table 5 Primers for subcloning of Thc_cut1, Thc_cut2 and Thh_est into pQE80L

primer name	sequence (from 5' to 3')	Tm [°C]
pQE80L_up (BPp239)	45 nt hom atagattcaattgtgagcggataacaatttcacaca <i>EcoRI</i> gaattc attAAGGAGATATACAT <i>start</i> ATGGCCAACC	61.4
pQE80L_down (BPp240)	45 nt hom aggtcattactggatctatcaacaggagtccaagctcagctaatt <i>stop</i> AAGCT <i>HindIII</i> TCA <i>His6</i> STGGTGGTGG	59.7

2.1.4. Instruments and Devices

Table 6 List of instruments and devices used in this work

instrument	supplier
autoclave VX150	Systex, Wetttemberg, Germany
analytical scale	Santorius Stedim, Göttingen, Germany
Avanti J-20XP centrifuge	Beckmann Cloutier Inc., California, USA
baking oven	Binder, Tuttlingen, Germany
Bradford reagent (Cat.Nr. 500-0006)	Biorad, Vienna, Austria (Cat.Nr. 500-0006)
centrifuge tubes, 50 mL and 500 mL	Thermo Scientific Inc., Massachusetts, USA
centrifuges	Centrifuge 5415R, Eppendorf, Hamburg, Germany Centrifuge 5424, Eppendorf
column (5 mL HisTrap)	GE Healthcare (Cat.Nr. 17-5247-01)
cryo vials	Thermo Scientific
desalting column (HisTrap 26/10)	GE Healthcare, Buckinghamshire, UK (Cat.Nr. 17-5087-01)
bioreactor	DASGIP technology, Jülich, Germany
electrophoresis gel chambers: PowerPac™ Basic + Sub_CellGT	BioRad, Hercules, USA
electrotransformation: BioRad Micropulser	BioRad
electroporation cuvettes (2 mm)	Peqlab Biotechnology GmbH, Erlangen, Germany
Eppendorf tubes	Sarstedt, Nümbrecht, Germany
Falcon tubes	Greiner bio-one International AG, Kremsmünster, Austria
flasks	2000 mL (Schott Duran), Bartelt, Graz, Austria 1000 mL (SIMAX), Bartelt 250 mL (Schott Duran), Bartelt
FPLC	Äkta Purifier, GE Healthcare Äkta Prime, GE Healthcare
G:Box HR	Syngene, Cambridge, UK
gel kits	QIAprep Spin Miniprep Kit (250), Quiagen QIAquick Gel Extraction Kit, Quiagen
Gravity Flow Affinity purification equipment	Ni-NTA resin, Quiagen, Hilden, Germany Disposable 10 mL Polypropylen Columns, Thermo Scientific
HPLC/UV	Agilent Technologies, Santa Clara, USA
ddH ₂ O device (arium® basic)	Santorius Stedim
incubator HT MultitronII	InforsAG, Bottmingen, Swiss
lab Scale	Binder
laminar flow chamber	CleanAir, Woerden, The Netherlands

HisProbe-HRP working solution	Thermo Scientific (Cat.Nr. 15165)
Luminol/Enhancer Solution + Stable peroxide solution (HRP detection)	Thermo Scientific (Cat.Nr. 15168)
Nanodrop	Thermo Scientific
PD10 Desalting Columns	GE Healthcare (Cat.Nr. 17-0851-01)
PCR machines (GeneAmp [®] PCR System 2700)	Applied Biosystems, California, USA
PCR tubes	Geiner bio-one International AG
petridishes	Geiner bio-one International AG
photometer	Beckmann Cloutier Inc. BioPhotometer, Eppendorf
pipette tips	Geiner bio-one International AG
pipettes	1000 µL, 200 µL, 20 µL, Deville, South Plainfield, USA 10 µL, Biohit, Santorius Stedim
plate reader (SPECTRAmax Plus384)	Molecular Devices, Silicon Valley, USA
scanner	Tevion USB Scanner, Mühlheim, Germany
serological pipettes	Geiner bio-one International AG
silica plates 60 F254	Merck, Darmstadt, Germany
sterile syringe filters	Scientific Startegies, Oklahoma, USA
sterile filters	Santorius Stedim
sonifier	Branson, Danbury, USA
TLC chamber	Sigma-Aldrich
UV cuvettes	Greiner bio-one International AG
vortex	IKA [®] -Werke GmbH & Co. KG, Staufen, Germany

2.1.5. Chemicals and enzymes

Table 7 List of reagents and enzymes used in this work

reagent	Cat. Nr.	supplier
acetic acide	6755.2	Roth, Kalsruhe, Germany
acetonitrile LC-MS grade	9017	J.T. Baker, München, Germany
agarose LE	840004	Biozyme, Hessisch-Oldendorf, Germany
aluminium chloride hexahydrate	1010841000	Merck, Darmstadt, Germany
ammonia	5460.1	Roth
ampicillin	A0166	Sigma-Aldrich, St.Louis, USA
ammonium chloride	K298.2	Roth
antifoam	LM1207072	Bussetti & Co GmbH, Vienna, Austria
ammonium persulfate (APS)	13375.01	Serva, Heidelberg, Germany
Acrylamide/Bis solution, 37.5:1 (30 % w/v), 2.6 % C	10688.01	Serva

boric acid	1001625000	Merck
n-butanol	7171.2	Roth
calcium chloride dihydrate	CN93.1	Roth
cobalt chloride hexahydrate	1025390100	Merck
Comassie Blue-250R	3862.2	Roth
copper(II)chloride dihydrate	1027330250	Merck
DNAse I	DN25-100mg	Sigma-Aldrich
dNTP Set I(100 mM each)	K039.1	Roth
1,4-dithiothreitol (DTT)	6908.1	Roth
DMSO	4720.3	Roth
EDTA	CN06.1	Roth
ethanol	20821.330	VWR International, Pennsylvania, USA
ethidium bromide	46066	Fluka, St. Louis, USA
α -D-glucose monohydrate	6780.2	Roth
glycerol	3908.3	Roth
glycin	3908.3	Roth
hydrochloric acid 32%	4625.2	Roth
hydrochloric acid, fuming	4625.1	Roth
imidazole	1047161000	Merck
iron(II)sulphate heptahydrate	1039650500	Merck
isoleucine	3922.2	Roth
isopropyl β -D-1-thiogalactopyranoside (IPTG)	CN03.3	Roth
kanamycin sulfate	T832.2	Roth
LB-Agar Lennox	X65.3	Roth
LB-medium Lennox	X964.2	Roth
leucine	1699.1	Roth
lysozyme	8259.2	Roth
magnesium chloride	8.14733.0500	Merck
magnesium sulfate heptahydrate	A537.4	Roth
mangan(II)sulphate monohydrate	1059991000	Merck
β -mercaptoethanol	4227.1	Roth
methanol HPLC Gradient grade	87-56-1	J.T. Baker
methionine	1702.1	Roth
NAD		Roth
norleucine	HAA113.0025	Iris Biotech GmbH, Marktredwitz, Germany
norvalin	HAA1114.0005	iris
PageRuler prestained protein ladder	SM0671	Thermo Scientific, Massachusetts, USA
<i>para</i> -nitrophenyl acetate (pNPA)	N8130-10G	Sigma-Aldrich
<i>para</i> -nitrophenyl butyrate (pNPB)	N9376-5G	Sigma-Aldrich

PEG-8000	P5413-1KG	Sigma-Aldrich
phosphoric acid	6366.1	Roth
Phusion [®] High-Fidelity DNA polymerase	M0530S	NEB, Frankfurt am Main, Germany
di-potassium hydrogen phosphate	T875.2	Roth
potassium dihydrogen phosphate	P018.2	Carl Roth, Germany
pyridin	270970-100mL	Sigma-Aldrich
ribonuclease A (RNase I)	R5503-100mg	Sigma-Aldrich
SOB medium	AE27.1	Roth
di-sodium tetraborate decahydrate	CN07.1	Roth
sodium chloride (NaCl)	9265.1	Roth
di-sodium hydrogen phosphate	T876.2	Roth
sodium dihydrogen phosphate monohydrate	T879.2	Roth
sodium dodecyl sulfate (SDS)	2326.1	Roth
sodium hydroxid	P031.2	Roth
sodium hydrogen carbonate	0965.1	Roth
sodium molybdate dihydrate	1065241000	Merck
sterile water	-	Fresenius Cabi, Graz, Austria
T5 exonuclease	162340	Biozyme
Taq ligase	M0208S	NEB
tetramethylethylenediamin (TEMED)	35930.01	Serva
tris base	4855.3	Roth
Triton-X100	3051.3	Roth
valin	4879.1	Roth
yeast extract (Charge: 269107355)	2363.4	Roth
zinc sulphate heptahydrate	1088830500	Merck

2.1.6. Media and buffers

Unless otherwise specified all media and buffers were autoclaved.

2.1.6.1. **LB**

Medium: 10 g/L tryptone, 5 g/L yeast extract, 5 g/L NaCl

Agar: 10 g/L tryptone, 5 g/L yeast extract, 5 g/L NaCl, 20 g/L agar

1 mL of the appropriate antibiotic stock (1000 X) was added per liter of medium or agar.

2.1.6.2. SOC medium

5 g/L yeast extract, 20 g/L tryptone, 0.6 g/L NaCl, 0.2 g/L KCl, 10 mM MgCl₂, 10 mM MgSO₄, 20 mM glucose

2.1.6.3. 5 X ISO buffer

Table 8 Composition 5 X ISO buffer

component	C _{stock}	volume / amount
25% (w/v) PEG-8000	PEG-8000	1.5 g
500 mM Tris/Cl pH 7.5	1 M Tris/Cl pH 7.5	3000 µL
50 mM MgCl ₂	2 M MgCl ₂	150 µL
50 mM DTT	1 M DTT	300 µL
1 mM dATP	100 mM dATP	60 µL
1 mM dCTP	100 mM dCTP	60 µL
1 mM dGTP	100 mM dGTP	60 µL
1 mM dTTP	100 mM dTTP	60 µL
5 mM NAD	100 mM NAD	300 µL
	sterile ddH ₂ O	up to 6000 µL

The PEG-8000 was weighed out first and then all other ingredients were added out of stock solutions. All ingredients were mixed by vortexing and filter sterilized by using 0.45 µm sterile syringe filters. 100 µL aliquots were stored at -20 °C.

2.1.6.4. M9 medium supplementations

Table 9 Composition M9 salt stock

component	amount
Na ₂ HPO ₄	33.9 g/L
KH ₂ PO ₄	15 g/L
NaCl	2.5 g/L
NH ₄ Cl	5 g/L

Table 10 Composition trace element stock

component	amount
FeSO ₄ x 7 H ₂ O	40.0 g/L
MnSO ₄ x H ₂ O	10.0 g/L
AlCl ₃ x 6 H ₂ O	10.0 g/L
CoCl ₂ x 6 H ₂ O	7.3 g/L
ZnSO ₄ x 7 H ₂ O	2.0 g/L
Na ₂ MoO ₄ x 2 H ₂ O	2.0 g/L
CuCl ₂ x 2 H ₂ O	1.0 g/L
H ₃ BO ₄	0.5 g/L
HCl conc. (37%, fuming)	414 mL/L
ddH ₂ O	up to 1000 mL

2.1.6.5. M9 based media

Table 11 Composition M9 medium

component	C _{stock}	C _{final}	1 L/ OD ₆₀₀ 3.6
M9 salts ²	5 X		1 X 200 mL
MgSO ₄ ²	1 M	0.1 g/g CDM	1 mL
CaCl ₂ ²	1 mg/mL	1 µg/L	1 mL
glucose ²	1 M	3 g/g CDM	20 mL
trace elements ²	~18.7 X	50 L/g CDM	60 µL
antibiotic ²	1000 X		1 X 1 mL
amino acid supplementation ²	100 mM	1 mM (~0.13 g/g CDM)	10 mL
yeast extract ¹	-	3.5 g/L	3.5 g
ddH ₂ O ¹	-	-	up to 1000 mL

CDM, cell dry mass

¹ 3.5 g YE were dissolved in ddH₂O and autoclaved.

² All other ingredients were supplemented afterwards as sterile stock solutions.

Table 12 Composition M9 medium adapted for the bioreactor

component	C _{stock}	V _{St[mL]} /1000 mL
M9 salt stock ²	5 X	200
MgSO ₄ ²	1 M	10
Ca ²⁺ / citric acid ^{2,3,4}	24 mg/mL	10
glucose ²	1 M	200
trace elements ²	~18.7 X	0.600
yeast extract ¹	-	35 g
ddH ₂ O ¹	-	up to 1000 ml
antifoam (1:10) ^{2,3}	-	1

¹ 35 g YE were dissolved in ddH₂O and autoclaved directly in the bioreactor.

² All other ingredients were supplemented afterwards as sterile stock solutions via a septum.

³ Ca²⁺ and antifoam were added under stirring.

⁴ 120 mg/mL citric acid were added to Ca²⁺ as chelating reagent.

Table 13 M9 medium adapted for Nle production

component	C _{stock}	V _{St[mL]} /1000 mL
M9 salt stock ²	5 X	200
MgSO ₄ ²	1 M	1
Ca ^{2+;2,3}	1 mg/mL	1
glucose ¹	1 M	60 g
trace elements ²	~18.7 X	0.060
H ₂ O ¹	-	up to 1000 mL
Val+Ile ²	10 g/L	1
antifoam (1:10) ^{2,3}	-	1

¹ 60 g glucose were dissolved in ddH₂O and autoclaved directly in the bioreactor.

² All other ingredients were supplemented afterwards as sterile stock solutions via a septum.

³ Ca²⁺ and antifoam were added under stirring.

2.1.6.6. Ni-chelate lysis Buffer / Ni-chelate Buffer A (ÄKTA)

50 mM NaH₂PO₄ x H₂O, 300 mM NaCl, 10 mM imidazole, pH 8.0; For resuspension of cell pellets 1 mg/ml lysozyme, 4 µg/ml DNase, and 10 µg/ml RNase were added.

2.1.6.7. Ni-chelate wash buffer

50 mM NaH₂PO₄ x H₂O, 300 mM NaCl, 20 mM imidazole, pH 8.0

2.1.6.8. Ni-chelate elution buffer / Ni-chelate Buffer B (ÄKTA)

50 mM NaH₂PO₄ x H₂O, 300 mM NaCl, 250 mM imidazole, pH 8.0

For ÄKTA purification following elution buffer (Buffer B) was used: 50 mM NaH₂PO₄ x H₂O, 300 mM NaCl, 500 mM imidazole, pH 8.0

2.1.6.9. storage buffer

20 mM Tris/Cl, pH 7.0

2.1.6.10. reaction buffer (PET / 3PET degradation)

100 mM Tris/Cl, pH 7.0

2.1.6.11. 5 x SDS sample buffer

10% (w/v) SDS, 0.08 M Tris/Cl (pH 6.8), 12.5% (v/v) glycerol, 0.2% (w/v) bromphenol blue, 4% (v/v) β-mercaptoethanol (added fresh before use)

2.1.6.12. 10 X Running buffer

1% (w/v) SDS, 1.92 M glycine, 0.25 M Tris

2.1.6.13. staining solution

0.1% (w/v) Coomassie Blue R-250, 40% (v/v) ethanol, 10% (v/v) CH₃COOH, up to 1000 mL with H₂O

2.1.6.14. destaining solution

40% (v/v) ethanol, 10% (v/v) CH₃COOH, up to 1000 mL with H₂O

2.1.6.15. HPLC (Buffer A)

20 mM KH₂PO₄, pH 8.0

2.1.6.16. 10x TBS buffer

60 g/L Tris, 87 g/L NaCl, adjust with HCl to pH 8.0

2.2. Methods

2.2.1. Preparation of electrocompetent *E. coli* cells

A 20 mL LB overnight culture (ONC) of the desired *E. coli* strain was incubated at 37 °C and vigorous shaking. The next day a main culture of 500 mL LB was inoculated with 15 mL of the ONC and incubated at 37 °C and vigorous shaking until an OD₆₀₀ of 0.7 and 0.8 was reached. Cells were harvested in pre-chilled 500 mL centrifuge bottles at 5000 x g for 15 minutes at 4 °C. The supernatant was discarded and the cells were gently resuspended in 500 mL of sterile, ice-cold 10% (w/v) glycerol. The centrifugation step was repeated and the supernatant was discarded. The cells were again resuspended in 500 mL sterile, ice-cold 10% (w/v) glycerol. Cells were harvested again and the supernatant was poured off. The remaining pellet was resuspended in 1 mL of sterile, ice-cold glycerol. 80 µL aliquots were frozen in N₂ and stored at -80 °C.

2.2.2. Electroporation of *E. coli*

The transformation of plasmids into electrocompetent *E. coli* cells DH5α followed a standard protocol [80]. 40 µL electrocompetent cells were thawed on ice and mixed with 50-100 ng of the plasmid DNA. The mixture was transferred to a pre-chilled electroporation cuvette and incubated on ice for 5 minutes. Immediately after pulsing in the electroporator (Bio-Rad micropulser fixed program EC2: 2.50 kV, 1 pulse) 1 mL of SOC media was added and the cells were regenerated at 37 °C for 1 hour at 700 rpm. After regeneration, cells were plated on

selective media or directly transferred into fresh LB supplemented with the appropriate antibiotic for an ONC.

2.2.3. PCR

Inserts for Gibson cloning were prepared by PCR. A 40-50 nucleotide homology region for the desired vector was added at the 5'-ends of PCR primers. The following PCR mix in a thin-walled PCR tube was used:

component	C_{final}	volume to add
dsDNA template	5 – 500 ng	x μL
forward primer [25 pmol/ μL]	0.2 – 1.0 μM	0.5 μL
reverse primer [25 pmol/ μL]	0.2 – 1.0 μM	0.5 μL
10 X reaction buffer	1 X	2.5 μL
dNTP's [2.5 mM each]	0.2 mM each	2.0 μL
DNA-polymerase [5 U/ μL]	1.0 – 2.5 U	0.5 μL
ddH ₂ O	-	up to 25 μL

Plasmid preparations were used as PCR template in the listed amounts.

A standard 3 step PCR was performed:

step	T	time	cycles
initial denaturation	95 °C		5 min
denaturation	95 °C		30 sec
annealing	T_{anneal}		1 min 25 x
extension	72 °C	1 min/kb of aplicon length	
end-elongation	72 °C		10 min

T_{anneal} is 4-5 °C lower than the T_m calculated with the OligoExploerer software [81]

After the PCR reaction, the mixes were treated with *DpnI* to digest the template. 1 μL of *DpnI* was added to each PCR mix (25 μL) and incubated at 37 °C for 3 hours. *DpnI* was heat inactivated at 80 °C for 10 minutes. The PCR product was analyzed or further purified on an agarose gel.

2.2.4. Gel electrophoresis

The analysis and purification of DNA fragments by agarose gel-electrophoresis was performed according to a standard protocol [82]. 1% agarose gels were run in 1 X TAE buffer at 90 V for preparative and 120 V for analytical gels. The size of the DNA fragments was estimated by comparison with the standard "Gene Ruler DNA Ladder Mix" in Figure 4 (Thermo Scientific).

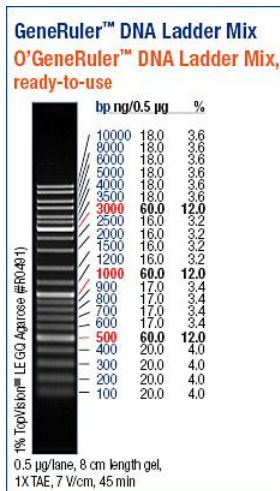


Figure 4 GeneRuler™ DNA Ladder Mix

2.2.5. Gibson assembly

2.2.5.1. Fragment design

The method for cloning by *in vitro* recombineering was used as described by Gibson [83]. The used DNA fragments must be linear carrying a 40-60 bp overlapping homology region for efficient recombination. For that reason, homology hooks for the desired vector were attached to the 5'-ends of the primers for target gene amplification. The scheme in Figure 5 shows the cloning strategy for TTL (A) and the cutinases (B). Sequence homology of all three enzymes facilitated the primer design as two pairs could be used for the PCR amplification of all three cutinase genes. Primers for amplification are listed in Table 3 (TTL subcloning into pQE80L and pet26b(+)), Table 4 (Thc_cut1 and Thc_cut2 subcloning into pMS470) and Table 5 (Thc_cut1, Thc_cut2 and Thh_est subcloning into pQE80L). The vectors pET26b(+), pMS470 and pQE80L were double digested with the appropriate digestion enzymes *NdeI/HindIII* (pEt26b(+)), *NdeI/HindIII* (pMS470), *EcoRI/HindIII* (pQE80L) to generate linear fragments.

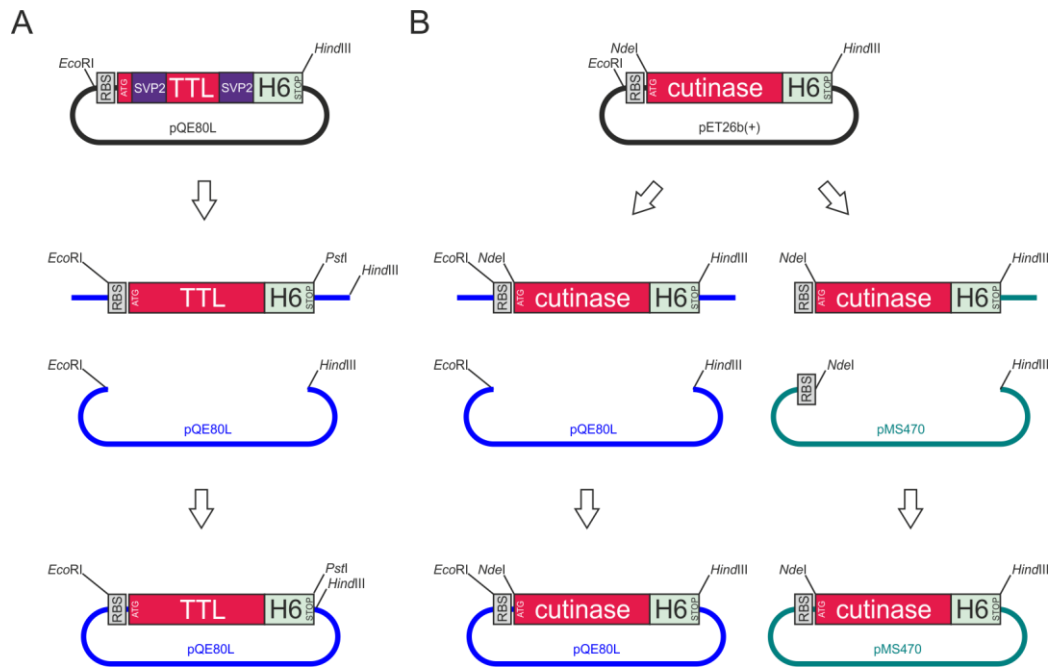


Figure 5 Cloning strategy via Gibson Assembly

A: The TTL-h₆ gene was PCR amplified using the primers described in Table 4 together with the template vector pQE80L-SVP2-TTL-h₆ to release SVP2 signal peptide. The PCR fragment was assembled with *EcoRI/HindIII* cut pQE80L by *in vitro* homologous recombination yielding the expression construct pTTL.

B: The template vectors pET26b(+)-Thc_cut1, pET26b(+)-Thc_cut2 and pMS470-Thh_est were used for PCR amplification of the inserts using the primers shown in Table 4 and Table 5. The target backbone vectors pQE80L and pMS470 were cut with *EcoRI/HindIII* and *NdeI/HindIII*, respectively. The corresponding linear fragments were assembled into the final expression constructs by *in vitro* homologous recombination.

RBS, ribosomal binding side; H6, hexahistidine-tag; SVP2, signaling peptide

All DNA fragments were gel purified before the Gibson assembly.

2.2.5.2. Preparation of the assembly master mix

The 5 X isothermal buffer (5 X ISO) was prepared as described in section 2.1.6.3. The assembly master mix was prepared by mixing the following components:

component	volume to add
5 X ISO buffer	320 μ L
T5 exonuclease (10 U/ μ L)	0.64 μ L
Phusion® High-Fidelity DNA Polymerase, (2 U/ μ L)	20 μ L
Taq DNA ligase, 40 U/ μ L	160 μ L
sterile ddH ₂ O	fill up to 1200 μ L

The mixes can be stored in 15 μ L aliquots at -20 °C.

2.2.5.3. Cloning by *in vitro* recombination

A 15 μ L aliquot of the assembly master mix was thawed on ice. 5 μ L of DNA to be assembled were added to the master mix and incubated at 50 °C for 60 minutes. The DNA fragments were used in equimolar amounts. The reactions contained at least 100 ng of each DNA fragment. The assembled DNA fragments were transformed into *E. coli* DH5 α after Gibson

Assembly. Positive clones were selected on LB agar plates containing appropriate antibiotics depending on the resistance marker of the two used vectors, i.e., 100 mg/L ampicillin for pQE80L constructs and 50 mg/L kanamycine for pET26b(+) constructs. 4 positive clones of each construct were checked by restriction enzyme digest and two clones with the correct restriction pattern were sequence verified.

2.2.6. Preparation of plasmids, PCR products and DNA fragments

All plasmids were isolated with the Quiagen “QIAprep Spin Miniprep Kit (250)” according to the user manual and finally eluted with 50 μ L of ddH₂O. An 10 mL overnight culture in LB medium was used as starting material.

DNA fragments and PCR products were purified on standard agarose gels and extracted with the commercial “QIAquick Gel Extraction Kit” by Quiagen. Elution volume was 25 μ L.

2.2.7. Restriction enzymes

Restriction digests were performed with FastDigest enzymes (Thermo Scientific) at 37 °C following the manufacturer’s instructions. Analytical restrictions were performed for 1 h and preparative cuts for 3 h.

2.2.8. Sequencing

All expression constructs were sequenced by LGC Genomics GmbH (Berlin, Germany). 10 - 20 μ L of plasmid preparation with a concentration of 100 ng/ μ L was sent for analysis with standard forward and reverse primers for the vectors by LGC Genomics.

2.2.9. Titration of the optimal yeast extract concentration as Met limiting growth source

For titration experiments, glycerol stocks with an OD₆₀₀ of 1 were required. For that purpose an ONC of B834(DE3) carrying one of the expression plasmids was grown at 37 °C with appropriate antibiotic supplementation. An amount of cells was harvested such that after resuspension in x mL of fresh LB medium the OD₆₀₀ would be 2. Afterwards, x mL of sterile 70% (v/v) glycerol were added. 1 mL aliquots in sterile cryo vials were frozen in liquid N₂ and store at -80 °C until used.

In sterile 250 mL baffled flasks, 10 mL of 1 g/L, 2 g/L, 3 g/L, 4 g/L, and 6 g/L yeast extract YE solutions were prepared by diluting a sterile 60 g/L YE stock with sterile water. As the positive control, a 250 mL baffled flask with 10 mL of 1 g/L YE and 1 mM of Met was prepared. 600 mL of 1.1 X M9 medium were mixed as described in section 2.1.6.5 and inoculated with 660 μ L of the prepared glycerol stocks (OD_{600} 1). 90 mL of the cell suspension were added to each 250 mL flask containing 10 mL of the YE dilution. The cultures were incubated at 37°C with vigorous shaking until stationary phase was reached. The OD_{600} was read in regular intervals and an OD_{600} vs. time growth curve was recorded. The reading intervals were shortened in the log phase in order to get better resolution.

2.2.10. High cell density SPI in *E. coli*

The strain must be auxotrophic for Met to incorporate Met analogs, i.e. Nle, into target proteins. Every SPI experiment is separated in two phases. In phase I (growth phase) the auxotrophic strain is grown with a limiting concentration of Met. After Met depletion the ncAA Nle (analog culture) or Met (canonical culture) are added to the medium and protein expression is induced by IPTG (Phase II). The protocol can be adapted for other cAAs and their ncAA analogs.

2.2.10.1. Shake flask

Phase I:

1 L of M9 medium containing YE as limiting Met source (2.1.6.5) for Nle incorporation (analog culture) and Met control (canonical culture) in 2 L baffled flasks were prepared. Main cultures were inoculated out of a fresh ONC or with a 1 mL glycerol stock (OD_{600} 1) of strain B834(DE3) carrying the inducible expression plasmid. The cultures were incubated at 37 °C with vigorous shaking until the OD_{600} remained constant for 30 minutes. The growth arrest indicated Met depletion.

Phase II:

The non-induced analog culture was supplemented with 1 mM of Nle, as well as the non-induced canonical culture with 1 mM Met.. Expression of the target protein was induced by adding 0.4-1 mM IPTG to each culture and was performed for 4 hours with vigorous shaking. The induction temperature was dependent on the target protein. The three cutinases were expressed at 28 °C and the TTL at 30 °C. At the end of the induction the OD_{600} was read. Cells

were harvested by low speed centrifugation (20 min, $\sim 4000 \times g$, 4 °C) and resuspended in 5 mL Ni-chelate lysis buffer per gram cell wet weight (CWW). After 1 hour incubation on ice, cells were directly used for protein purification or the suspensions were stored at -80 °C until use.

2.2.10.2. Bioreactor

All experiments done in a bioreactor were performed with a DASGIP bioreactor system. The bioreactors were suitable for up to 1400 mL working volume and equipped with a pH and an oxygen electrode. For stirring, a 6-flat blade disc turbine was used. Basically, the medium formulation followed the list of ingredients outlined in section 2.1.6.5. The pH was pre-set to 7 and adjusted automatically with 10% (v/v) H_3PO_4 and 12.5% (v/v) NH_3 . The partial pressure of oxygen (pO_2) was pre-set to a minimum concentration of dissolved oxygen of 30% and was regulated via the stirrer velocity.

2.2.10.2.1. Production of Nle-labeled proteins in the bioreactor

The ICDF protocol established in 1 L shake flask cultures was scaled up for the bioreactor. M9 adapted for the bioreactor (2.1.6.5) was used. The process was scaled up 10-fold compared to shake flask cultivations and was designed to yield a theoretical final OD_{600} of 36 (equals to 12 g cell dry mass, CDM). According to the theoretical amount of YE as Met source to lead to growth arrest at an OD_{600} of 30, 35 g/L YE were anticipated (section 3.1.1). In comparison to the shake flask experiment, all ingredients were added in a 10-fold excess, except of the M9 salt and Ca^{2+} stocks. The Ca^{2+} stock contained 24 mg/mL $CaCl_2 \times 2H_2O$ and 120 mg/mL citric acid (molar ratio Ca^{2+} / citric acid is ~ 1) as a chelating agent to prevent precipitation of calcium phosphate in the medium adapted for the bioreactor. Each culture in a bioreactor was inoculated with 1 mL glycerol stock of B834(DE3) {pTTL} ($OD_{600} \sim 1$) and grown at 37 °C to the point of Met depletion as indicated by the constant OD_{600} for 30 min. Then the bioreactor was cooled to 30 °C and 20 mM of the amino acid (Met or Nle) were supplemented. The expression was induced by 1 mM IPTG and was performed for 4 h at a pH 7 and a pO_2 minimum of 30%. At the end of the bioreactor process, the cells were harvested by low speed centrifugation, resuspended in lysis buffer and stored at -80 °C.

2.2.10.2.2. Nle production

M9 medium adapted for Nle production was used (section 2.1.6.5).. The process was developed to be limited by Val/Ile supplementation (100 mg each) to yield a theoretical final

OD₆₀₀ of about 3 (equals to 1 g CDM). Nle production should be increased in resting cells under fermentative conditions. The bioreactor was inoculated with an ONC of BWEC10 to an OD₆₀₀ of 0.01 and grown at 32° C to presumed Val depletion after 20 hours as indicated by constant OD₆₀₀. Then the bioreactor was kept at 32 °C for 52 hours. At the end of the bioreactor process, the cells were harvested by low speed centrifugation, the supernatant was sterile filtered (0.45 μM), aliquoted in 50 mL falcons and stored at -80 °C. Samples for thin layer chromatography were taken after 38 h, 46 h and 66 h. For that purpose, 1 mL culture was harvested and 2 μL of the supernatant were spotted on silica gel plate. Metabolic samples were also taken for amino acid analysis by HPLC-UV.

2.2.10.2.3. Production of synthetic proteins containing biosynthesized Nle

The medium was based on M9 medium adapted for the bioreactor (section 2.1.6.5), but slightly altered for each process. Details are summarized in Table 14. All supplementations during the bioreactor process are shown in Table 15.

Nle production in growing cells (bioreactor 1)

The process was designed to yield a theoretical final OD₆₀₀ of 6 (equals 2 g CDM). Accordingly, 7 g/L YE were anticipated to lead to Met depletion at OD₆₀₀ 6. The bioreactor was inoculated with BWEC14{pTTL + pLeu*} to an initial OD₆₀₀ of 0.01 and grown at 37 °C to Met depletion as indicated by constant OD₆₀₀ for 30 min. Then the bioreactor was cooled to 30 °C and expression was induced by the addition of 1 mM IPTG. Expression was performed for 4 h at a pH 7 and a pO₂ minimum of 30%. At the end of the bioreactor process, the cells were harvested by low speed centrifugation, resuspended in lysis buffer and stored at -80 °C until further processing.

Nle production in resting cells (bioreactor 2)

The process was designed to yield a theoretical final OD₆₀₀ of 10 (equals to 3.3 g CDM). A two-step process was planned: (1) Accumulation of cell mass up to OD₆₀₀ 3 then depletion of Val and production of Nle (zero-growth phase); (2) growth restart by the addition of Val, further accumulation of cell mass until depletion of Met at OD₆₀₀ 10; then induction of target protein production in the presence of Nle biosynthesized in the zero-growth phase. 3.5 g/L YE were anticipated to lead to Val depletion at OD₆₀₀ 3 (section 3.1.1)). In order to ensure that Met was not depleted at the first growth arrest, 280 μM Met were supplemented to support growth until OD₆₀₀ 10 (previous observation). The bioreactor was inoculated with

BWEC14{pTTL} to an initial OD₆₀₀ of 0.01 and grown at 37 °C to Val depletion as indicated by a constant OD₆₀₀. After depletion, a zero-growth period for Nle production was performed at 37°C, pH 7, pO₂ of 30%. 0.5 mM valine were added for growth restart to bioreactor 2, but the strain did not restore growth. All supplementations tested for growth restart were inefficient. Thus, bioreactor 2 was shut down with any further processing.

Nle production in resting cells (bioreactor 8)

The process was designed as in bioreactor 2. In contrast to bioreactor 2, strain BWEC14{pTTL + pLeu*} was used. As supplementation with Ile and glucose did not promote growth after zero growth phase, yeast extract was added. Addition of YE restored growth and after reaching constant OD₆₀₀ the bioreactor was cooled to 30 °C and expression was induced by 1 mM IPTG and was performed for 4 h at a pH 7 and a pO₂ minimum of 30%. At the end of the bioreactor process, the cells were harvested by low speed centrifugation, resuspended in lysis buffer as before and stored at -80 °C until further processing.

Metabolic samples were frequently taken from bioreactors 1, 2, and 8. 1 mL culture was harvested and the supernatant was filter sterilized and stored at -20°C.

Table 14 Composition of media adapted for Nle production in a bioreactor

		bioreactor 1	bioreactor 2	bioreactor 8
component	c_{st}	volume/amount	volume/amount	volume/amount
M9 salts ²	5 X	200 mL	200 mL	200 mL
MgSO ₄ ²	1 M	1 mL	1 mL	1 mL
Ca ^{2+,2,3}	1 mg/mL	1 mL	1 mL	1 mL
glucose ²	1 M	55.6 mL	111.1 mL	111.1 mL
trace elements ²	~18.7 X	60 μ L	180 μ L	180 μ L
yeast extract ¹	-	7 g	3.5 g	3.5 g
ddH ₂ O ¹	-	up to 1000 mL	up to 1000 mL	up to 1000 mL
ampicillin ²	100 mg/mL	1 mL	1 mL	1 mL
kanamycin ²	50 mg/mL	1 mL	1 mL	1 mL
antifoam ^{2,3}	1:10	1 mL	1 mL	1 mL

st, stock

¹ 7 g YE were dissolved in 741.4 mL ddH₂O and autoclaved directly in the bioreactor.

² All other ingredients were supplemented afterwards as sterile stock solutions via a septum.

³ Ca²⁺ and antifoam were added under stirring.

Table 15 Supplementations during the bioreactor process

		bioreactor 1	bioreactor 2	bioreactor 8
component	c_{st}	volume/amount	volume/amount	volume/amount
Val	100 mM	-	5 mL	
Ile	100 mM	-	5 mL	5 mL
Met	100 mM	-	5 mL	
glucose	1 M	-	50 mL	50 mL
YE (3.5 g/L)	60 g/L	-	-	60 mL

The analytics was the same for all cultures. Cell growth was monitored by measuring OD₆₀₀. Additionally, the CDM was determined as followed. 1 mL of cell suspension was harvested in pre-baked (105 °C, 48 h) tared Eppendorf tubes. Pellets were washed with 1 mL water and spun again. The supernatant was discarded and the Eppendorf tubes were dried at 105 °C until their mass remained constant.

Expression was analyzed by SDS PAGE. To ensure approximately equal amounts of cellular protein in each lane, samples corresponding to 1 OD₆₀₀ were sampled before and after 4 h of induction.

2.2.11. SDS-PAGE

All proteins were analyzed by SDS-PAGE as described by Laemmli ([84]). The polyacrylamide gels were composed of 5% stacking gel on top and 10% separating gel at the bottom. To follow protein expression, 1 OD₆₀₀ samples were harvested (13.000 rpm, RT, 2') and the

pellet was resuspended in 80 μL H_2O and 20 μL 5 X SDS LD were added. 10 μL were loaded. To analyse the protein purification, 40 μL of the relevant FPLC fractions were mixed with 10 μL of 5 X SDS LD. 5-10 μL were loaded. To follow protein purification samples after every step were taken according to the following scheme:

Table 16 SDS sample overview FPLC purification

sample	abbreviation	v_{sample} [μL]	5 X SDS LD [μL]	v_{load} [μL]
lysate	P3	80	20	2-10
pellet	P4	80	20	2-10
flow through	P5	80	20	2-10
wash	P6	80	20	10-15
eluate	P7	40	20	5-10

Standard amounts for shake flask experiments are the maximum levels of v_{load} . For the bioreactor experiments the amounts loaded on the gels were adapted.

Samples were heated at 98°C for 10 min and loaded onto the gel. To analyze TTL containing biosynthesized Nle NuPAGE® gels were used (Life technologies) according to the manufacturer’s instructions. The size of the DNA fragments was estimated by comparison with the standard “Gene Ruler DNA Ladder Mix” shown in Figure 6 (Thermo Scientific).

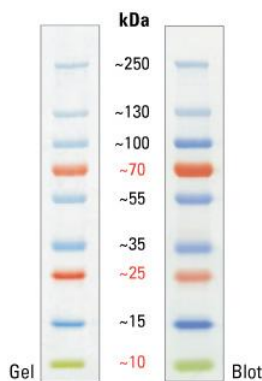


Figure 6 Band profile of the Thermo Scientific PageRuler Plus Prestained Protein Ladder

2.2.12. Protein purification

All proteins used in this work carried a hexahistidine-tag and were purified by Ni-chelate affinity chromatography using one of the two methods. Cutinases from shake flask experiments and TTL containing biosynthesized Nle were purified by gravity flow. The other TTL variants produced in a bioreactor were purified on an ÄKTA purifier system.

2.2.12.1. Ni-chelate chromatography by gravity flow

Frozen cell pellets in lysis buffer were thawed and chilled on ice. Fresh pellets were resuspended in 5 mL lysis buffer per gram CWW and pre-treated for 1 h on ice. Cell rupture was performed by sonication (sonication tip $\Phi \sim 1$ cm, output control: 8, duty cycle: 70-80%, time: 6-8 minutes). Cell debris was removed by high speed centrifugation (40 min, 20000 x g, 4 °C). Supernatant (cleared lysate) was transferred to a fresh vessel and the volume was estimated. The sonication pellet was resuspended in the same volume of 2% SDS. Cleared lysate (P3) was immediately used for purification. Columns (Thermo Scientific) were packed by gravity flow. 2 mL of nickel resin (Quiagen) led to 1 column volumes (CV). The protocol is summed up in Table 17.

Table 17 Ni-chelate chromatography by gravity flow

step	CV	buffer	comment
equilibration	20	lysis buffer	
load lysate	-	-	collect flow through
wash	50	wash buffer	collect wash fraction
elution	4	elution buffer	collect eluates
regeneration	30	0.5 M NaOH	
resin wash	10	30% (v/v) EtOH	store column in 30% (v/v) EtOH

Columns were only reused for the same variants.

2.2.12.2. FPLC purification on an ÄKTA purifier system

For protein purification a cooled ÄKTA purifier system with sample collector was used. The composition of Buffer A (lysis buffer) and Buffer B (elution buffer, see section 2.1.6.8) is shown in 2.1.6. A 5 mL HisTrap column (GE Healthcare) was used. To avoid cross-contamination, the synthetic variant was always purified first. A step gradient was chosen. The whole lysate volume (20 to 30 mL) was loaded onto the column by using an external pump. The flow for sample loading was 2 mL/min and for the rest of the purification process 4 mL/min. The method is described in Table 18.

Table 18 Ni-chelate purification protocol for ÄKTA purifier

step	CV	buffer	comment
equilibration	7	Buffer A	
wash	7	2% Buffer B	2 mL fractions
step I	5	10% Buffer B	1.5 mL fractions
step II	5	35% Buffer B	1.5 mL fractions
step III	5	100% Buffer B	2 mL fractions

Column purification and storage was performed as described in the manual.

Fractions in peaks were checked by SDS-PAGE and further processed or analyzed.

2.2.12.3. Desalting / buffer exchange

The buffer exchange for all proteins was performed on an ÄKTA prime system. A HisTrap 26/10 Desalting column (GE Healthcare) was used at a flow of 8 mL/min. The separation column was always equilibrated with 20 CV storage buffer, see section 2.1.6.9) At maximum, 15 mL of sample could be loaded via a 20 mL sample loop. 5 mL fractions were collected. Fractions containing protein as indicated by SDS-PAGE analysis were pooled.

2.2.13. Protein concentration

Protein concentrations were double checked either by Nanodrop (Thermo Scientific) or by Biorad protein assay (Biorad). For both methods the user's manual was followed.

2.2.14. PET, PLA & 3PET degradation assay

2.2.14.1. PET (poly-ethylene-terephthalate) and PLA (poly-lactic acid)

PET/PLA films (1 mm x 0.5 mm) were washed with 30 mL TritonX solution (5 g/L), 30 mL of Na₂CO₃ (2 g/L) and ddH₂O. All washing steps were performed at 50 °C and 100 rpm for 30 minutes. In between, the PET films were washed with ddH₂O. PET degradation was performed in 1.5 mL Eppendorf tubes in a 200 µg/mL enzyme solution at 50 °C and 500 rpm for 24 hours.

2.2.14.2. 3PET (bis(benzoyloxyethyl) terephthalate)

10 mg of 3PET were put in a 1.5 µL Eppendorf tube and incubated with an enzyme solution (200 µg/mL) at 50 °C at 500 rpm for 3 hours.

The enzymes were diluted with 100 mM Tris/Cl (pH 7.0) to a final concentration of 200 µg/mL. For both assays the reactions were stopped by mixing 500 µL reaction mixture

with 500 μL ice-cooled MeOH. The samples were provided to A. Marold (ACIB, AG Gubitz) for HPLC analysis of the release products after centrifugation at 4000 rpm and 0 $^{\circ}\text{C}$ for 15 minutes.

2.2.15. Esterase activity assay

The assay is based on an internal protocol (ACIB, AG Ribitsch). The used substrate concentration was 6.7 mM for *para*-nitrophenyl acetate (pNP-acetate) and 7.86 mM *para*-nitrophenyl butyrate (pNP-butyrate). Reactions were performed in 96 well microtiter plates at room temperature. The release of *para*-nitrophenol was detected photometrically. The absorbance was followed over time and the initial reaction velocity (v_{in} , slope) was determined. The activity per volume (U/mL) was calculated using the formula shown in Figure 7. 20 μL of enzyme solution (V_{enzyme}) were used in a total reaction volume of 220 μL (V_{tot}). The enzymes were diluted with 100 mM Tris/Cl (pH 7.0) to a final concentration of 200 $\mu\text{g}/\text{mL}$.

Figure 7 Volumetric activity on pNP-acetate and pNP-butyrate

The enzymatic cleavage of pNP-esters releases p-nitrophenol. Under basic conditions the p-nitrophenol anion can be photometrically detected at 405 nm. The increase of absorbance is followed over time. The initial reaction velocity (v_{in}) was deduced from the slope of the curve. Based on Lambert Beer's Law the shown formula was used to calculate the specific enzyme activity (U/mL).

V_{tot} , total volume of reaction mixture; V_{enzyme} , volume of enzyme solution; F, dilution factor of the enzyme solution

2.2.16. PET adhesion assay (HisProbe HRP)

Prepared PET films (procedure see section 2.2.14) were incubated with a defined amount of enzyme in 600 μL of 100 mM Tris/Cl (pH 7.0) buffer at 30 $^{\circ}\text{C}$ for 2 hours. Afterwards, PET films were washed twice by dipping in 100 mM Tris/Cl (pH 7.0) at room temperature and transferred to a new 2.0 mL Eppendorf tube. The films were incubated with 1.5 mL of HisProbe-HRP (Thermo Scientific, a 1:2500 dilution in TBS) at room temperature and 400 rpm for 40 minutes. Afterwards, the PET films were washed twice by dipping in 100 mM Tris/Cl (pH 7.0) at room temperature. The films were incubated with 600 μL of SuperSignal West Pico Substrate Working Solution (Thermo Scientific, equal amounts of Luminol/Enhancer solution and Stable Peroxide Solution) and incubated at room

temperature for 5 minutes. The luminescence signal was developed in a G-box for 5-10 minutes.

2.2.17. Thin layer chromatography (TLC)

Silica gel plates (Merck) were used for separating amines out of culture supernatants with a thin layer chromatography. A mixture of n-butanol: H₂O: CH₃COOH in the ratio 3:1:1 was used as the mobile phase. Chromatograms were developed in standard TLC chambers. Amino acids (amines) were stained with ninhydrine solution (0.1 g ninhydrine dissolved in 0.5 mL acetic acid and 100 mL acetone). Samples were spotted with capillaries (Hirschmann Laborgeräte). Stained TLC plates were heated until the purple color of spot of calibration substance was clearly visible.

2.2.18. HPLC-UV for amino acid analysis

Based on the data obtained from thin layer chromatography a HPLC method for branched chain amino acids (Ile, Leu, Nle, Nva, Val) analysis was developed. For UV detection at 338 nm, the amino groups of the amino acids were derivatized in-needle ([85] & internal communication K. Weinhandl (ACIB-Graz) with OPA (*ortho*-phthaldialdehyde)/MCE (β -mercaptoethanol) (Figure 8).

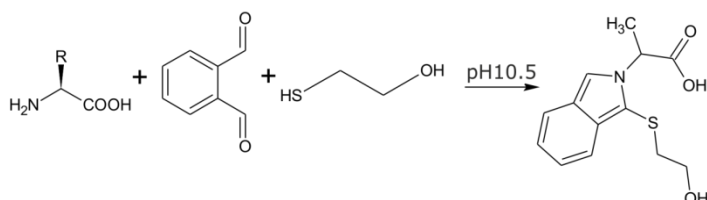


Figure 8 scheme of OPA/MCE derivatization reaction

2.2.18.1. Preparation of derivatization reagent

18 mg of OPA were dissolved in 1 ml of acetonitrile. Then, 14 μ l of MCE were added and the mixture was mixed and transferred to a HPLC vial.

2.2.18.2. Preparation of samples for HPLC analysis

Samples were filtered (0.2 μ m PES filters) to avoid blocking of the HPLC column. All samples were diluted appropriately in borate buffer (0.1 mM NaB₄O₇, pH 10.5). Amino acid standards were diluted 5 times.

2.2.18.3. HPLC method

An Agilent HPLC-UV (Agilent technologies) equipment was used. The settings for the HPLC method are summarized in Table 19. The derivatization program for the in-needle reaction is shown in Table 20.

Table 19 HPLC method for branched chain amino acid analysis

parameter	Set up
column flow	0.700 mL/min
stop time	25 minutes
maximum pressure	250 bar
oven temperature	25 °C
column	Litochrat 250 Purospher Star RP18e 5 μ M
Solvent A	70% 20 mM KH_2PO_4 (pH 8.0)
Solvent D	30% acetonitrile
$\lambda_{\text{det},1}$	338 nm
$\lambda_{\text{det},2}$	210 nm

Table 20 Injection program

step	command	amount [μ L]	reagent	comment
1	draw	30	sample	
2	draw	0	H_2O	exterior needle wash
3	draw	10	OPA/MCE	derivatization reagent
4	draw	0	H_2O	exterior needle wash
5	mix max. amount in seat	-	-	6 times
6	eject	30	-	into empty vial
7	inject	-	-	residual 10 μ L
8	needle wash	-	-	2 times

For a calibration curves of branched chain amino acids (Ile, Leu, Nle, Nva, Val) 5 stock solutions each with following concentrations 25 mg/mL, 50 mg/mL, 100 mg/mL, 150 mg/mL and 200 mg/mL of the amino acid dissolved in 0.1 M HCl were used. Calibration curves were calculated by linear curve fit using EXCEL. All calculation for the amino acid quantification was based on the obtained calibration curves.

2.2.19. Mass analysis

Samples for mass analysis were provided in 20 mM Tris/Cl buffer (pH 7.0) to the ACIB Core Facility Metabolomics (Medical University of Graz) for analysis. Deconvoluted masses were plotted against intensity using QTI Plot software [86]. Theoretical masses were calculated using MassXpert [87] extended for nCAA. For calculations the ionization level was set to zero.

3. Results

3.1. Synthetic protein production by external non-canonical amino acid supplementation

3.1.1. High cell density fermentation

The methionine Met auxotrophic *E. coli* strain B834(DE3) had previously been described as a suitable host for supplementation based incorporation experiments of Met analogs [33]. Therefore, it was chosen as the host strain for SPI of norleucine (Nle) in the present study. Strain B834(DE3) is a B strain carrying a mutation in the Met biosynthesis pathway [88] which makes it dependent on exogenous Met supply in minimal medium.

Budisa et al. introduced New Minimal Medium (NMM; [33]) containing limiting amounts of Met for incorporation of Met analogs by B834(DE3). Being a multi-component medium, NMM is badly customizable for increased cell density fermentations (ICDF). In this study the original recipe of NMM was progressively changed to reduce the number of ingredients to the essential ones (see section 2.1.6.5)

In NMM, the cells grow to a final OD_{600} of 2 and the depletion of the canonical amino acid (cAA) is usually designed to occur at mid log (OD_{600} 1) [89]. As growth is not restored by the addition of the ncAA during target protein expression, the final cell numbers are comparably low (OD_{600} 1 vs. $OD_{600} \geq 4$ for routine protein expression in LB medium [90]). Lower cell numbers often yield less protein, therefore, we sought to establish a ICDF (final OD_{600} 3.6 in minimal medium) protocol in order to produce high amounts of synthetic proteins.

As outlined above, auxotrophic cells must be supplemented with the cAA in the medium in order to grow (first phase of SPI, see section 1.2. Higher cell densities require more supplements and the water solubility especially of the aromatic amino acids is quite low. To overcome the problem of amino acid solubility for ICDFs the applicability of yeast extract (YE) as the Met source was evaluated. The titration experiment in Figure 9 shows that YE is a suitable Met supply for the growth of B834(DE3). B834(DE3) transformed with an expression plasmid of TTL (pTTL) was used in order to evaluate the amount of YE necessary and sufficient to sustain growth and plasmid maintenance to a certain OD_{600} . The culture medium was designed such that it contained enough glucose and other nutrients except Met for the cells to reach a final OD_{600} of 3.6. The medium was inoculated with the cells (2.2.9)

and 100 ml each in a shake flask were supplemented with a specific amount of YE as indicated in Figure 9. The positive control contained 1 g/L YE and an excess of 10 mM Met. 1 mM Met per g CDM is determined to be sufficient for Met auxothrophic strains (internal communication G. Striedner, ACIB Vienna). The cultures were grown at 37 °C and samples withdrawn for OD₆₀₀ determination at repeated intervals over 24h. The results (Figure 9) indicate a direct correlation between the amounts of YE added and the arrest of growth: As the amount of YE raises the cells grow to a higher OD₆₀₀. Met is indeed the limiting factor in the growth medium: B834(DE3) supplemented with only 1 g/L YE grow to a final OD₆₀₀ of ~0.8 while they reach the expected maximal OD₆₀₀ ~3.5 if 10 mM Met is added in excess on top of 1 g/L YE.

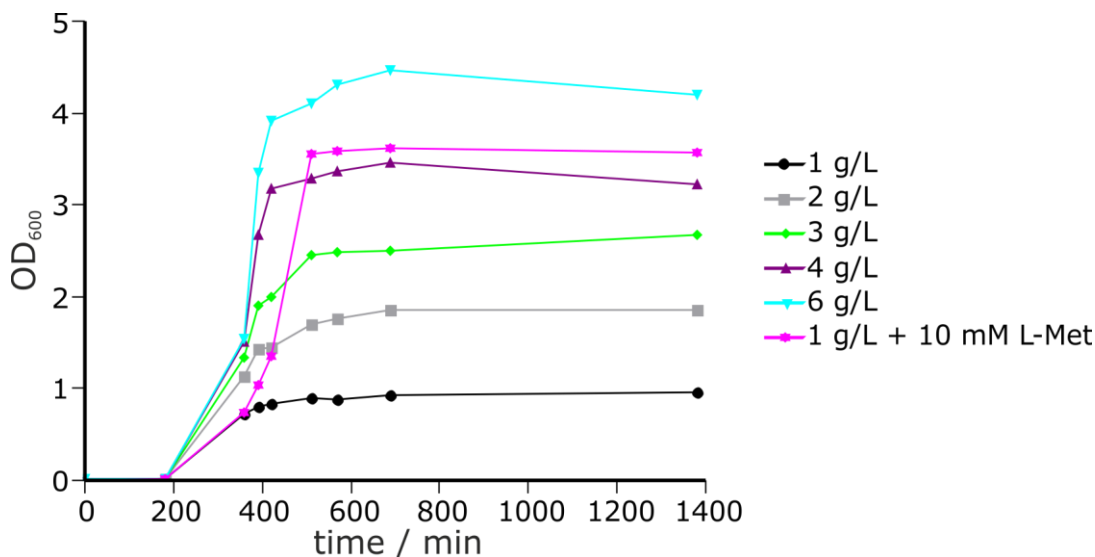


Figure 9 Yeast extract (YE) is suitable to control Met depletion

YE dependent growth of the Met-auxothrophic strain B834(DE3) carrying {pTTL} in 100 mL shake flask cultures in M9 medium containing 1 g/L (black curve), 2 g/L (grey curve), 3 g/L (green curve), 4 g/L (purple curve), and 6 g/L (cyan curve) YE in comparison to 1 g/L YE + supplementation with excess Met (pink curve). OD₆₀₀ values higher than 3.6 were normalized to CDM according to the correlation in Figure 10. All values were determined in triplicates. The error bars are very close to the average data point and, therefore, are omitted for clarity.

Starvation of *E. coli* strains may influence the optical density (internal communication). For that reason, the correlation between cell density and cell dry mass (CDM) was determined for the culture supplemented with 1 g/L YE and excess of Met. The results in Figure 10 show that for this experiment a linear correlation between OD₆₀₀ and CDM was obtained for OD₆₀₀ values ≤3.6. The OD₆₀₀ values >3.0 for the pink curve in Figure 9 were corrected according to this correlation. For all further experiments the correlation between OD₆₀₀ and CDM was linear for all further experiments. OD₆₀₀ values >3.6 were obtained for the culture

supplemented with 6 g/L of YE. This is most probably due to the introduction of extra carbon source by YE.

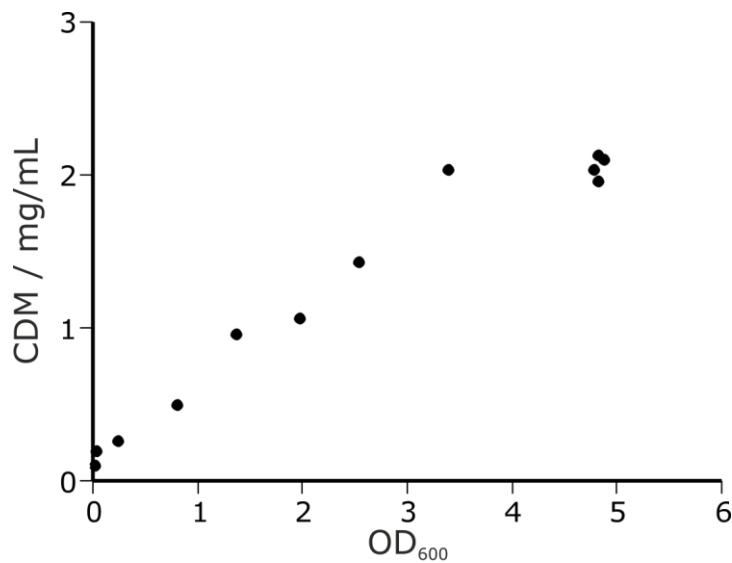


Figure 10 Correlation of cell dry mass (CDM) and optical density (OD₆₀₀)

A linear correlation between OD₆₀₀ and CDM was observed for OD₆₀₀ ≤ 3.6 for a culture supplemented with 1 g/L YE and excess Met (10 mM). All values were determined in triplicates. The error bars are very close to the average data point and, therefore, were omitted for clarity.

In order to validate the data obtained from the 100 mL shake flask cultures, the cultivation volume was 10-fold up-scaled while the final OD₆₀₀ 3.6 remained unchanged. The cultures were supplemented with 1 or 3.5 g/L YE as the Met source. As shown in Figure 11, B834(DE3){pTTL} showed comparable growth behavior in 1 L shake flask cultures. To ensure that Met was the growth limiting factor, 1 mM Met was added to two cultures after an initial growth arrest at OD₆₀₀ ~1 (1 g/L YE; Figure 11, pink curve) and OD₆₀₀ ~3 (3.5 g/L YE; Figure 11, black curve). Both cultures reached the maximum OD₆₀₀ of 3.6, comparable with the positive control containing 1 g/L YE and an 1 mM of Met (Figure 11, green curve). Supplementation with 3.5 g/L YE caused the cells to enter log phase earlier than supplementation with only 1 g/L (Figure 11, black and grey curves vs. green and pink curves, respectively).

The optimal YE concentration for limited Met supplementation was found to be 3.5 g/L. This YE concentration provoked the growth arrest due to Met depletion in the late log phase (OD₆₀₀ ~3) of cultures containing enough glucose and other nutrients to reach a final OD₆₀₀ of 3.6 (high cell density).

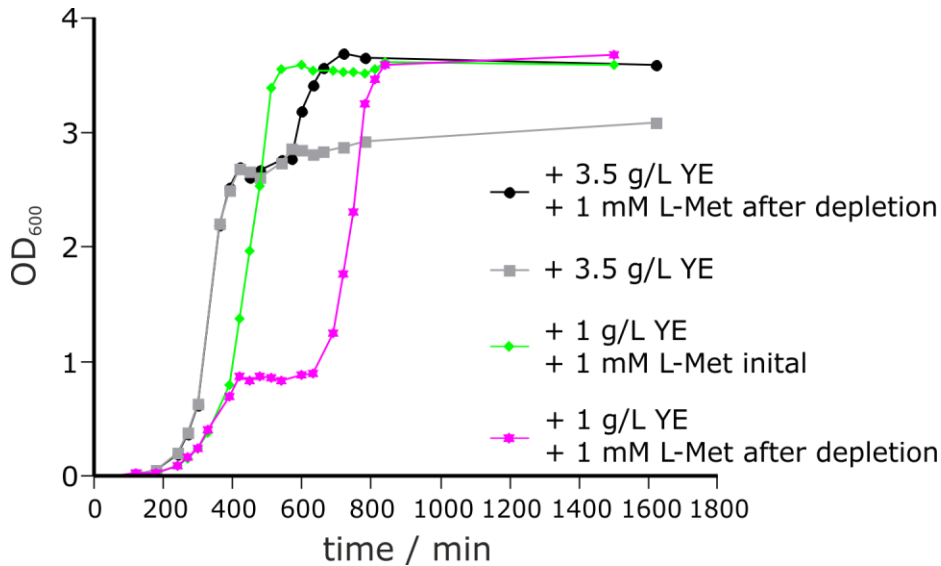


Figure 11 The scale-up from 100 mL to 1 L high density shake flask cultures is feasible

Growth of Met-auxotrophic strain B834(DE3) {pTTL} in 1 L M9 medium in 2 L shake flasks with different supplementations. After growth arrest, two cultures (black and pink curves) were supplemented with 1 mM Met and restored growth as expected. As positive control, a culture was grown in the presence of excess Met. All values were determined in triplicates. The error bars are very close to the average data point and, therefore, are omitted for clarity.

The optimized recipe of M9 based minimal medium for SPI of Met analogs in high cell density cultures is summarized in Table 21. The amount of carbon source was calculated to yield a final OD₆₀₀ of 3.6. The optimal YE concentration ($C_{YE,opt}$) of 3.5 g/L was deduced from the titration experiment in Figure 9 and leads to Met depletion with a concomitant growth arrest at a OD₆₀₀ 3. The medium was used for all global incorporation experiments with Nle in shake flask cultures.

Table 21 M9 medium for SPI of Met analogs in high cell density shake flask cultures

ingredient name	C_{stock}	C_{final}	1 L / OD ₆₀₀ 3.6
M9 salt stock ²	5 X	1 X	200 mL
MgSO ₄ ²	1 M	1 mM	1 mL
CaCl ₂ ²	1 mg/mL	1 µg/L	1 mL
glucose ²	1 M	20 mM	20 mL
trace elements ²	~ 18.7 X	1 X	60 µL
yeast extract ¹		3.5 g	3.5 g
H ₂ O ¹			780 mL
appropriate antibiotics ²			1 mL

¹ 3.5 g YE were dissolved in 780 mL ddH₂O and autoclaved.

² All other ingredients were supplemented afterwards as sterile stock solutions.

When the glucose concentration of the medium is high but the amount of dissolved oxygen is limited in shake flask cultures, the *E. coli* cells start to acidify the medium, which subsequently leads to “acid death” of the cells [70]. *E. coli* B strains are valued for their

comparably modest tendency to acidify the medium. However, due to a drop in pH below 5, optical densities above 4 could not be obtained for B834(DE3) in shake flask cultures (data not shown). For that reason, all shake flask SPI experiments with Nle described in this study were performed in M9 medium with 3.6 g/L glucose and 3.5 g/L YE.

3.1.2. Applications

The ICDF protocol described above was examined for its applicability to biotechnologically relevant enzymes.

3.1.2.1. Synthetic TTL

The substitution of all Met residues in TTL by Nle increased the enzyme activity by approximately ten-fold [38]. For that reason, TTL was used as the model protein to establish the ICDF protocol for SPI of non-canonical amino acids (ncAA), specifically Met analogs, into target proteins. For SPI experiments an appropriately inducible expression system is needed. Therefore, the TTL expression construct carrying a C-terminal h₆tag described by [38] was reproduced by Gibson Assembly [83]. Homology regions for cloning of the target gene were introduced by PCR. Both PCR reactions yielded the expected fragment of about 890 bp (Figure 12, A). The backbone vectors pQE80L and pET26b(+) were prepared by restriction double digest and purified by gel extraction. Vectors containing an irrelevant insert were used to ensure double digest of restriction enzymes. Due to a different promoter the pET26b(+) vector was used for the construction of a second alternative expression construct. Because of the successful expression of TTL with the already published pQE80L construct that was never used in this study.

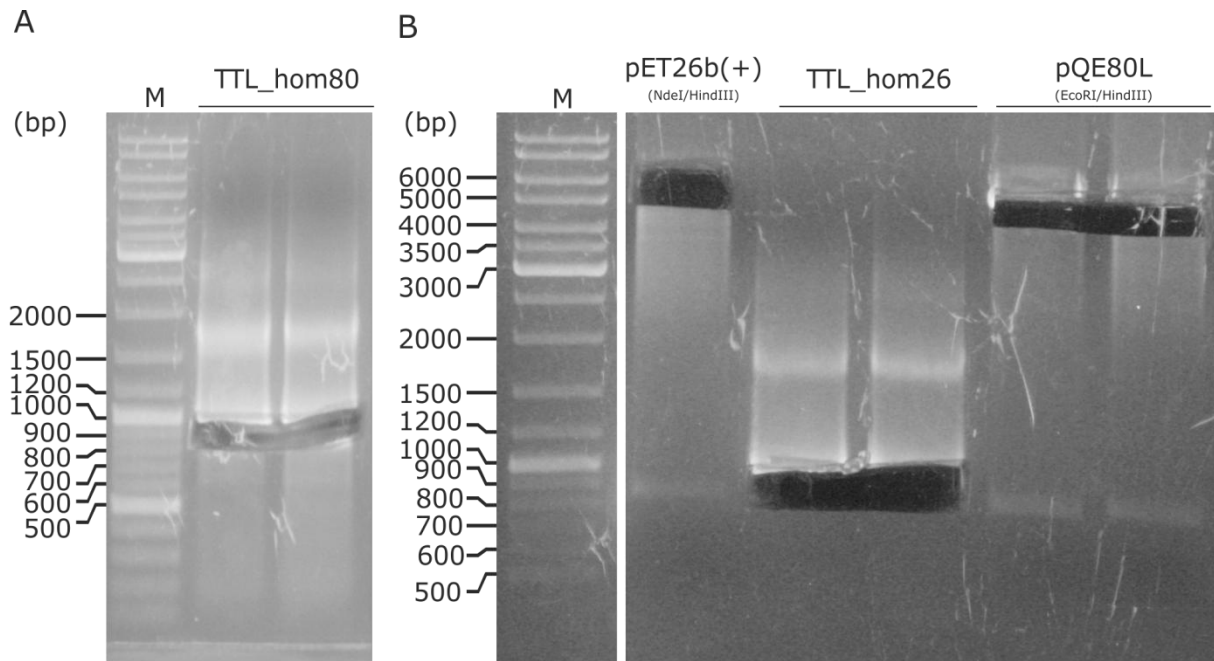


Figure 12 Preparation of inserts and vectors for Gibson assembly

1% agarose gel, the size of the relevant marker bands is indicated.

A: The PCR with primers BpP 244 and BpP 245 (Table 3) yielded the TTL gene carrying flanking homologies for assembly with the pQE80L vector (TTL_hom80).

B: PCR with primers BpP 241 and BpP 243 (Table 3) yielded a TTL fragment carrying flanking overlapping homologies for the pET26b(+) vector (TTL_hom26). The vectors pQE80L and pET26b(+) were double digested with the indicated digestion enzymes.

Two PCR samples were analyzed each, both contained the expected 890 bp fragment. All fragments were excised and purified.

The prepared vectors and purified inserts were assembled. Four obtained clones each were checked by restriction digest and sequence verified (Figure 13; A and B). Positive clones could be received for both constructs.

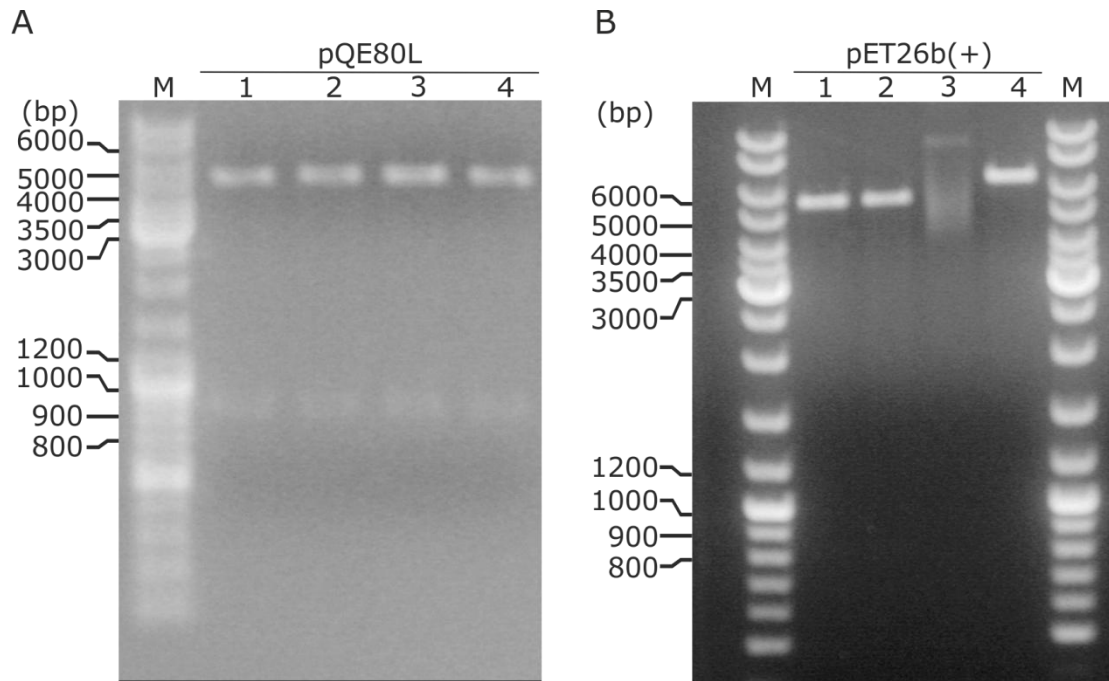


Figure 13 Control restriction of four different clones of each expression construct

1 % agarose gel; the size of the relevant molecular weight marker bands is indicated.

A: Restriction double digest of pTTL constructs with *EcoRI/HindIII* yielded to the expected fragments of 4660 bp and 834 bp.

B: The constructs cloned into pET26b(+) were double digested with *NdeI/HindIII* and yielded the expected fragments of 5246 bp and 834 bp for clones 1 and 2. Only the vector band at 5300 bp is clearly visible. The quality of the gel picture is too bad to see the rather small second fragment at about 800 bp

Budisa and co-workers showed that active TTL can be expressed in shake flask cultures using the expression construct pTTL [38]. Hence, the generated pQE80L construct was used for further expression and incorporation experiments. A test expression in M9 medium in 100 mL shake flask cultures was performed to test whether our expression plasmid works and the ICDF protocol could be used for Nle incorporation,. The results of the experiment shown in section 3.1.1 could be reproduced and the cultures grew to a final OD_{600} of 3. As Met should be depleted at this point 1 mM of Nle was added to the culture medium. A second culture was supplemented with 1 mM Met as a control. Protein expression was induced by adding 1 mM of IPTG as soon as the *E. coli* culture reached 1 OD_{600} . Samples were taken before and after induction for SDS-PAGE analysis. The clear over-expression bands in the induced samples (gel in Figure 14, lane i) indicate that both TTL variants were successfully over-expressed. The Met-variant and the Nle-variant showed different migration behavior on SDS-PAGE gels as reported in previous publications [38], indicating the successful incorporation of Nle into the target protein. The IPTG induction also led to a second over-expression band of an unidentified smaller protein. The amount of the TTL[Nle] variant was reduced compared to the TTL[Met] one.

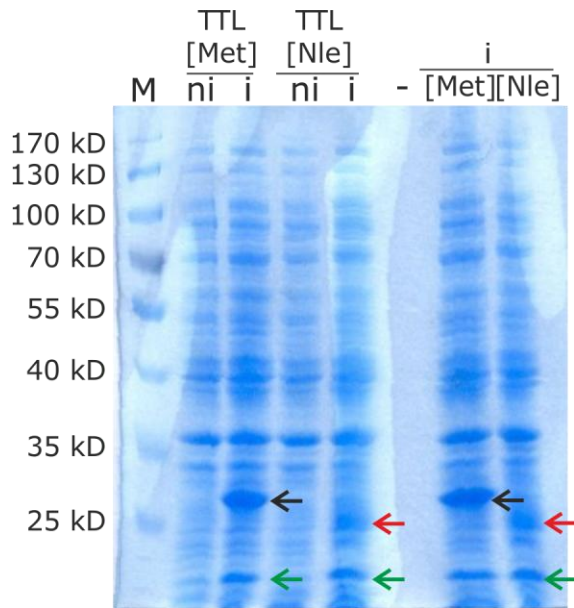


Figure 14 Expression of TTL[Met] and TTL[Nle] in 100 mL cultures

10% SDS polyacrylamide gel; Coomassie blue stain. The size of the relevant molecular weight marker bands is indicated on the left gel margin. M, pre-stained protein ladder mix; ni, non-induced culture; i, induced culture; -, empty lane. In the induced sample an over expression band of TTL[Met] (black arrow) and TTL[Nle] (red arrow) is detectable. In addition, a second smaller unknown protein is present in the induced samples (green arrow).

The TTL variants used for activity measurements and substrate screenings were produced in a bioreactor. The expression and purification is described in section 3.1.3. A photometrical assay with *para*-nitro-phenyl acetate (pNP-acetate) and *para*-nitro-phenyl butyrate (pNP-butyrate) was chosen to detect the successfully expressed active TTL in a bioreactor. Results in Figure 15 indicate that the two protein variants have different activity towards esterase substrates. The non-canonical TTL[Nle] variant is slightly more active.

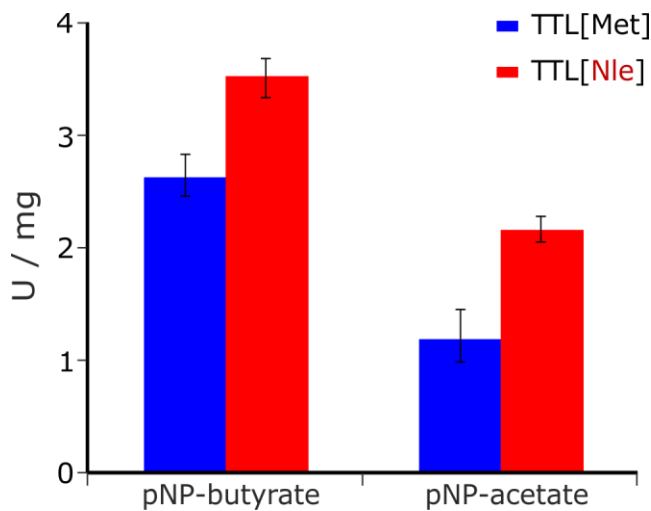


Figure 15 Increased activity of purified synthetic TTL on standard esterase substrates

Division of the value calculated with the formula in Figure 7 by the total amount of protein (in mg) led to the specific activity (U/mg). All values were determined in triplicate. The error bars are indicating the maximal and minimal value.

Substrates relevant for biotechnological use were screened to identify whether there is a general trend of Nle incorporation into the TTL enzyme. Enzymatic degradation of polymers, especially plastics degradation and surface modification, is a growing and important field as described in literature [65]. Although TTL is described as a lipase of a thermophile bacterium the results in Figure 16 show that the enzyme has esterase activity. Thus, we tested the enzyme on polymeric substrates, like polyesters poly-ethylene-terephthalate (PET) and poly-lactic-acid (PLA)). The smaller and therefore soluble degradation products mono(2-hydroxyethyl)terephthalate (MHET), terephthalic acid (TA) and ethylene glycol were monitored. According to previous reports [38] the temperature optimum of TTL[Nle] is 75 °C. However, standard temperature for PET degradation by polyesterases is 50 °C [65]. Both temperatures were tested in our assays. As indicated in Figure 16 TTL shows PET hydrolase activity at 75 °C. An interesting observation was the two-fold increased activity of the Nle variant. The release product obtained in highest concentrations was TA. There was no detectable enzyme activity at 50 °C neither for the TTL[Nle], nor for the parent protein TTL[Met] (data not shown). PLA is not thermo-stable and therefore the degradation was performed at lower temperatures. To overcome the problem of the optimal temperature of the TTL, the enzyme was heat activated ([38]) for 10 minutes at 80 C before degradation of PLA films of defined size (1 mm x 0.5 mm) at 37 °C. Even so no enzyme activity on PLA was measured.

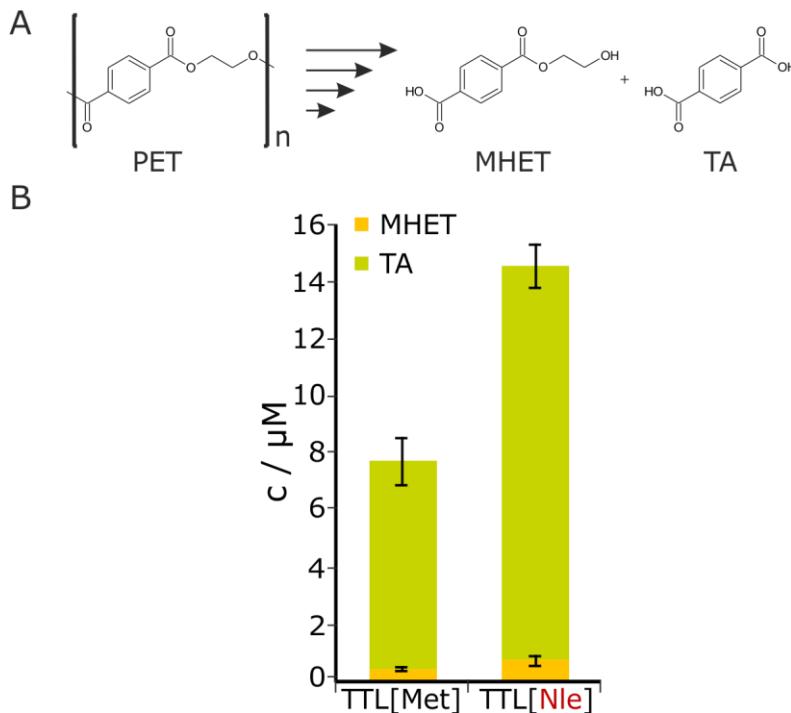


Figure 16 TTL shows PET hydrolyase activity

A: Schematic degradation of poly-ethylene-terephthalate (PET) to the detectable release products mono(2-hydroxyethyl) terephthalate (MHET) and terephthalic acid (TA).

B: Activity of TTL[Nle] variant shows a two times increased activity on PET compared to the parent variant at 75 °C. All values were determined in triplicate. The error bars are indicating the maximal and minimal value.

3.1.2.2. Synthetic cutinases

The cutinases Cut1 and Cut2 from *Thermobifida cellulositytica* (Thc_Cut1 and Thc_Cut2), as well as an esterase from *Thermobifida halotolerans* (Thh_est) are used for poly-ethylene-terephthalate surface modification and degradation [65]. The concept of positive effects of Nle incorporation seen in the case of the TTL should be expanded to other enzymes of the alpha/beta hydrolase family with biotechnological relevance. Minor amount of soluble protein can be expressed with a pET system, but the expression is not optimal (personal communication D. Ribitsch, ACIB Graz). We designed other constructs with different promoters, which were then tested for protein expression. Cloning of the target genes into the chosen expression vectors pQE80L (T5 promoter) and pMS470 (tac promoter) was performed by Gibson assembly. The insert was amplified by PCR and two 50 nucleotide homology regions for two different expression vectors were introduced (shown in Figure 17, B). The PCR reactions yielded the expected fragment of about 890 bp for all 3 cutinases. The vectors were prepared by restriction double digest and purified via a gel extraction kit. Vectors containing an irrelevant insert were used to ensure double digest of restriction enzymes (Figure 17, A).

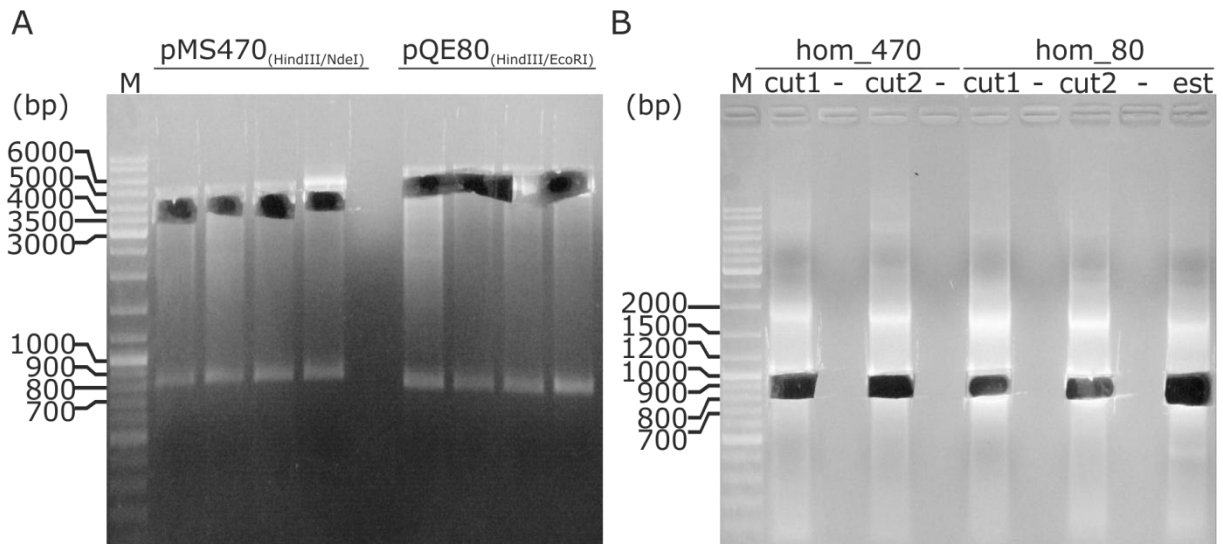


Figure 17 Preparation of inserts and vectors for Gibson Assembly

1 % agarose gel; the size of the relevant molecular weight marker bands is indicated.

A: The double digests of pMS470 and pQE80L with the indicated restriction enzymes yielded the expected size for pMS470 (3900 bp) and pQE80L vector (4652 bp). The fragments were cut for further purification.

B: PCR with the designed primers BpP 241+242 (pMS470, Table 4) and BpP 239+240 (pQE80L, Table 5) yielded the expected fragment for the 3 different cutinases Thc_Cut1, Thc_Cut2 and Thh_Est carrying homology regions for the pMS470 vector (left, hom_470) and pQE80L vector (right, hom_80). The product bands with the expected size of 890 bp were cut for further purification. -, empty lane

Obtained clones were checked by restriction digest and sequence verified [Figure 18; A (pMS470) and B (pQE80L)]. Positive clones could be received for both constructs.

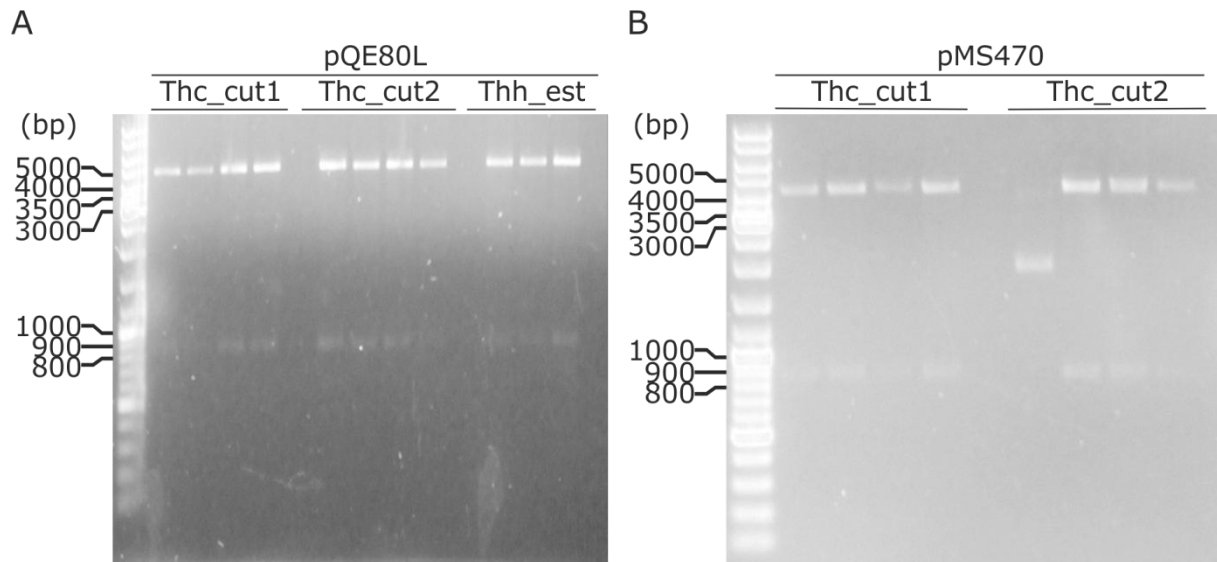


Figure 18 Control restriction of four different clones of each expression construct

1 % agarose gel; the size of the relevant molecular weight marker bands is indicated.

A: The double digest of pQE80L constructs with *EcoRI/HindIII* yielded to the expected fragments of 4652 bp and 838 bp.

B: The constructs cloned into pMS470 were double digested with *NdeI/HindIII* and yielded the expected fragments of 3980 bp and 818 bp for clones 1-4 (Thc_cut1) and clones 2-4 (Thc_cut2).

Promoters for the highest expression of synthetic cutinases were tested in 100 mL LB medium cultures. Induction with 1 mM of IPTG led to the expression of a protein with the size of approximately 30 kD. All other bands are identical for induced (i) and non-induced (ni) culture samples. All three cutinases were successfully expressed as soluble proteins. The expression levels of Thh_Est seemed lower than for Thc_Cut1 and Thc_Cut2. The pMS470 constructs yielded predominantly soluble cutinases (Figure 19). After the expression with pQE80L construct, no soluble cutinase fraction could be detected. Therefore, all further incorporation experiments were done with the pMS470 constructs.

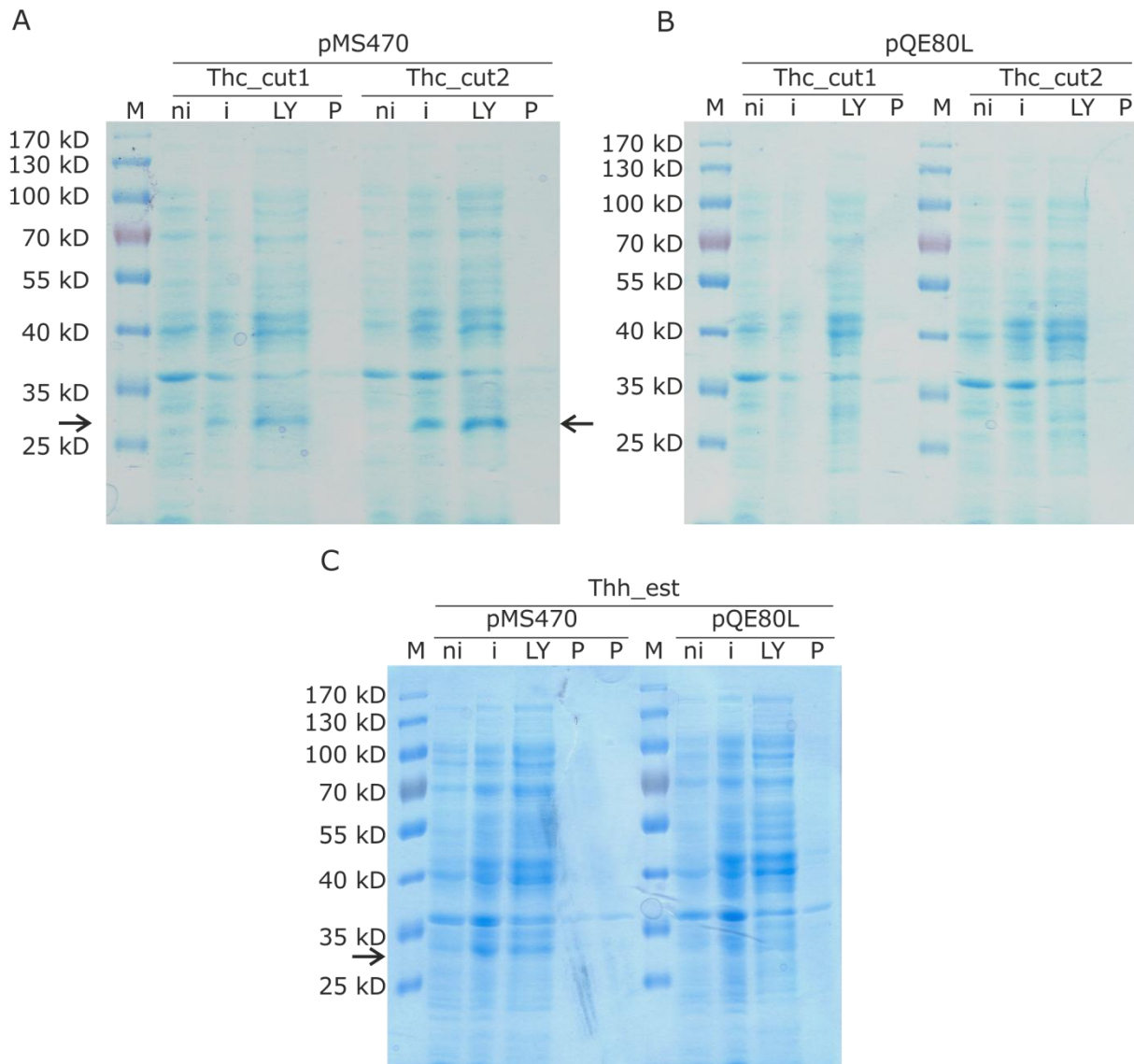


Figure 19 Expression of different cutinases in B834(DE3) (LB medium)

10% SDS polyacrylamide gel; Coomassie blue stain. The size of the relevant molecular weight marker bands is indicated on the left gel margin. The calculated molecular weight of all 3 cutinases is approximately 30 kD. M, pre-stained protein ladder mix; ni, non-induced culture; i, induced culture; LY, cleared lysate with soluble proteins; P, insoluble proteins

A: Expression of Thc_Cut1 and Thc_Cut2 using a pMS470 expression vector leads to soluble protein at the expected size in the induced and lysate samples (indicated by black arrow).

B: Expression of Thc_Cut1 and Thc_Cut2 using a pQE80L expression vector did not lead to any expression of the target proteins at all.

C: The same result was obtained for the third enzyme Thh_Est. Using a pMS470 vector for expression lead to soluble protein in the induced and lysate sample (indicated by black arrow).

The intensive band in the induced samples, as well as in the lysate samples indicate that the expression of soluble Met & Nle variants of all three cutinases was successfully performed in M9 medium (Figure 20, Thc_Cut1 (A[Met] and B[Nle]); Thc_Cut2 (C[Met] and D[Nle]), Thh_Est (E[Met] and F[Nle])). Only low amounts of protein were detected in the pellet, flow through, and in the wash fraction, indicating that the incorporation of Nle into cutinases do

not effect solubility and purification behavior. The reduction in protein yields for the synthetic cutinase variants were comparable to the observations made for the TTL.

The expression level of the third cutinase, Thh_Est, was insufficient and led to almost no protein for Thh_Est[Met], and Thh_Est[Nle] (details see Figure 20). None of the two plasmid constructs led to over-expressed, soluble Thh_Est[Met] or Thh_Est[Nle], the third protein of the cutinase group we examined.

After Ni²⁺-affinity chromatography Thc_Cut1[Met & Nle] and Thc_Cut2[Met & Nle] could be obtained. More than 20 mg/L culture medium of pure protein was produced from the canonical protein variants of the two cutinases. The amount of synthetic variants was almost 50% reduced. (see concentrations in Table 22 and Figure 21).

The incorporation efficiency was determined for all three cutinases by LC-MS analysis (CF Proteomics). The incorporation efficiency is shown in Figure 22. The major mass signal in all three cases corresponds to that of fully labeled proteins, although species with partial exchange of the Met were detectable (Thc_Cut1[Met]: calculated mass (m_{calc}): 29289.70 Da (Table 23); experimental mass (m_{exp}): 29289.75 Da (Table 23 and Figure 22, A); Thc_Cut1[Nle]: m_{calc} : 29236.83 Da (Table 23); m_{exp} : 29235.92 Da [3 Nle], 29253.78 Da [2 Nle] and 29270.71 Da [1 Nle] (Table 23 and Figure 22, B)) (Thc_Cut2[Met]: m_{calc} : 29513.80 Da (Table 23); m_{exp} : 29512.88 Da (Table 23 and Figure 22, C); Thc_Cut2[Nle]: m_{calc} : 29459.93 Da (Table 23); m_{exp} : 29458.98 Da [3 Nle], 29476.87 Da [2 Nle] and 29494.81 Da [1 Nle] (Table 23 and Figure 22, D)) (Thh_Est[Met]: m_{calc} : 29671.44 Da (Table 23); m_{exp} : 29671.54 Da (Table 23 and Figure 22, E); Thh_Est[Nle]: m_{calc} : 29599.61 Da (Table 23); m_{exp} : 29598.65 Da [4 Nle], 29617.60 Da [3 Nle] and 29633.61 Da [2 Nle] (Table 23 and Figure 22, F)). The second highest peaks in the spectra of Thc_Cut1[Met] (Figure 22, A) and Thh_Est (Figure 22, E) could be identified as a TFA (trifluoroacetic acid) adduct of the proteins.

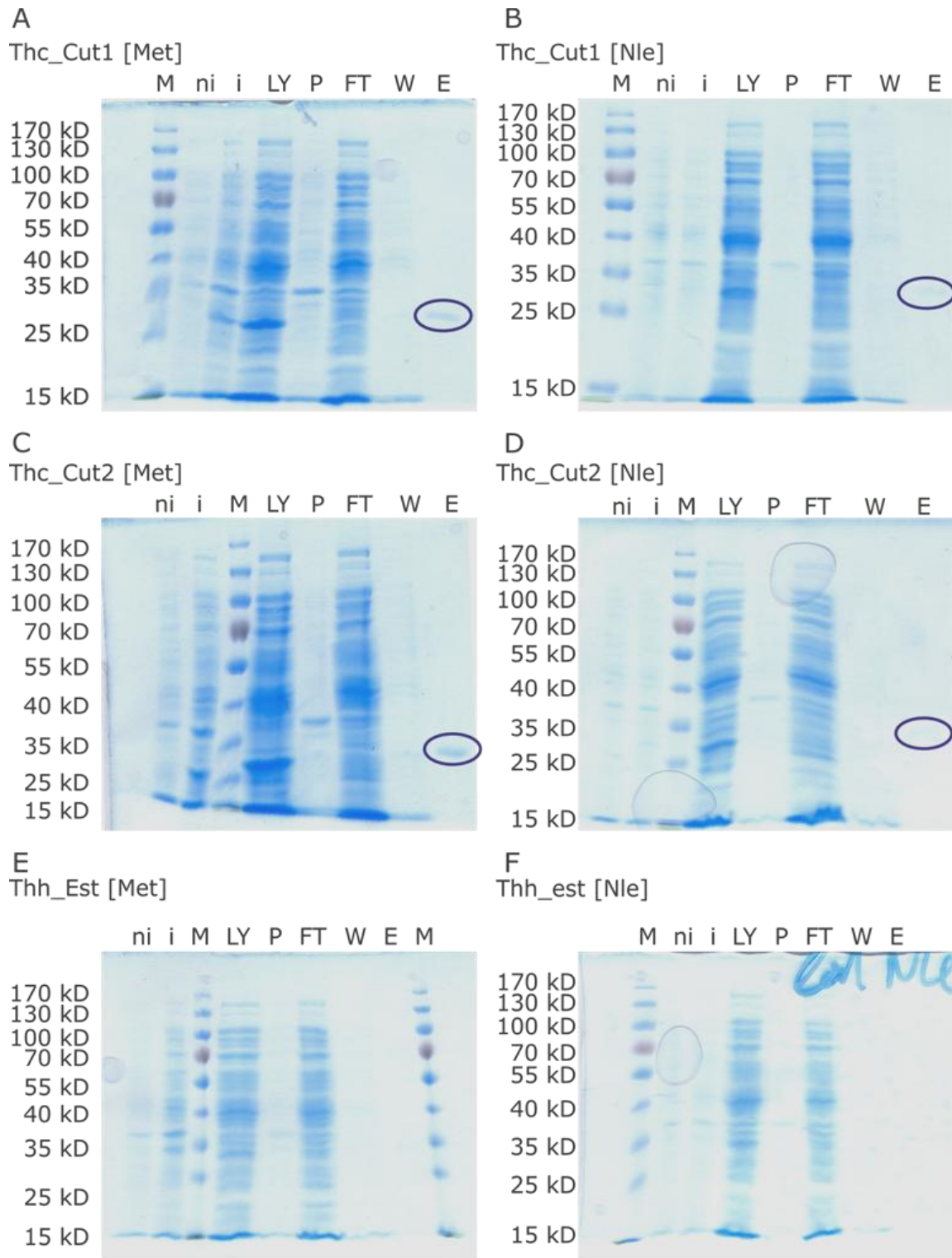


Figure 20 Expression and purification of parent cutinases [Met] and synthetic variants [Nle] 10% SDS polyacrylamide gel; Coomassie blue stain. The size of the relevant molecular weight marker bands is indicated. The calculated molecular weight of all 3 cutinases is approximately 30 kD. M, pre-stained protein ladder mix; ni, non-induced culture; i, induced culture; LY cleared lysate with soluble proteins; P, insoluble proteins; FT, flow through; W, wash; E, eluate.

Purification progress was followed for the indicated cutinases in pictures A-F. Pure cutinases are marked in the eluate fractions (blue circle). No pure protein was obtained for both Thh_Est variants.

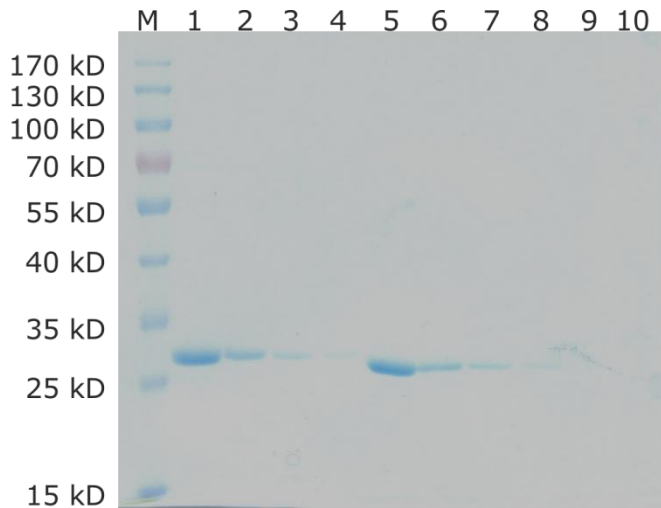


Figure 21 Purified cutinase variants

10% SDS polyacrylamide gel; Coomassie blue stain. The size of the relevant molecular weight marker bands is indicated on the left gel margin. The calculated molecular weight of all 3 cutinases is approximately 30 kD. M, pre-stained protein ladder mix; Lane 1+2, Thc_Cut1 [Met]; Lane 3+4 Thc_Cut1 [Nle]; Lane 5+6, Thc_Cut2 [Met]; Lane 7+8, Thc_Cut2 [Nle]; Lane 9, Thh_Est [Met]; Lane 10, Thh_Est [Nle]

Pure cutinase variants were obtained except of Thh_Est (inadequate amounts, lane 9 and 10).

Table 22 Total amount of pure cutinases produced in 100 mL shake flask cultures

enzyme variant	c [mg]
Thc_Cut1 [Met]	24
Thc_Cut1 [Nle]	12
Thc_Cut2 [Met]	30
Thc_Cut2 [Nle]	14
Thh_Est [Met]	4
Thh_Est [Nle]	4

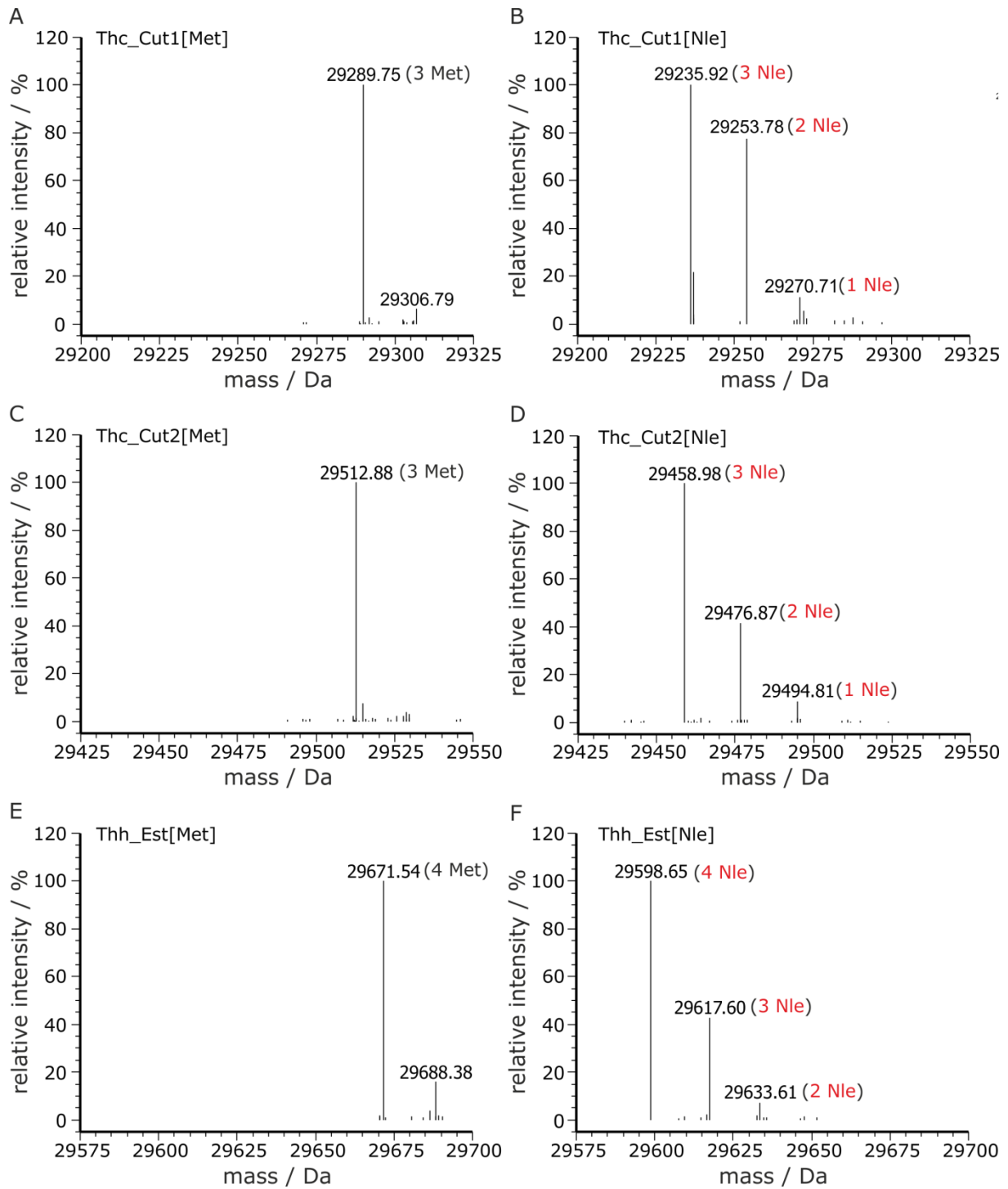


Figure 22 Efficiency of Nle incorporation into cutinase variants

The total mass of intact proteins were determined by ESI-MS. Due to an Ala as the penultimate amino acid, the N-terminal Met was excised. Therefore, accordingly reduced mass values were obtained. The main species are labeled with the experimentally determined mass values and the number of introduced Nle residues is shown in brackets. The MS spectra of following proteins are shown: A (Thc_Cut1[Met]), B (Thc_Cut1[Nle]), C (Thc_Cut2[Met]), D (Thc_Cut2[Nle]), E (Thh_Est[Met]) and F (Thh_Est[Nle]).

Table 23 Mass analysis for incorporation efficiency determination

Mass data were calculated with the MassXpert software [87]. The isotopic mass determination is very accurate ($\Delta m \leq 1$ Da) and the found masses allow to speculate that one disulfide bond is present in the protein. That is the reason why the mass calculations include 1 disulfide bond. Due to an Ala as the penultimate amino acid the N terminal was excised. This fact was taken into account for the mass calculations. n.d., not detectable

Thc_Cut1			
species	mass _{calculated} [Da]	mass _{experimental} [Da]	Δm
-N _{term} Met	29290.70	29289.75	0.95
1 Nle	29272.74	29270.71	2.03
2 Nle	29254.78	29253.58	1.20
3 Nle	29236.83	29235.92	0.91
Thc_Cut2			
species	mass _{calculated}	mass _{experimental}	Δm
-N _{term} Met	29513.80	29512.88	0.92
1 Nle	29495.85	29494.81	1.04
2 Nle	29477.89	29476.87	1.02
3 Nle	29459.93	29458.98	0.95
Thh_Est			
species	mass _{calculated}	mass _{experimental}	Δm
-N _{term} Met	29671.44	29671.54	0.10
1 Nle	29653.48	n.d.	-
2 Nle	29633.52	29633.61	0.09
3 Nle	29617.57	29617.60	0.03
4 Nle	29599.61	29598.65	0.96

Thc_Cut1 and Thc_Cut2 showed activity on pNP-esters indicating that functional proteins were expressed. (data not shown).

Synthetic cutinases of Thc_Cut1 and Thc_Cut2 were also tested for PET degradation activity and compared to the parent proteins. The results in Figure 23 show that the Nle variant of Thc_Cut 1 is less active than the parent, but shows an entirely different pattern of release products. The MHET:TA ratio was shifted from 1:6 in the parent protein to 1:1 in the synthetic variant. In this regard Thc_Cut 1[Nle] displayed a similar behavior as the Thc_Cut 2 parent. Thus, exchange of Met for Nle in Thc_Cut 1 shifts the substrate selectivity towards that of Thc_Cut 2. The synthetic Thc_Cut2 variant showed no PET degradation activity.

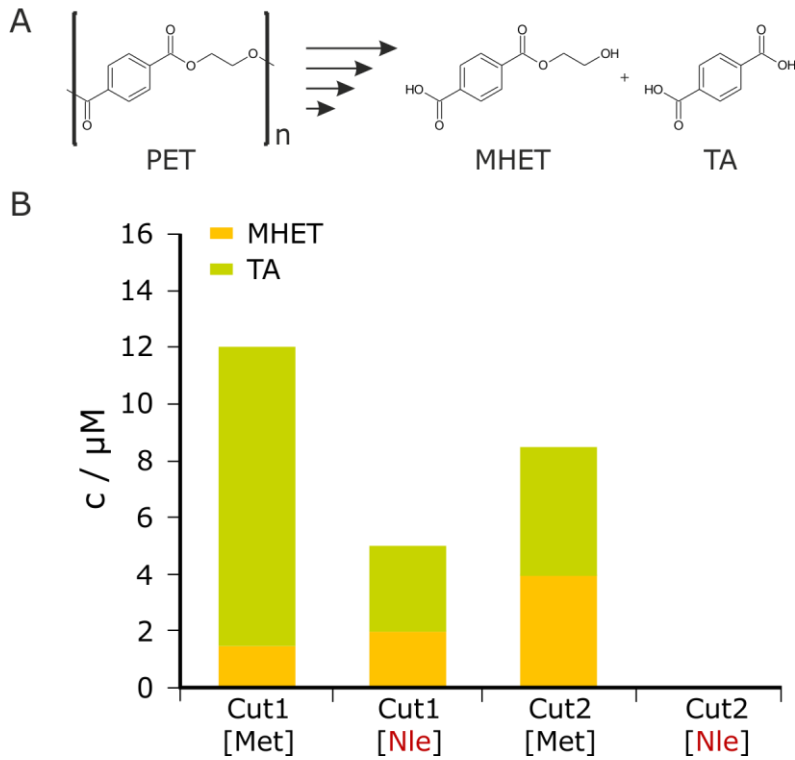


Figure 23 PET degradation by Thc_Cut1 and Thc_Cut2 variants

A: Schematic degradation of poly-ethylene-terephthalate (PET) to the detectable release products mono-(2-hydroxyethyl) terephthalate (MHET) and terephthalic acid (TA) is shown.

B: The detectable release products mono(2-hydroxyethyl) terephthalate (MHET) and terephthalic acid (TA) were detected by HPLC measurements. All values were determined in duplicates and the mean value is shown.

Comparable effects were observed for the degradation of the model substrate 3-PET, where the difference in activity is more obvious between parent and synthetic variant. The pattern of release products is also different for parent and synthetic Thc_Cut1. Only a minor activity of Thc_Cut 2[Nle] was detectable (Figure 24).

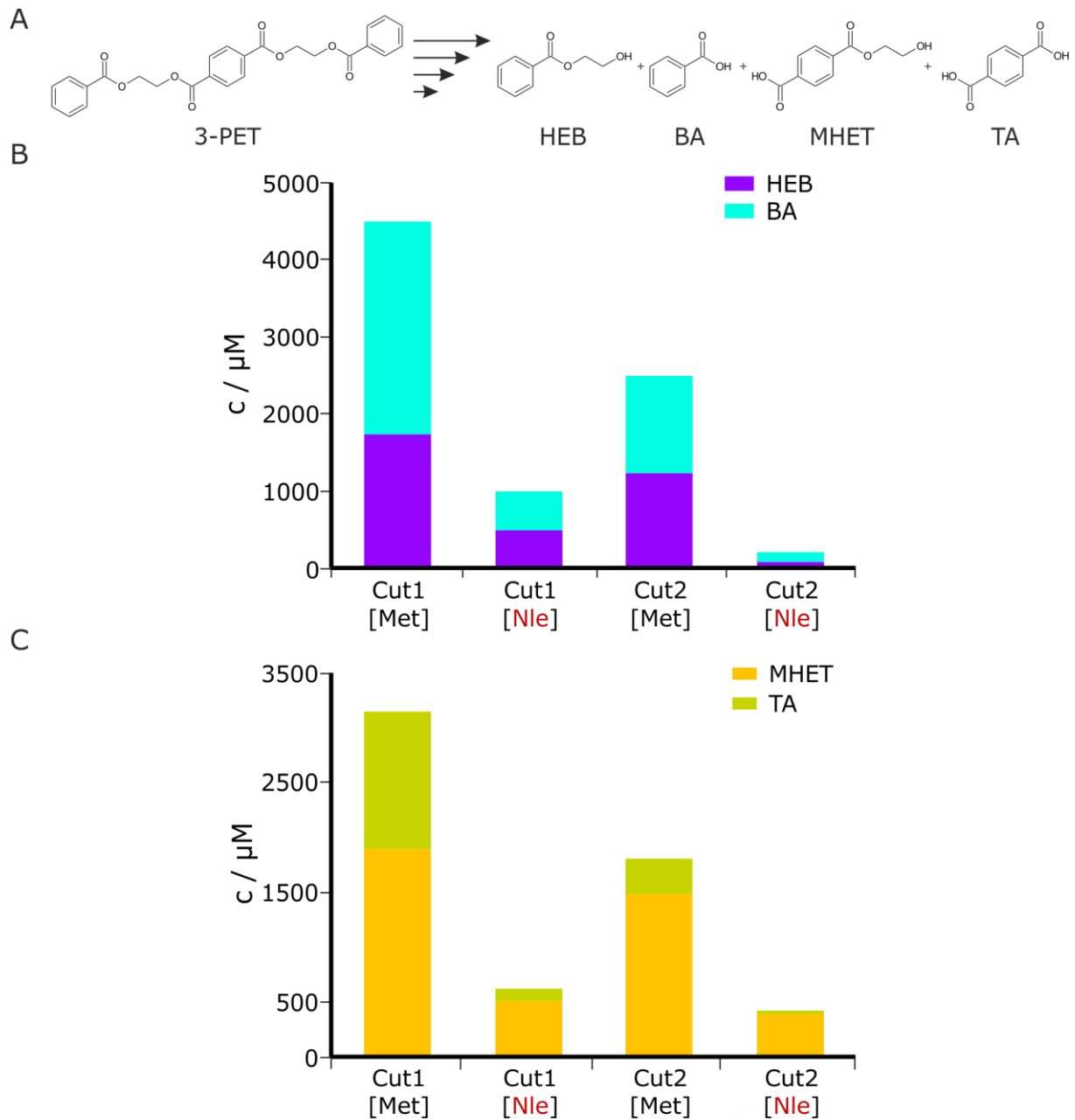


Figure 24 3-PET (model substrate) degradation by Thc_Cut1 and Thc_Cut2 variants

A: Schematic degradation of the model substrate bis(benzoyloxyethyl) terephthalate (3PET) to the detectable release products mono-(2-hydroxyethyl) terephthalate (MHET), terephthalic acid (TA), 2-hydroxyethyl benzoate (HEB) and benzoic acid (BA).

B: HEB, BA.

C: MHET, TA.

All values were determined in duplicates and the mean value is shown.

Figure 25 shows the results of the HRP Western probe of h₆-tagged Thc_Cut 1 on PET films. Because of the intensity of the luminescence signal it can be assumed that Thc_Cut 1[Nle] has a better absorbance affinity to the PET films. Two different concentrations of the parent protein were measured because previous experiments performed by other groups indicated

the weak affinity of the Thc_Cut1[Met] protein to PET films (oral communication D. Ribitsch, Figure 25, C & D).

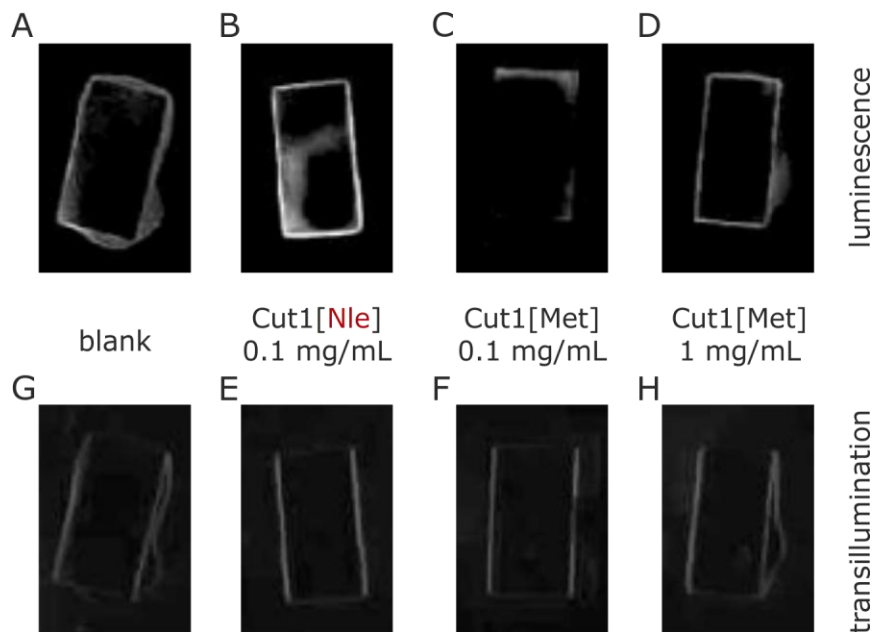


Figure 25 PET adhesion assay of PET films incubated with Thc_Cut1 wild type and [Nle] variant

PET films were incubated with HisProbe HRP working solution. For development the HRP marked PET films were incubated with SuperSignal West Pico Substrate working solution for 5 minutes and the luminescence was detected with a Gbox. The luminescence picture of the PET films incubated with solutions A (50 mM Tris/Cl (pH 7.0), blank); B (100 µg/mL Thc_Cut1[Nle]); C (100 µg/mL Thc_Cut1[Met]); D (1 mg/mL Thc_Cut1[Nle]) are shown. The transmission images of the PET films incubated with solutions: E (50 mM Tris/Cl (pH 7.0), blank); F (100 µg/mL Thc_Cut1[Nle]); G (100 µg/mL Thc_Cut1[Met]); H (1 mg/mL Thc_Cut1[Nle]) are shown.

3.1.3. Production of synthetic proteins in a bioreactor

From the data presented in section 3.1.1 it was clear that the incorporation of ncAA into target proteins can be performed with the newly developed ICDF protocol for SPI in *E. coli*. The next step was to validate the suitability of the protocol for ICDFs in larger scales. A DASGIP bioreactor equipment was chosen to test which cell densities are necessary for sufficient protein expression and incorporation of ncAA into the model enzyme TTL. A ten times up-scaled batch process for a final OD₆₀₀ of 30 was designed. Previous results had shown that it was crucial to increase the amount of cAA and ncAA supplemented for the expression to successfully produce TTL[Met] & TTL[Nle] (data not shown). Based on these results a threshold of 100 mg/g CDM of added Met and Nle was defined. This corresponds to ~0.5-1 mM /g CDM depending on the molecular mass of the amino acid. Growth behavior in the DASGIP bioreactors was reproducible. Growth arrest after 600 min indicated Met

depletion after reaching the expected OD_{600} of about 25-30 (Figure 26). After supplementation with Met the strain restarted growth, but also the strain supplemented with Nle started growing again. That was unexpected for the bioreactors supplemented with Nle, because in theory the strain should not be able to grow on the ncAA. However, the total increase in biomass is about 20% lower in the Nle supplemented bioreactor (Figure 29). The CDM behaved similarly (Figure 27). A linear correlation was observed between OD_{600} and CDM (Figure 28).

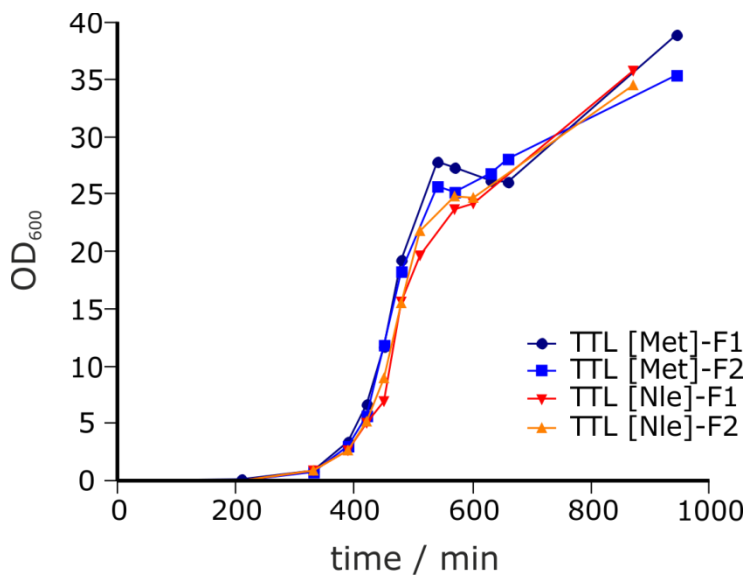


Figure 26 Growth curves OD_{600} vs. time of B834(DE3) during the bioreactor process

Both variants showed comparable growth behavior in two separate bioreactors. The expected OD_{600} of 30 was reached.

All values were determined in triplicates. The error bars are very close to the average data point and, therefore, are omitted for clarity.

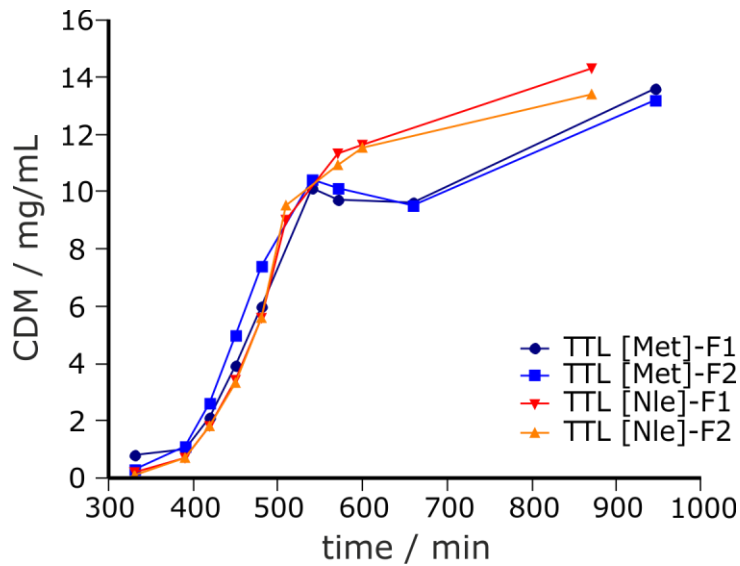


Figure 27 Growth curves CDM vs. time of B834(DE3) during the bioreactor process

For the cell dry mass comparable results to the OD_{600} was obtained.

All values were determined in triplicates. The error bars are very close to the average data point and, therefore, are omitted for clarity.

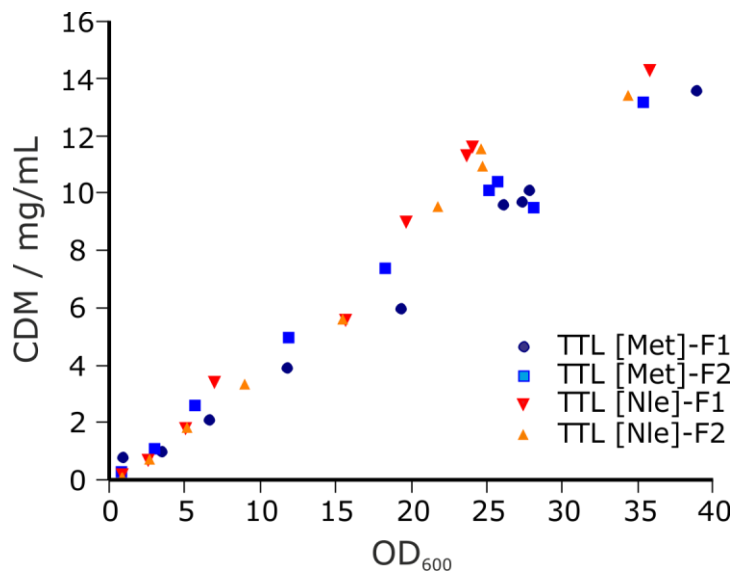


Figure 28 Linear correlation of OD_{600} and CDM over whole bioreactor process for both variants.

The error bars are very close to the average data point and, therefore, are omitted for clarity.

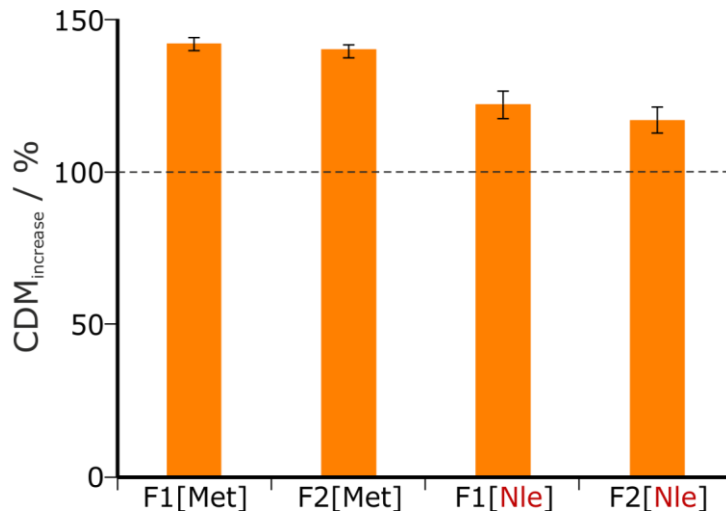


Figure 29 CDM after induction and amino acid supplementation

CDM before induction was set as 100 % (dashed black line) and the increase after induction and amino acid supplementation is shown relative to the non-induced value. All values were determined in triplicate. The error bars indicate the determined maximum and minimum values.

The significant visible over-expression band in all induced culture samples confirmed successful TTL expression in the presence of Met (parent, A), as well as in the presence of Nle (synthetic protein, B) in the bioreactor. A comparison of the band intensities in Figure 30 implies that the expression in the shake flask (A, lane Met; B, lane Met and lane Nle) yielded higher protein amounts than that in the bioreactor (A, lane I (F1+F2); B, lane I (F1+F2)). The reduced yield in synthetic protein (Figure 30, B, lane i) compared to parent (Figure 30, A, lane i) is comparable to previous shake flask results (Figure 14, lanes i[Met] and i[Nle]).

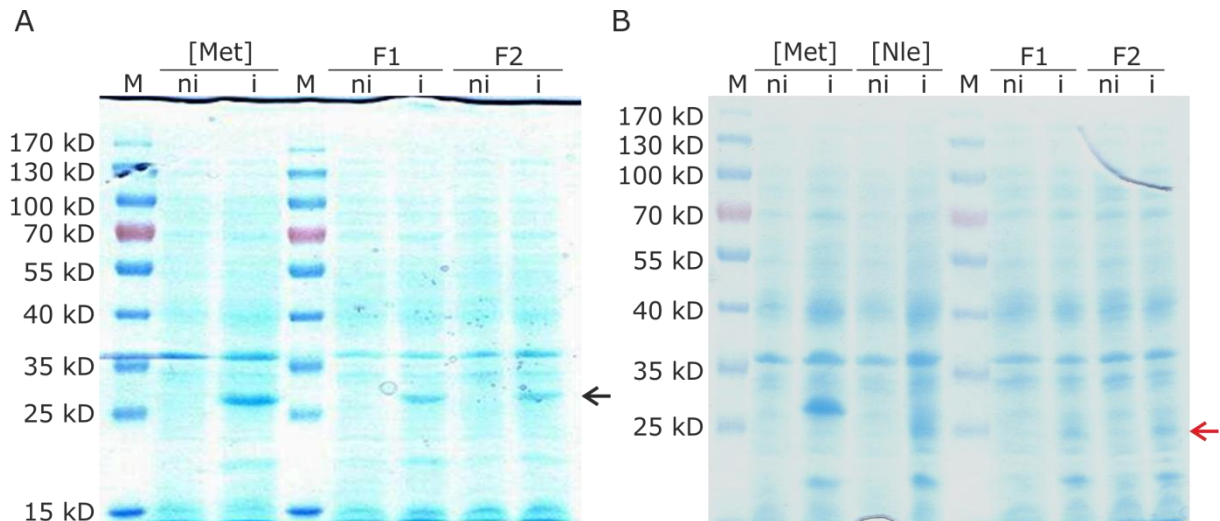


Figure 30 Expression of TTL variants in B834(DE3) in a DASGIP bioreactor system

10% SDS polyacrylamide gel; Coomassie blue stain. The size of the relevant molecular weight marker bands is indicated. The amount of loaded sample corresponds to 1 OD₆₀₀. M, pre-stained protein ladder mix; ni, non-induced culture; i, induced culture, Met (ni+i) and Nle (ni) as positive controls (out of 100 mL shake flasks see Figure 14); F1, F2, two independent cultures.

A: Cultures F1 and F2 were supplemented with Met to produce the parent protein (30 kD, black arrow).

B: Cultures F1 and F2 were supplemented with Nle to produce the synthetic variant (25 kD, red arrow).

The introduced N-terminal h₆-tag was used to purify the proteins by Ni²⁺-affinity chromatography. The elution profiles are shown in Figure 31 for the parent (A), as well as the synthetic protein (B). A stepwise increase of imidazole concentration led to 3 different elution fractions. SDS-PAGE analysis of the 3 peaks revealed that the collected fractions differed in purity. The bulk fraction (peak at 185 mM imidazole, see Figure 31) was highly pure (Figure 33) and was used for all further activity tests described in section 3.1.2.1. The purest fraction of protein was eluted with 500 mM imidazol. This fraction was further used for the determination of the Nle incorporation efficiency by LC-MS.

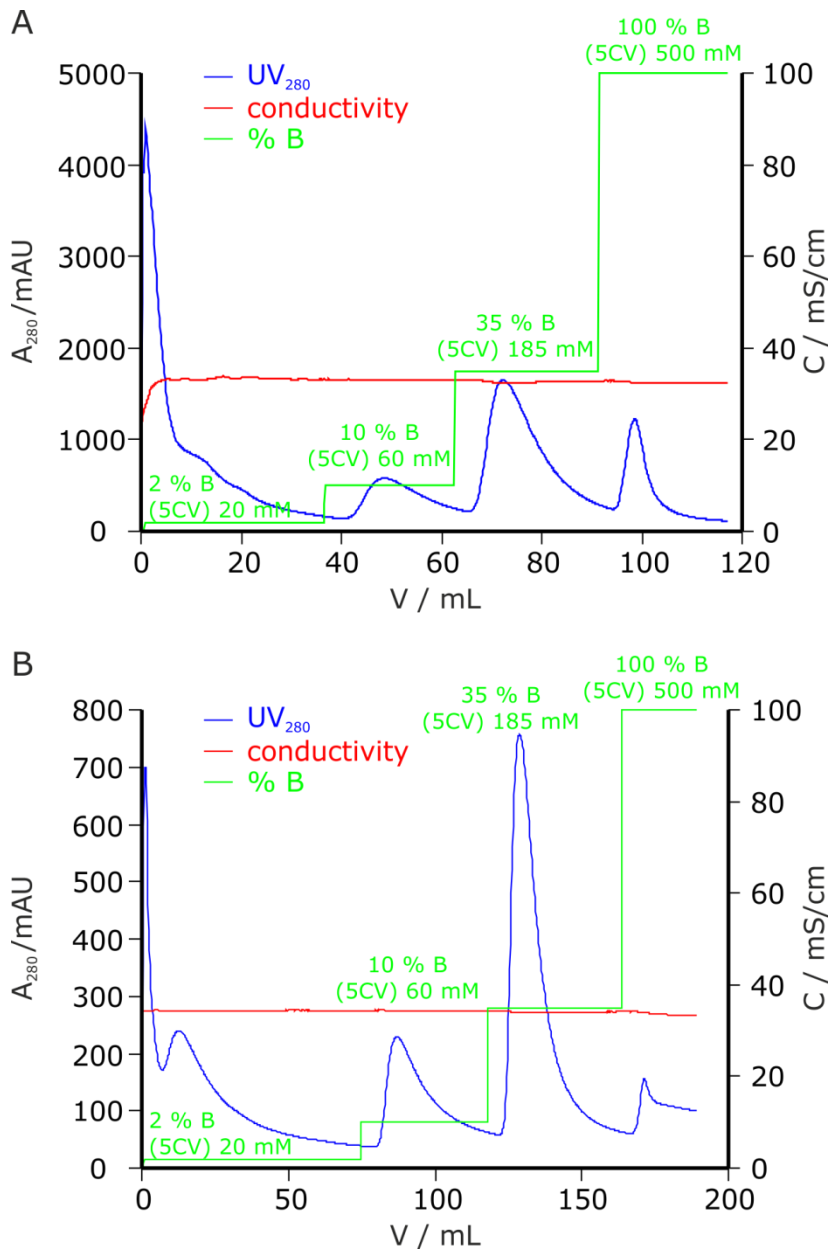


Figure 31 Purification of TTL variants on an ÄKTA purifier system

Buffer A: 50 mM NaPi, 300 mM NaCl, 10 mM imidazole. Buffer B: 50 mM NaPi, 300 mM NaCl, 500 mM imidazole. Column: HisTrap 5 mL; flow load: 2 mL/min, flow: 4 mL/min; A₂₈₀ = UV absorption at 280 nm (blue); C = conductivity (red); %B = amount of buffer B (green).

The fractions corresponding to the 3 peaks were pooled to yield 3 elution fractions with different purity.

A: TTL [Met]

B: TTL [Nle]

The purification was successful for both enzymes (Figure 32). TTL[Met] was predominantly found in the cleared lysate (Figure 32, A, lane LY), indicating soluble protein expression. The same observation was made with the synthetic variant (Figure 32, B, lane LY). Almost no parent protein was detectable in the pellet (Figure 32, A, lanes P1, P2), flow through (lane FT) or wash (lane w) fraction leading to high amounts of pure protein (lane E). This was slightly different in the case of the synthetic variant. Intensive bands running slightly below

the TTL[Nle] in the eluate (Figure 32, B, lanes FT and W) indicate that a considerable amount of the protein is insoluble. This suggests that there is a difference in purification behavior between parent and synthetic protein. The smear above the main band in the eluate fraction of TTL[Nle] may indicate partially labeled protein species (Figure 32, B, lane E).

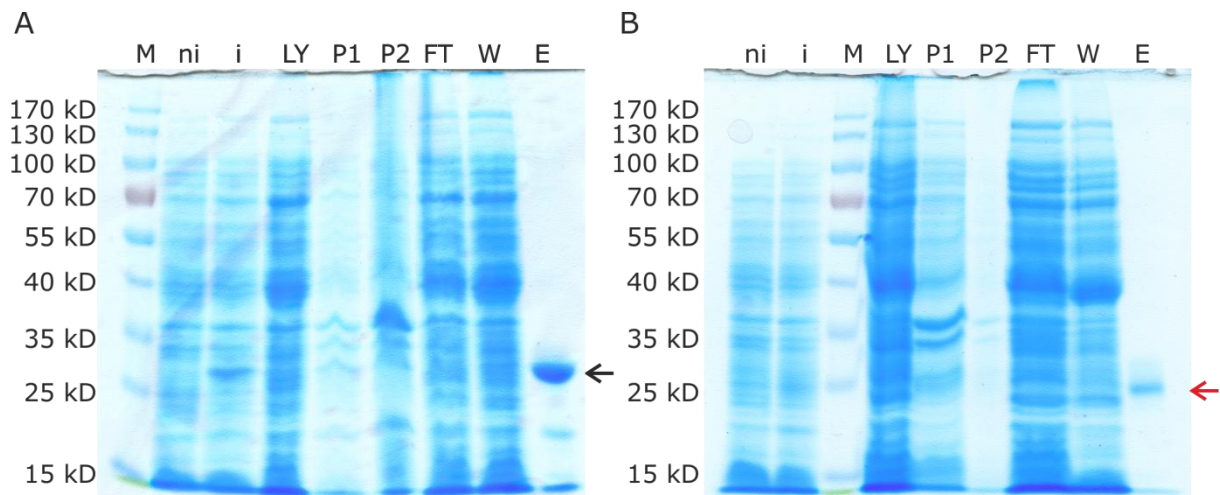


Figure 32 Purification of TTL [Met] and TTL [Nle] by Ni-affinity chromatography

10% SDS polyacrylamide gel; Coomassie blue stain. The size of the relevant molecular weight marker bands is indicated. M, pre-stained protein ladder mix; ni, non-induced culture; i, induced culture; LY cleared lysate with soluble proteins; P1, insoluble proteins (supernatant dissolved in 2 % SDS); P2, insoluble proteins (residue dissolved in SDS loading buffer); FT, flow through; W, wash; E, eluate.

A: Purification of parent protein performed on an ÄKTA purifier system (see Figure 31 A). The black arrow indicates the expected size of TTL[Met].

B: Purification of synthetic variant performed on an ÄKTA purifier system (Figure 31 B). The red arrow indicates the expected size of TTL[Nle].

Figure 33 shows the protein of the bulk elution fraction (peak at 185 mM imidazole, Figure 31) indicating that pure TTL[Met], as well as TTL[Nle] were obtained. In the TTL[Met] preparation, a second smaller band is visible (~18 kD) which is suspected to be a degradation product (see supporting information of [38]). The determination of the protein concentrations (Table 24) confirmed that the expression of the synthetic variant was less effective than that of the parent protein. The total amount of produced TTL[Met] protein was five-times higher (100 mg) than the concentration of TTL[Nle] (25 mg).

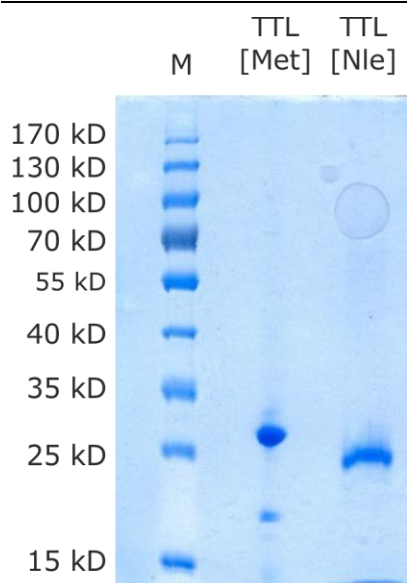


Figure 33 Purified TTL variant

10% SDS polyacrylamide gel; Coomassie blue stain. The size of the relevant molecular weight marker bands is indicated on the left. M, protein ladder; Lane 1, TTL (Met); Lane 2, TTL (Nle). The samples shown were taken from the bulk fraction (peak at 185 mM imidazole in Figure 31).

Table 24 Total amount of purified TTL variants

3 fractions with different purity after ÄKTA purification (see Figure 31).

variant	c [mg/mL]	v [mL]	m [mg]	m_{total} [mg]
TTL Met_1	1.44	15	22	100
TTL-Met_2	1.9	30	57	
TTL-Met_3	1.19	15	18	
TTL-Nle_1	0.11	17.5	2	25
TTL-Nle_2	0.54	35	19	
TTL-Nle_3	0.12	25	3	

The LC-MS results for incorporation efficiency determination of Nle into TTL indicate that fully labeled TTL[Nle] was produced in the bioreactor. The main species found for TTL[Nle] corresponds to fully labeled protein with all 11 Met residues exchanged (TTL[Met]: m_{calc} : 30111.32 Da of the (Table 25), m_{exp} : 30111.43 Da (Table 25 and Figure 34, A)) (TTL[Nle]: m_{calc} : 29913.80 Da (Table 25); m_{exp} : 29913.88 Da [11 Nle], 29931.75 Da [10 Nle] (Table 25 and Figure 34, B)). The other detectable peaks in the spectra could be identified as TFA adducts.

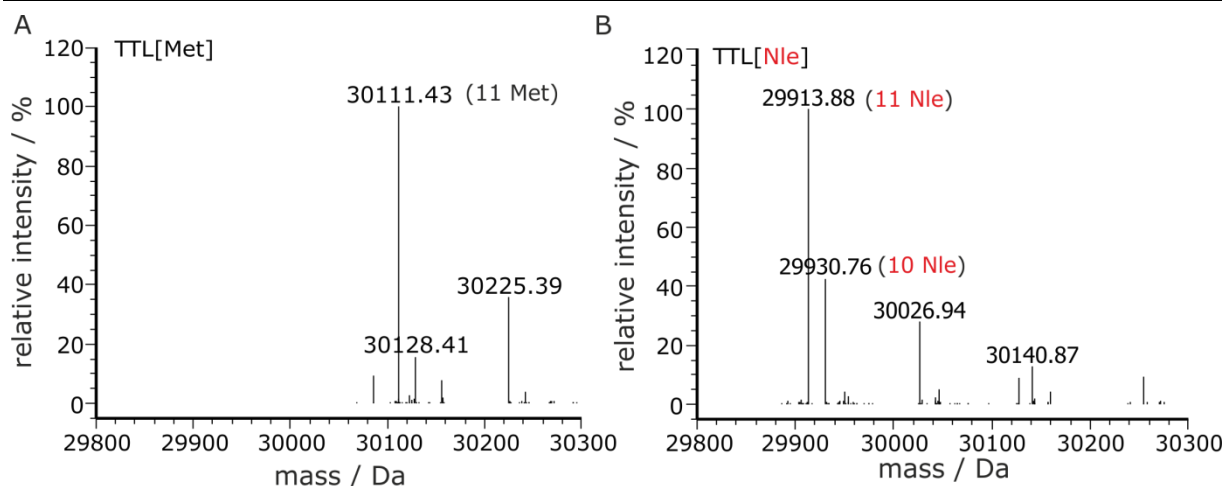


Figure 34 Efficiency of Nle incorporation into TTL

The total mass of intact proteins was determined by ESI-MS. The main species are labeled with the experimentally determined mass. The number of Met or Nle residues is shown in brackets.

A: Monoisotopic MS-spectrum of the parent TTL.

B: Monoisotopic MS-spectrum of TTL[Nle].

Table 25 Mass analysis for incorporation efficiency determination

Masses were calculated with MassXpert. n.d., not detectable

TTL			
species	mass _{calculated} [Da]	mass _{experimental} [Da]	Δm
11 Met	30111.32	30111.43	0.11
1 Nle	30093.36	n.d.	-
2 Nle	30075.40	n.d.	-
3 Nle	30057.45	n.d.	-
4 Nle	30039.49	n.d.	-
5 Nle	30021.53	n.d.	-
6 Nle	30003.58	n.d.	-
7 Nle	29985.62	n.d.	-
8 Nle	29967.66	n.d.	-
9 Nle	29949.71	n.d.	-
10 Nle	29931.75	29930.76	0.99
11 Nle	29913.80	29913.88	0.08

From the data of the first production of the TTL variants in the bioreactor, it was not totally clear whether an insufficient expression or loss during purification was responsible for the low amounts of purified TTL[Met] and TTL[Nle]. In a second bioreactor process under the same conditions, protein expression was monitored in more detail by SDS-PAGE. Both variants showed comparable growth behavior to the first bioreactor experiment (see Figure 26). The expected OD₆₀₀ of 25-30 was reached. After induction and Met or Nle supplementation the OD₆₀₀ increased for both bioreactors, comparably to the previous

experiment (Figure 35). The same observations were made for the CDM and the linear correlation between OD_{600} and CDM (Figure 36 and Figure 37). These results indicate that the process performed in a bioreactor was reproducible.

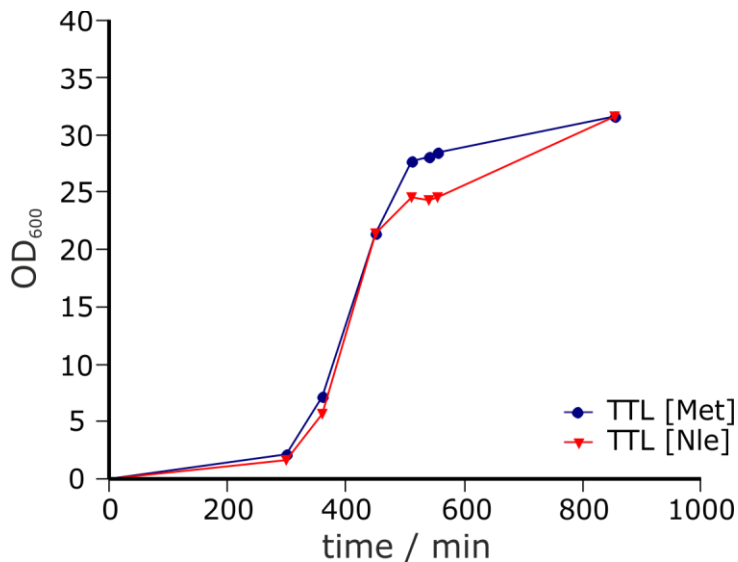


Figure 35 Growth curves OD_{600} vs. time of B834(DE3) during the bioreactor process

Both variants showed comparable growth behavior to the first bioreactor experiment (see Figure 26). The expected OD_{600} of 30 was reached.

All values were determined in triplicates. The error bars are very close to the average data point and, therefore, are omitted for clarity.

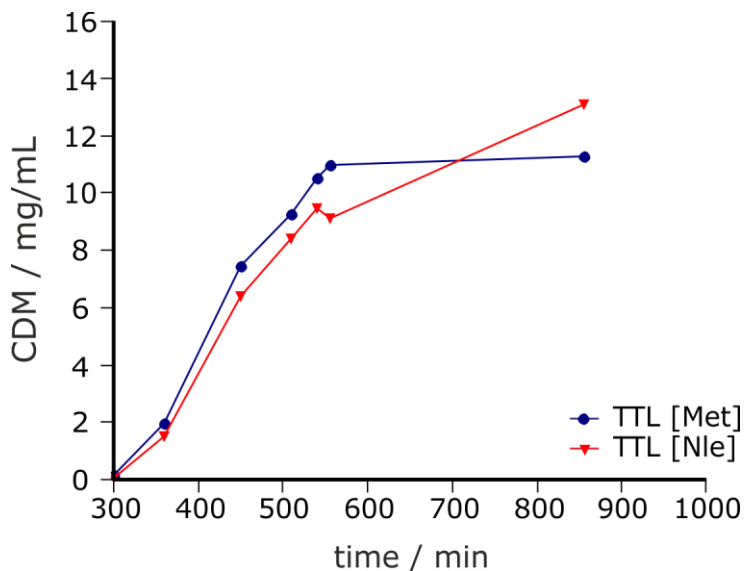


Figure 36 Growth curves CDM vs. time of B834(DE3) during the bioreactor process

For the cell dry mass comparable results to the OD_{600} was obtained.

All values were determined in triplicates. The error bars are very close to the average data point and, therefore, are omitted for clarity.

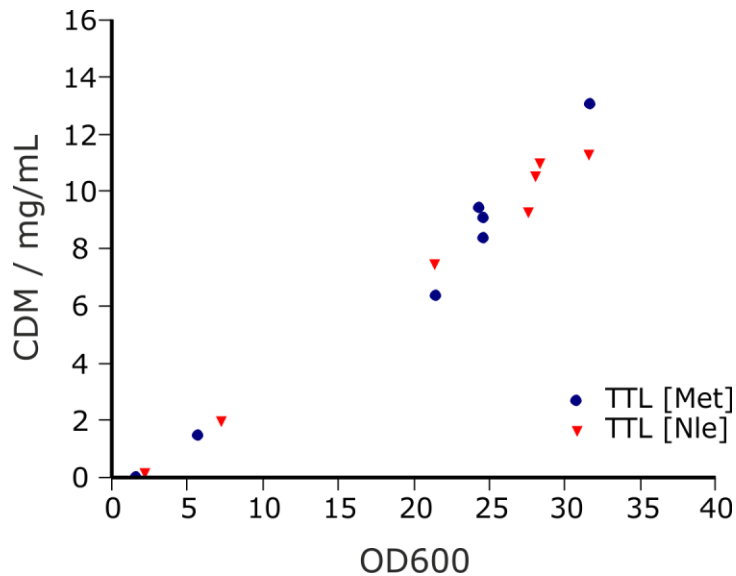


Figure 37 Linear correlation of OD₆₀₀ and CDM over the whole bioreactor process for both variants.

The error bars are very close to the average data point and, therefore, are omitted for clarity.

Compared to the positive controls (Figure 38, [Met]⁺ & [Nle]⁺) the induction of IPTG led to the expression of TTL[Met] with the expected apparent size of about 30 kD (Figure 38, black arrow), as well as TTL[Nle] with the expected apparent size of 25 kD (Figure 38, red arrow). The total amount of protein significantly increased over the first 3 hours. The comparison of the band intensities (Figure 38, lanes 1 implies that the expression in the shake flask (Figure 38, A, lane Met⁺; B, lane Nle⁺) still yielded higher amounts of protein, but in case of the parent protein the yields were higher than in the previous experiment. The reduced yield in synthetic protein compared to parent was comparable to the previous bioreactor experiment.

Apparently, the amount of TTL[Nle] isolated from the bioreactor had not proportionately increased in comparison to the shake flask approach. The amount of total protein loaded onto the gels in Figure 38 A (TTL[Met] and B(TTL[Nle])) (lanes 1 h-4 h (bioreactor), lanes +[Met] and +[Nle] (shake flask)) was normalized to 1 OD₆₀₀. A more pronounced TTL[Nle] band was visible in the shake flask culture in comparison to the bioreactor experiment. Still, it is reasonable to estimate that a higher amount of TTL[Nle] had been produced in the bioreactor than in the shake flask culture due to the 10 times higher cell density in the first. However, this issue needs further analysis by the relative quantification of the TTL[Nle] protein in cell extracts, e.g., by immunoblotting.

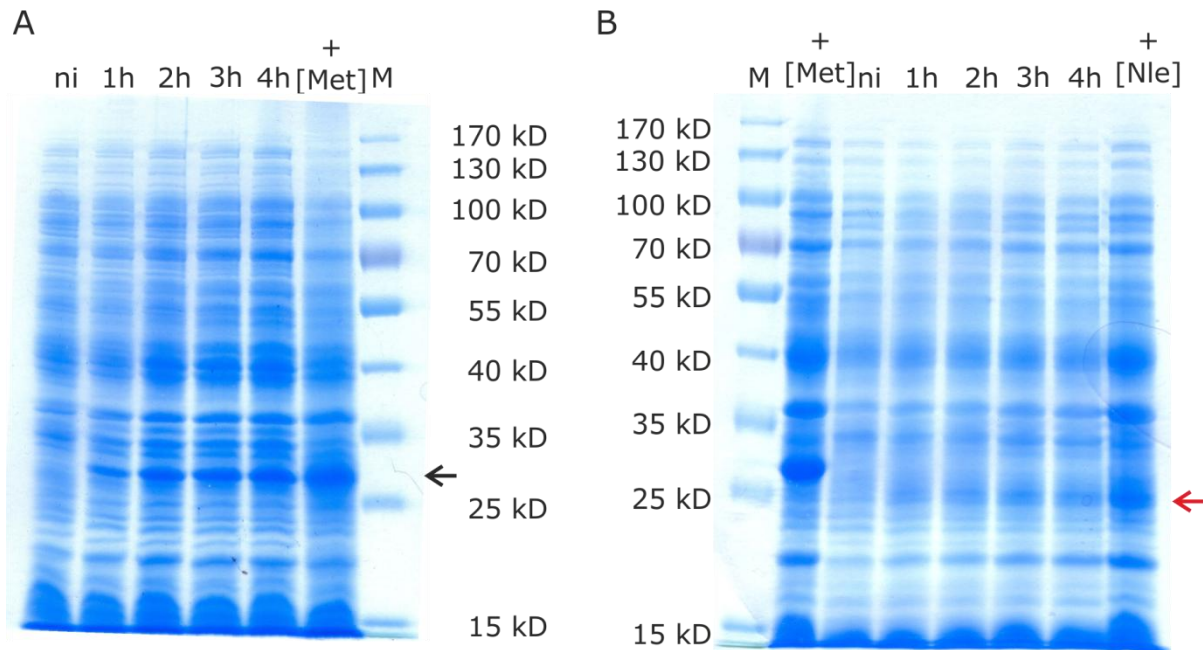


Figure 38 Expression study of TTL [Met] and TTL [Nle] in a DASGIP bioreactor system

10% SDS polyacrylamide gel; Coomassie blue stain. The amount of loaded sample corresponds to 1 OD₆₀₀. The size of the relevant molecular weight marker bands is indicated. M, pre-stained protein ladder mix; ni, non-induced culture, 1h, 2h, 3h, 4h (induced samples after time points), +, positive controls for TTL[Met] and TTL[Nle].

A: TTL[Met], apparent size 30 kD (black arrow)

B: TTL[Nle], apparent size 25 kD (black arrow)

3.2. Norleucine biosynthesis

It has been reported that *als* deficient *E. coli* strains can force the production of the two side products Nva and Nle of branched chain amino acid biosynthesis [31]. Based on that, a bioreactor process for Nle production by a metabolically engineered *E. coli* strain was developed. The aim was to determine if the genetically modified *als*- strain BWEC10 is able to produce Nle. The process was different than previous bioreactor experiments. The medium was based on that described by Sycheva and co-workers [31]. The cultivation in the bioreactor was performed without yeast extract, but an excess of glucose near the threshold of growth inhibition [66] was used. Controlling the concentration of dissolved oxygen by the stirrer velocity should drive the process into oxygen limitation. Leucine and isoleucine were added in limiting concentrations leading to a growth stop at OD₆₀₀ 3 because, as indicated in the above mentioned paper, Nva and Nle are mainly produced in resting cells. The growth behavior of BWEC10 with respect to OD₆₀₀ to a final value of 3 was as expected (Figure 39, A). The same behavior was observed with respect to CDM (Figure 39, B). The growth rate was lower compared to our previous experiments performed in a bioreactor

with yeast extract. During the starvation phase, OD₆₀₀ and CDM remained almost constant over 3 days.

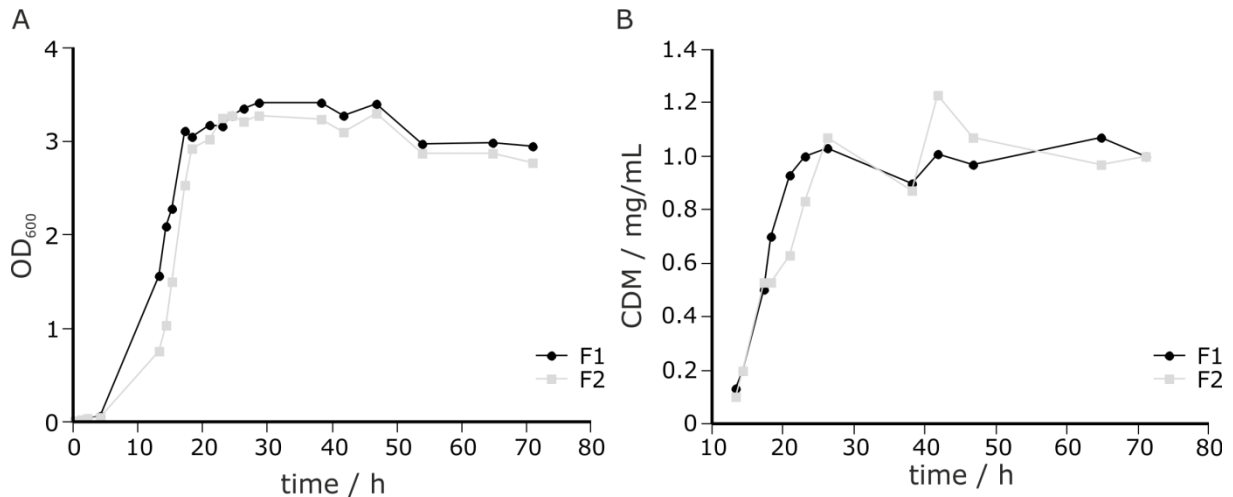


Figure 39 Growth behavior of BWEC10 in a bioreactor process for Nle biosynthesis

The process was performed under excess glucose conditions to facilitate Nle production. Two bioreactor processes were run in parallel. BWEC10 is a *als-* knockout in the BL21(DE3) strain background.

A: Growth curves OD₆₀₀ vs. time

B: Growth curves CDM vs. time

All values were determined in triplicates. The error bars are very close to the average data point and, therefore, are omitted for clarity.

Monitoring the concentration of branched chain amino acids (Val, Leu, Ile; Nle, and Nva) in complex samples, e.g. growth media supernatants, represents a challenge. Thin-layer chromatography was tested first for this task. In the thin layer chromatogram presented below (Figure 40) an increasing band with the same migration behavior as the Nle standard could be detected over time. Two other prominent bands were visible indicating other unknown amino acids or secondary metabolite amines in the culture supernatant. The results gave a first hint that a chromatographic method could be suitable for confirming the production of Nva and Nle with the metabolically engineered strain.

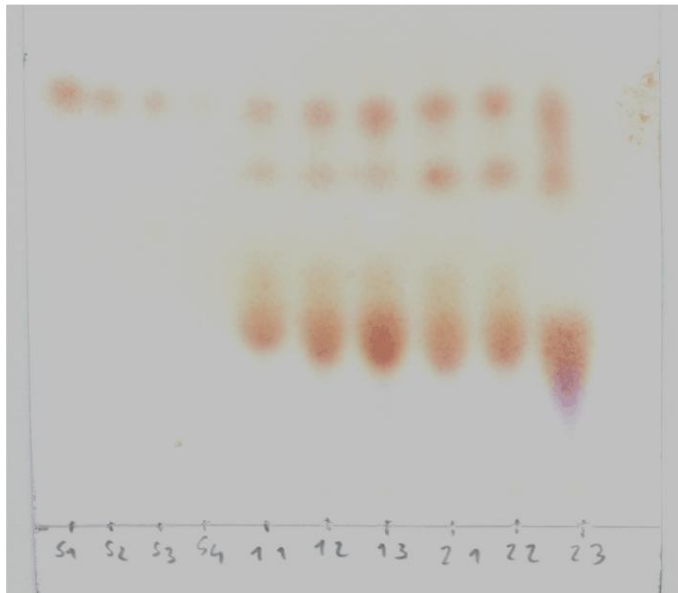


Figure 40 Thin layer chromatography of culture supernatants

Standard concentrations of Nle: S1, 0.5 g/L; S2, 0.25 g/L; S3, 0.125 g/L; S4, 0.0625 g/L

Supernatant samples: 1.1(F1, after 38 h); 1.2 (F1, after 46 h); 1.3 (F1, 66 h); 2.1 (F2, after 38 h); 2.2 (F2, after 46 h) and 2.3 (F2, after 66 h)

Nle standards dissolved in acidic EtOH, mobile phase n-butanol:H₂O:CH₃COOH = 3:1:1, ninhydrine detection was used to stain amino acids (primary amines). F1, bioreactor 1; F2, bioreactor 2

Based on the data obtained from thin layer chromatography, an HPLC method for branched chain amino acid (Leu, Ile, Nle, Nva, Val) analysis was developed. The amino acids in culture supernatants were derivatized for HPLC analysis. The separation procedure was validated using a calibration solution of the branched chain amino acids (Figure 41). The production of Nle and Nva could be confirmed by overlaying the chromatogram of the culture supernatant with the chromatogram of the amino acid standards (Figure 42). These results indicate that the metabolically engineered strain produced elevated amounts of Nva and Nle.

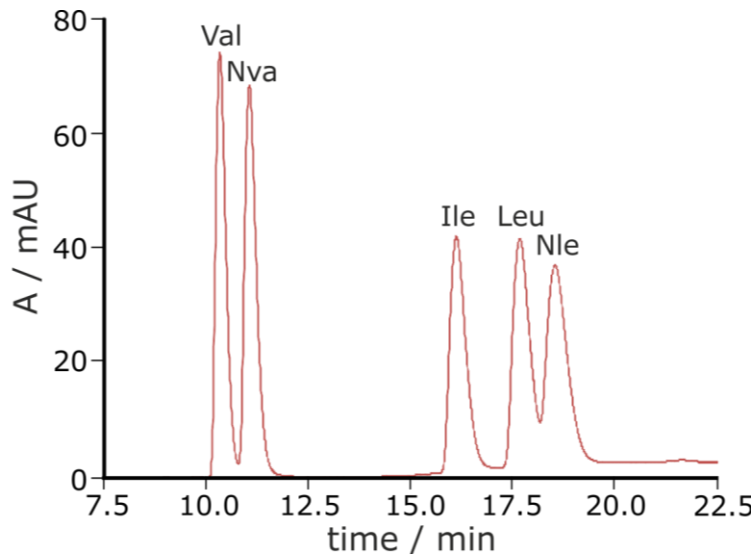


Figure 41 Branched chain amino acid analysis by HPLC UV

Chromatogram of a standard solution containing valine (L-Val), norvaline (L-Nva), isoleucine (L-Ile), leucine (L-Leu), norleucine (L-Nle) 5 mg/mL each diluted 1:50 with 0.1 M $\text{Na}_2\text{B}_4\text{O}_7$ buffer (pH 10.5). The UV trace at 338 nm is shown.

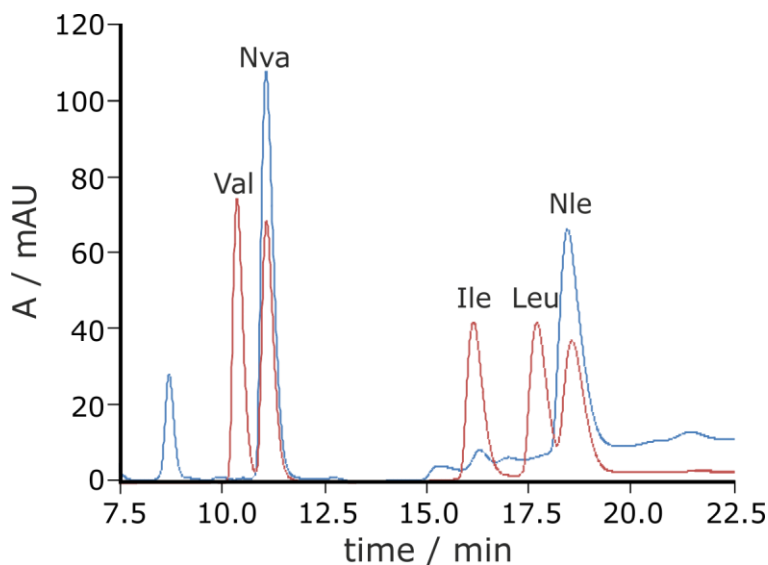


Figure 42 Culture supernatant analysis by HPLC UV

Chromatogram of supernatant diluted 1:5 with 0.1 M $\text{Na}_2\text{B}_4\text{O}_7$ buffer (pH 10.5) overlaid with a chromatogram of a standard solution containing valine (L-Val), norvaline (L-Nva), isoleucine (L-Ile), leucine (L-Leu), norleucine (L-Nle) 5 mg/mL each diluted 1:50 with 0.1 M $\text{Na}_2\text{B}_4\text{O}_7$ buffer (pH 10.5). The UV trace at 338 nm is shown.

3.3. Synthetic protein production by incorporation of biosynthesized Nle

Our previous results had shown that the ncAA Nle can be produced by a metabolically engineered *E. coli* strain. We had also proved that the incorporation of externally

supplemented Nle into target proteins can be performed in a bioreactor. Consequently, we aimed at combining the two approaches and intended to produce synthetic protein with biosynthesized Nle. Strain BWEC14 carries the gene knockouts $\Delta ilvBN::0$, $\Delta ilvIH::0$ and $\Delta ilvGM::0$ in a Met auxotrophic B834(DE3) background. To boost Nle production, the feedback-insensitive leucine operon *leuA*BCD* (pLeu*) was over-expressed. Due to the *als* knock out, BWEC14 is auxotrophic not only for met but also for Ile, Leu and Val. These auxotrophies must be appropriately supplemented, for which we used YE.

Three different experiments based on two different strategies were performed (details see in Figure 27). The canonical, branched chain amino acids Ile, Leu and Val, as well as the non-canonical ones Nle and Nva were analyzed by HPLC-UV. The expressed TTL was purified and the incorporation efficiency was determined by LC-MS.

Table 26 Strategies for incorporation of biosynthesized Nle

experiment	strain	plasmid	growth	abbreviation
growing cells	BWEC14{pTTL + pLeu*}	pQE80L-TTL-h ₆ + pLeuA*BCD	+	G+/leu*+
resting cells	BWEC14{pTTL + pLeu*}	pQE80L-TTL-h ₆ + pLeuA*BCD	-	G—/leu*+
resting cells	BWEC14{pTTL}	pQE80L-TTL-h ₆	-	G—/leu*—

3.3.1. Nle biosynthesis in growing cells

A one step protocol for Nle production in growth phase was applied to determine if the co-transformed over-expression plasmid pLeu* is sufficient to shift the productivity of BWEC14 in direction of the ncAA Nle (scheme shown in Figure 41). The analysis of OD₆₀₀ and CDM in Figure 44 shows that the expected OD₆₀₀ of 6, corresponding to 2 g/L CDM, was reached. Growth stop due to Met depletion occurred after 400 minutes. Growth after induction was marginal. This can also be ascribed to the fact that after induction no further amino acid source was added to the Ile, Leu and Val auxotrophic BWEC14 strain.

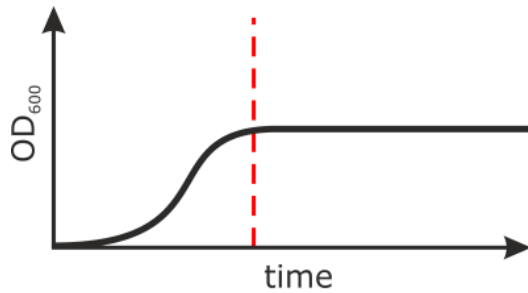


Figure 43 Scheme of Nle biosynthesis in growing cells and incorporation into TTL

Schematic overview of the process performed in bioreactor 1. Met auxotrophic BWEC14{pTTL + pLeu*} was cultivated in a DASGIP bioreactor using M9 medium with yeast extract as the limiting Met source. Nle production was anticipated to occur during growth. After Met depletion (dashed red line) TTL expression was induced by IPTG.

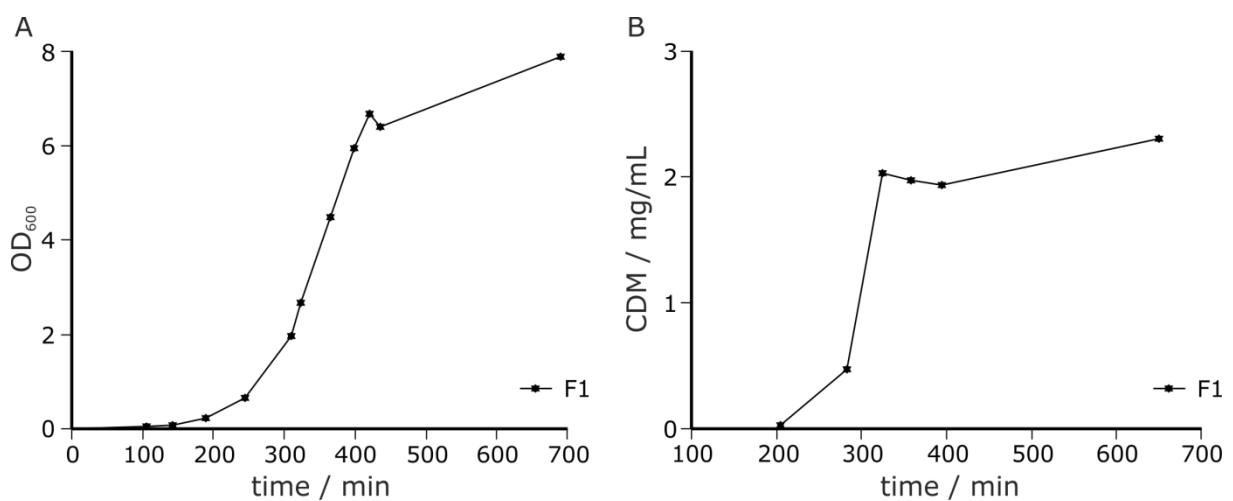


Figure 44 Bioreactor process analysis

A: Growth curves OD₆₀₀ vs. time for bioreactor 1

B: Growth curves CDM vs. time for bioreactor 1

All values were determined in triplicates. The error bars are very close to the average data point and, therefore, are omitted for clarity.

The amounts of branched chain amino acids in the supernatant are shown in Figure 45. The increase of Nva and Nle with time is plotted in correlation to the OD₆₀₀ (A). The exponential growth phase up to OD₆₀₀ 6 was sufficient to produce enough Nle for the standard SPI protocol as indicated by the red dotted line (100 mg/L). The branched chain amino acid concentrations decreased as expected (B). At the point of induction, all three amino acids were still present, although the free amount of Ile and Val was relatively low. Growth rates are comparable to previous bioreactor experiments with YE as the amino acid source (described in section 3.1.3).

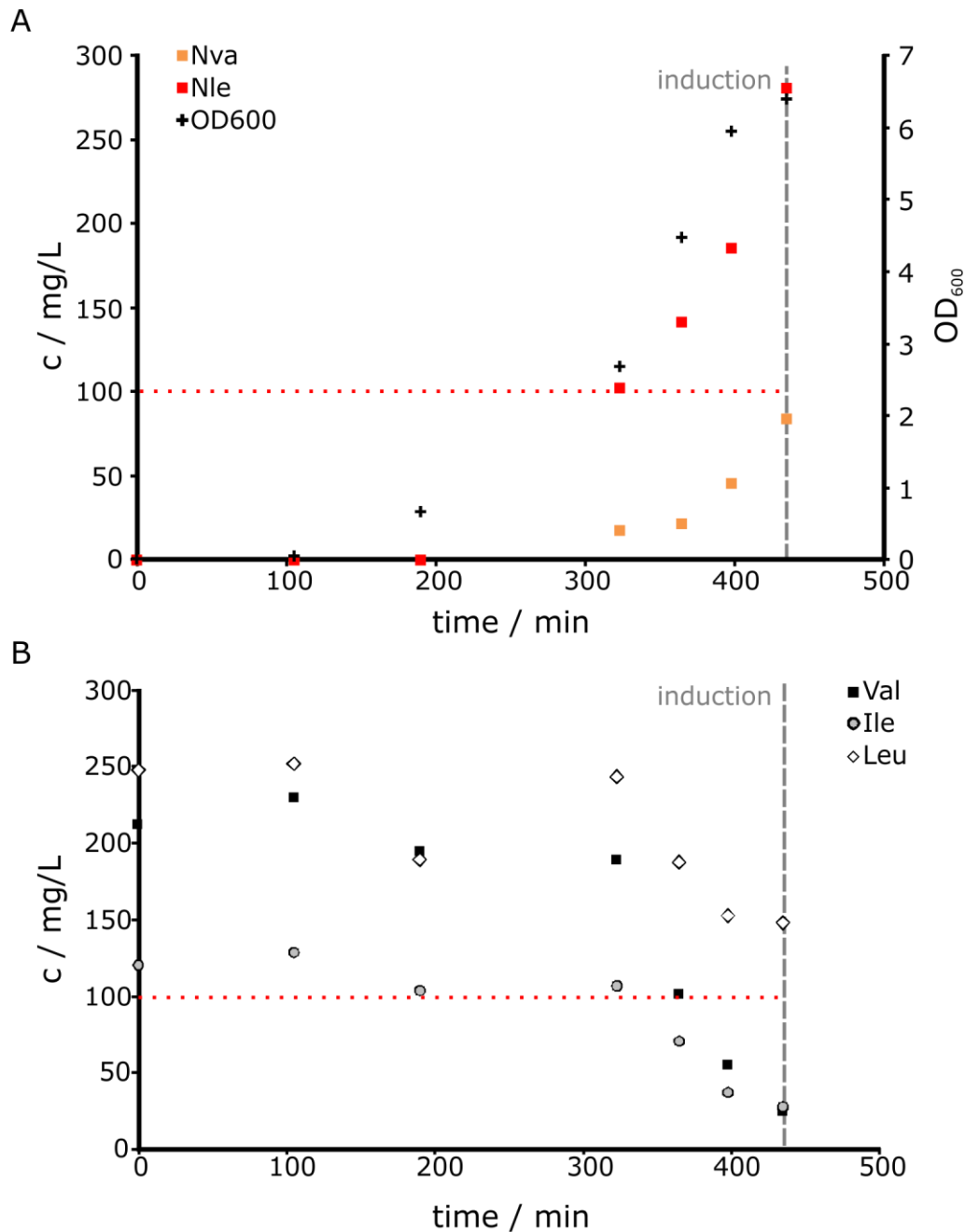


Figure 45 Amino acid analysis for BWEC14{pTTL + pLeu*} (bioreactor 1)

A: The total amount in mg/L of the two biosynthesized nCAA norvaline (Nva) and norleucine (Nle) over time is plotted. The correlation to the biomass production is shown (OD₆₀₀). Nva, norvaline (orange square); Nle, norleucine (red square); OD₆₀₀ (black cross)

B: The total amount of the cAAs valine (Val), isoleucine (Ile) and leucine (Leu) is plotted over time. Val, valine (black square); Ile, isoleucine (grey circle); Leu, leucine (white diamond). The red dotted line indicates the threshold of recommended amino acid concentrations for supplementation incorporation per liter culture medium. The grey dotted line indicates the time point of induction with 1 mM IPTG.

The analysis of TTL expression by SDS-PAGE revealed no visible difference between the non-induced and induced samples. This finding suggested that neither protein expression nor Nle incorporation had worked (Figure 46, A). In spite of the not very promising expression results, TTL was purified. Lanes E1 and E2 in the gel in Figure 46, A, indicate that expression

of TTL[Nle] had been successful although the protein was not visible in the whole cell sample (Figure 46, A, i). The main band shows the same migration behavior as the positive TTL[Nle] control. LC-MS confirmed that TTL had been fully labeled with biosynthesized Nle in the bioreactor. The main mass species corresponded to fully labeled protein with all 11 Met residues exchanged ($mass_{calc}$: 29913.80 Da (Table 27); $mass_{exp}$: 29912.85 Da (Figure 46, B)). The second biggest peak corresponded to the species with 10 methionines exchanged ($mass_{calc}$: 29931.75 Da (Table 27); $mass_{exp}$: (29930.80 Da) (Figure 46; B and Table 27)).

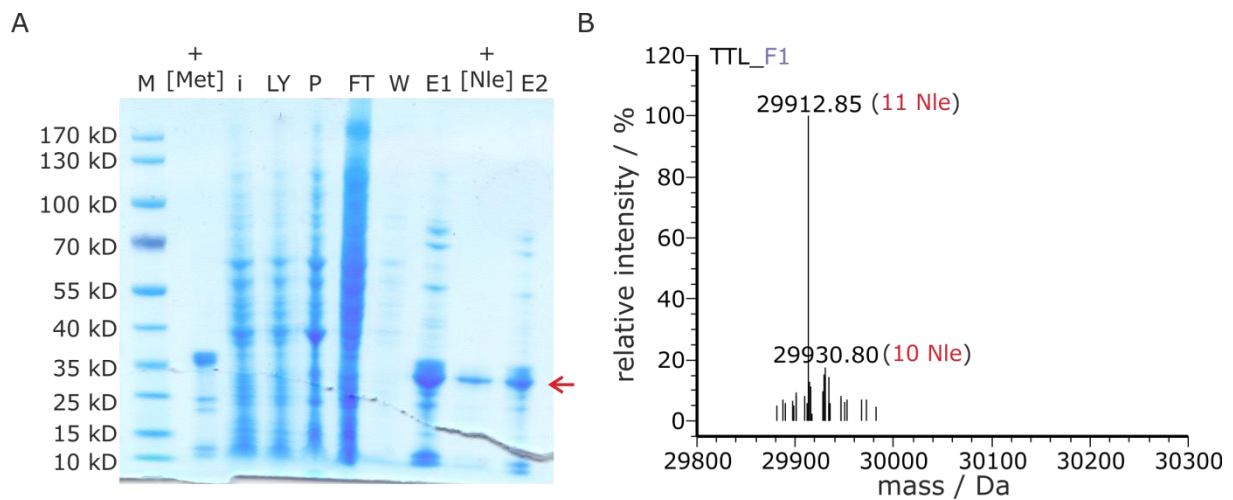


Figure 46 Protein purification + LC-MS analysis (bioreactor 1)

A: 10% SDS polyacrylamide gel; Coomassie blue stain. The size of the relevant molecular weight marker bands is indicated on the left gel margin. The expected size of TTL[Nle] variant is indicated by the red arrow. NuPAGE gels were used in this experiment, which explains the differences in size and migration behavior compared to self-made gels. M, prestained protein ladder mix; [Met]+, TTL[Met] positive control; i, P2-induced; LY, P3-cleared lysate; P, P4-insoluble fraction; FT, flow through; W, wash; E1, pure protein; [Nle]+, TTL[Nle] positive control; E2, pure protein

B: MS-spectrum of TTL_F8 is shown. The main species are labeled with the masses determined experimentally; the number of incorporated Nle residues is shown in brackets.

Table 27 Mass analysis for incorporation efficiency determination

Masses were calculated with the MassXpert software [87]. n.d., not detectable

TTL[F1]			
species	mass _{calculated} [Da]	mass _{experimental} [Da]	Δm
11 Met	30111.32	30111.43	0.11
1 Nle	30093.36	n.d.	-
2 Nle	30075.40	n.d.	-
3 Nle	30057.45	n.d.	-
4 Nle	30039.49	n.d.	-
5 Nle	30021.53	n.d.	-
6 Nle	30003.58	n.d.	-
7 Nle	29985.62	n.d.	-
8 Nle	29967.66	n.d.	-
9 Nle	29949.71	n.d.	-
10 Nle	29931.75	29930.80	0.95
11 Nle	29913.80	29912.85	0.95

3.3.2. Nle biosynthesis in resting cells

As described in section 3.2 resting cells of the *als-* knockout strain produce Nle. Therefore, I planned a two step protocol for the second experiment (scheme shown in Figure 47). After a short growth phase, Val depended growth arrest should occur. Nle production was anticipated to occur during the growth arrest in the resting cells. An excess of Met during the Nle-production phase was intended to prevent Nle incorporation into host proteins. Additional Val supplementation after Nle production phase should restore growth and lead to Met depletion (dashed red area). TTL expression was induced by IPTG

To investigate the effect of the *LeuA*BCD* over-expression, two different approaches were pursued: In bioreactor 2 a strain without the plasmid (BWEC14{pTTL}) and in bioreactor 8 a strain carrying the plasmid (BWEC14{pTTL+pLeu*}) were cultivated.

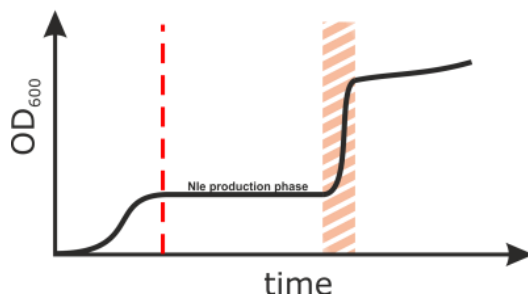


Figure 47 Scheme of Nle biosynthesis in resting cells and incorporation into TTL

Schematic overview of the process performed in bioreactor 2 and bioreactor 8. Met auxotrophic BWEC14{pTTL} and BWEC14{pTTL+pLeu*} strains were cultivated in M9 medium adapted for the bioreactor. After growth arrest (red dashed line) Nle biosynthesis should occur. TTL expression was induced after growth restart and Met depletion at higher OD₆₀₀ levels (red dashed area).

Growth restart after Val depletion with pure amino acids was impossible in bioreactor 2. Most probably, an essential nutrient was absent. In contrast to that the nutrient was present in YE because the culture in bioreactor 8 restored growth after Val depletion and starvation, however, growth stopped at OD₆₀₀ 8 already and the anticipated OD₆₀₀ 13 was not reached. There was almost no growth detectable after induction (Figure 48, A, t>1400 minutes). CDM shows comparable results to OD₆₀₀ (Figure 48, B).

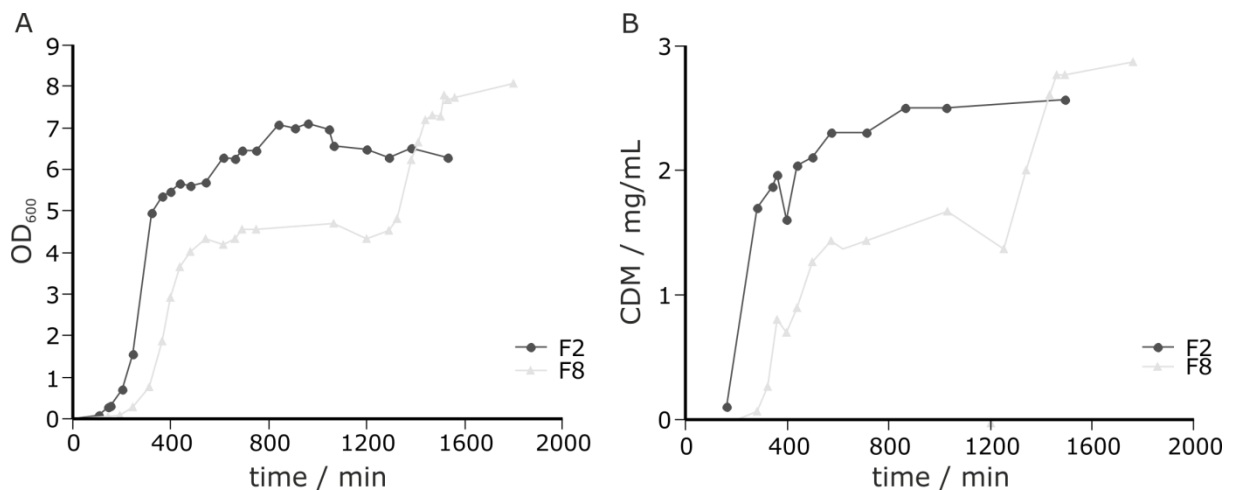


Figure 48 Bioreactor process analysis

A: Growth curves OD₆₀₀ vs. time for bioreactors 2 and 8

B: Growth curves CDM vs. time for bioreactors 2 and 8

All values were determined in triplicates. The error bars are very close to the average data point and, therefore, are omitted for clarity.

Figure 49 shows that in the absence of LeuA*BCD over-expression, only small amounts of Nle and Nva were produced (A). The amounts of Ile, Leu and Val are limited in YE, thus the branched chain amino acid concentrations decreased during the experiment as expected. The three amino acids decreased below the threshold for supplementation (red dotted line

in Figure 49, B) and, therefore, Ile and Val were replenished at the indicated time points. Leu was not added as this amino acid can be synthesized from Val as the precursor (see Figure 2). However, I observed that BWEC14{pTTL} did not restart growth, despite of the amino acid supplementataion. Likewise, neither Met addition, nor supplementation with glucose had a growth promoting effect (Figure 49, B). Thus, the experiment under G—/leu*— was stopped without any further processing.

As shown in Figure 50, YE can be used for growth restart of BWEC14{pTTL+pLeu*} after several hours of Val depletion, but Nle production stagnated 200 min after Val depletion (Figure 50, A) and could not be further boosted. Almost no Nle was produced during the starvation phase. After growth restart upon supplementation with YE, a significant increase in Nle production up to 3 g/L occurred (Figure 50, A, 1200 min). Thus, the amount of Nle required for standard SPI as indicated by the red dotted line (100 mg/L) was exceeded by 30 times. Nva was produced and highly efficiently converted to Nle under over-expression of the *leuA*BCD* operon (Figure 50, A). Again, the branched chain amino acid concentrations decreased as expected. Leu concentration was expected to increase due to the addition of YE, but the presumably small amounts of Leu present in YE might not be detectable in the presence of the huge amounts of Nle (Figure 50, B).

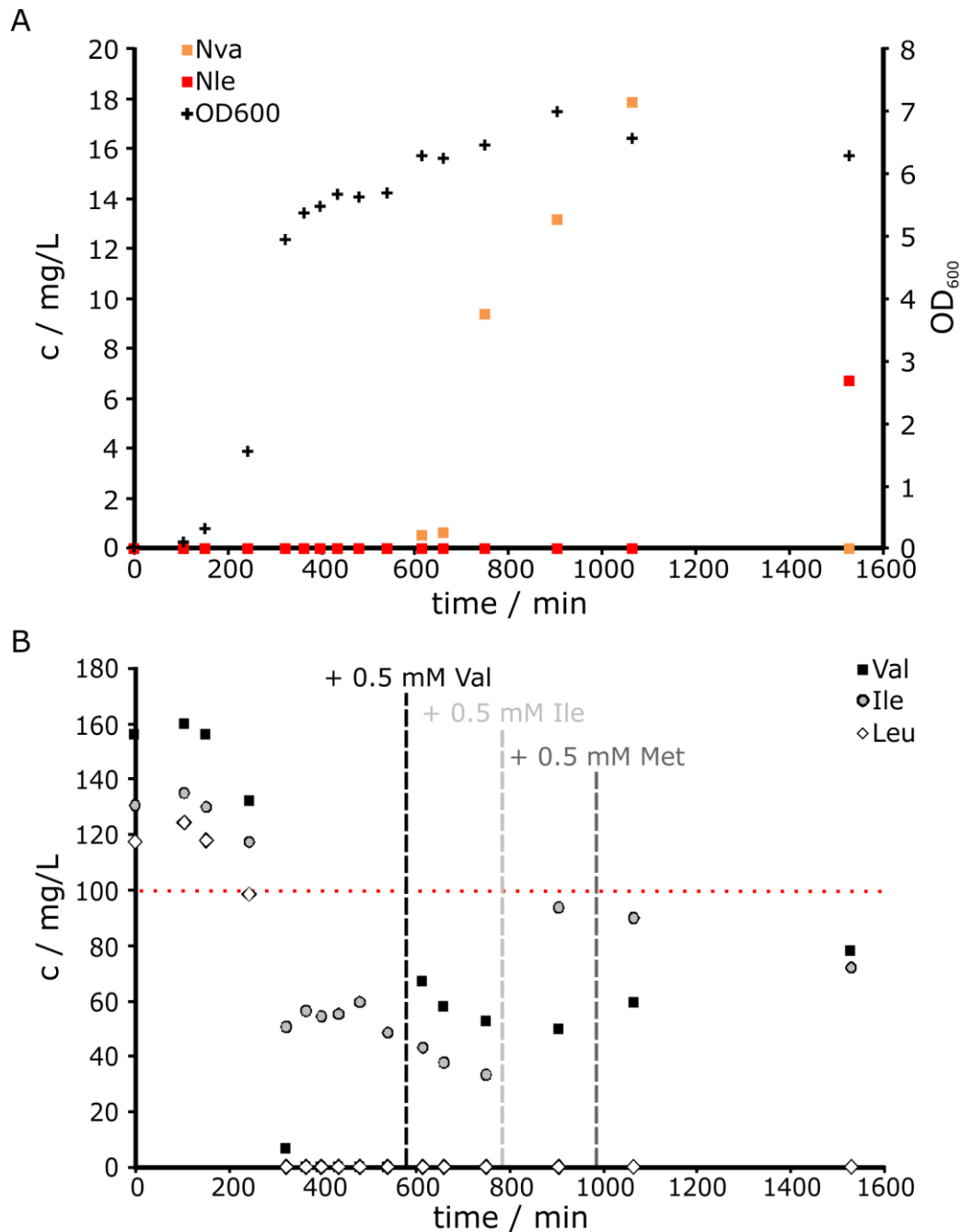


Figure 49 Amino acid analysis for BWEC14{pTTL} (bioreactor 2)

A: The total amount in mg/L of the two biosynthesized ncAA norvaline (Nva, orange square) and norleucine (Nle, red square) over time is plotted. The correlation to the biomass production is shown (OD₆₀₀, black cross).

B: The total amount of the cAAs valine (Val, black square), isoleucine (Ile, grey circle) and leucine (Leu, white diamond) over time is plotted. The grey dotted line shows the time point of Met supplementation (0.5 mM), the light grey dotted line shows the time point of Ile supplementation (0.5 mM) and the black dotted line shows the time point of Val supplementation (0.5 mM).

The red dotted line indicates the threshold of recommended amino acid concentrations for supplementation incorporation per liter culture medium. Nle production under the indicated conditions in bioreactor 2 did not reach this threshold.

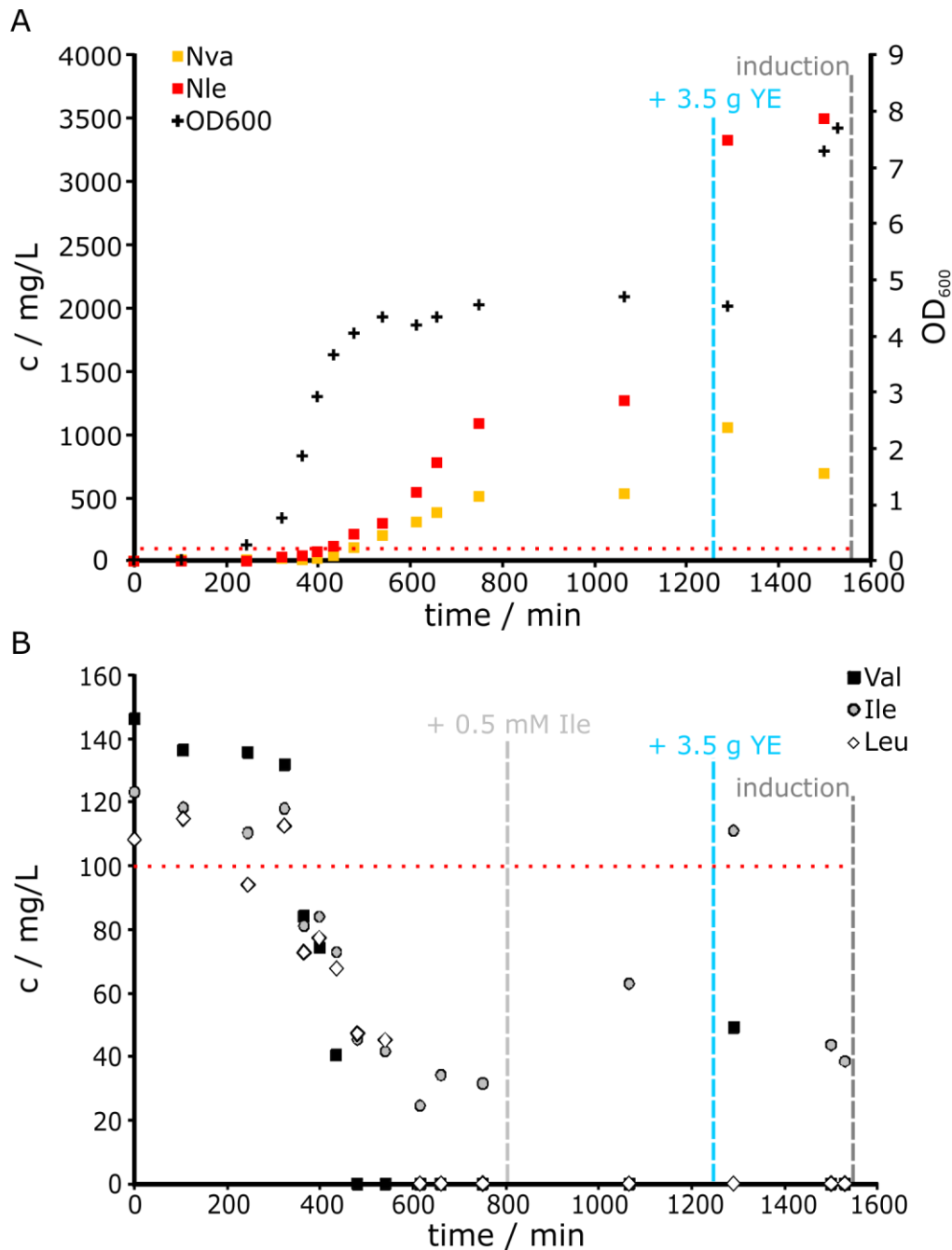


Figure 50 Amino acid analysis for BWEC 14{pTTL + pLeu*} (bioreactor 8)

A: The total amount in mg/L of the two biosynthesized ncAA norvaline (Nva, orange square) and norleucine (Nle, red square) over time is plotted. The correlation to the biomass production is shown (OD₆₀₀, black cross).

B: The total amount of the cAAs valine (Val, black square), isoleucine (Ile, grey circle) and leucine (Leu, white diamond) over time is plotted.

The red dotted line indicates the threshold of recommended amino acid concentrations for supplementation incorporation per liter culture medium. The grey dotted line indicates the time point of induction with 1 mM IPTG. The light grey dotted line shows the time point of Ile supplementation (0.5 mM) and the cyan dotted line shows the time point of YE (3.5 g/L, yeast extract) supplementation. Leu was not detectable from 600 min on.

The gel picture in Figure 51 (A) showed comparable results to the one in Figure 46 (A) The smear slightly above this band could originate from TTL with partial Nle incorporation caused by incomplete depletion of Met.

The mass analysis results (Figure 51, B and Table 28) confirmed the incorporation of Nle into TTL. However, a very inhomogeneous batch of TTL was produced in this two step process. The main species corresponded to partially labeled protein with 8 Met residues exchanged ($mass_{calc}$: 29967.66 Da (Table 28); $mass_{exp}$: 29665.79 Da (Figure 51, B and Table 28)). Other peaks corresponded to partially labeled species with 10 Met residues exchanged ($mass_{calc}$: 29931.75 Da (Table 28); $mass_{exp}$: 29928.85 Da (Figure 51, B and Table 28)), 9 Met residues exchanged ($mass_{calc}$: 29931.75 Da (Table 26); $mass_{exp}$: 29928.85 Da (Figure 51, B and Table 28)) and 6 methionines exchanged ($mass_{calc}$: 30003.58 Da (Table 26); $mass_{exp}$: 30000.68 Da (Figure 51, B and Table 28)). In addition, a small peak of fully labeled protein with all 11 Met residues exchanged was obtained ($mass_{calc}$: 29913.80 Da (Table 28); $mass_{exp}$: 29910.81 Da (Figure 51, B and Table 28)).

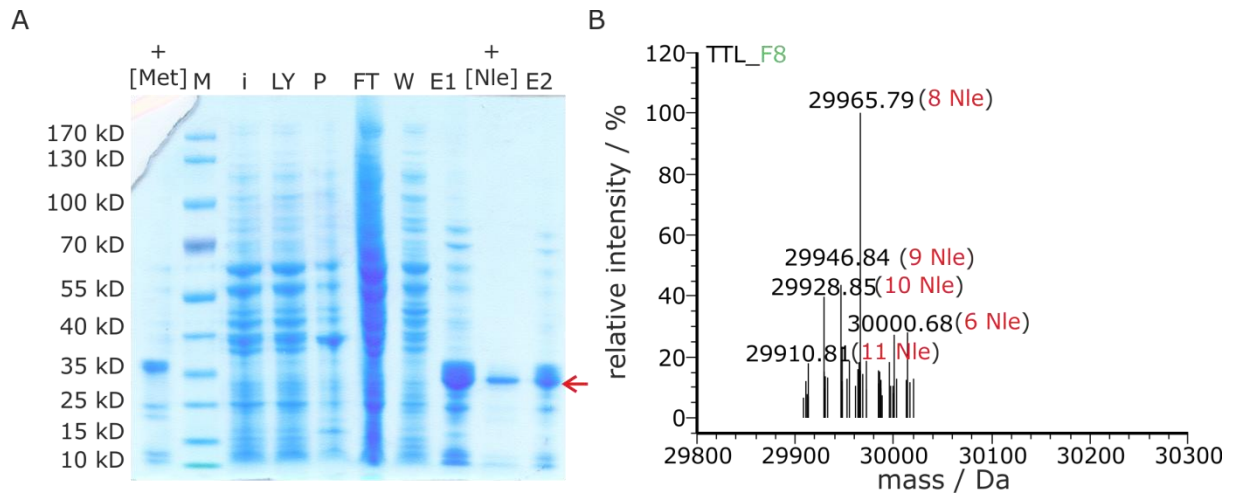


Figure 51 Protein purification and LC-MS analysis (bioreactor 8)

A: 10% SDS polyacrylamide gel; Coomassie blue stain. The size of the relevant molecular weight marker bands is indicated on the left gel margin. The expected size of TTL[Nle] variant is indicated by the red arrow. NuPAGE gels were used in this experiment, which explains the differences in size and migration behavior compared to self-made gels. M, prestained protein ladder mix; [Met]⁺, TTL[Met] positive control; i, P2-induced; LY, P3-cleared lysate; P, P4-insoluble fraction; FT, flow through; W, wash; E1, pure protein; [Nle]⁺, TTL[Nle] positive control; E2, pure protein

B: MS-spectrum of TTL_F8 is shown. The main species are labeled with the masses determined experimentally; the number of incorporated Nle residues is shown in brackets.

Table 28 Mass analysis for incorporation efficiency determination

Masses were calculated with the MassXpert software [87]. n.d., not detectable

TTL[F8]			
species	mass _{calculated} [Da]	mass _{experimental} [Da]	Δm
11 Met	30111.32	30111.43	0.11
1 Nle	30093.36	n.d.	-
2 Nle	30075.40	n.d.	-
3 Nle	30057.45	n.d.	-
4 Nle	30039.49	n.d.	-
5 Nle	30021.53	n.d.	-
6 Nle	30003.58	30000.68	2.90
7 Nle	29985.62	n.d.	-
8 Nle	29967.66	29965.79	1.87
9 Nle	29949.71	29946.84	2.86
10 Nle	29931.75	29928.85	2.9
11 Nle	29913.80	29910.81	2.99

4. Discussion

The establishment of ncAA incorporation as a new toolkit for protein engineering requires a method to produce synthetic proteins in large scales. Existing protocols for ncAA incorporation are performed at low cell densities ($OD_{600} \sim 1$, mid-log) [38] and Budisa, 1995 #4}. The present study focused on the development of ICDF protocols appropriate for large-scale, high-yield SPI experiments in *E. coli*. An important aspect of the work presented here was the validation of the protocol for synthetic protein production in a bioreactor.

As the ncAA, Nle was chosen. This amino acid is a side product of the branched chain amino acid biosynthesis [30]. Its cellular yields are increased in acetolactate synthase (als) knock-out strains and can be further pushed by simultaneous over-expression of a feedback insensitive *leuA*BCD* operon [31]. Previous studies had shown that global substitution of the Met residues in the thermophile lipase TTL by Nle substantially improved the activity of the enzyme without otherwise indispensable heat pre-treatment [38]. Thus, TTL was used as the model enzyme for the development of ICDF protocols for SPI in *E. coli*. In order to analyze whether global Met substitution by Nle would be beneficial for other enzymes of the alpha/beta-hydrolase class, synthetic Nle variants of the biotechnologically relevant enzymes of EC 3.1 were produced. Ultimately, biosynthesized Nle was incorporated *in situ* into TTL in the bioreactor.

4.1. Increased cell density fermentation

ICDF procedures for the production of synthetic proteins in shake flask cultures as well as the bioreactor were developed. New Minimal Medium described in the literature for SPI in *E. coli* consists of 12 components [33] which makes it tedious to prepare and rather expensive. Media for industrial scale fermentations should be as simple and inexpensive as possible [91]. Especially the amino acids are problematic for ICDF procedures. Feeding solutions of fed-batch processes are usually highly concentrated and if an amino acid must be included, the solubility of most of these compounds is easily exceeded.

In this study, a simple and low cost medium formulation was devised. Growth analysis (section 3.1.1) showed that the reduced medium very well supported growth of the B834(DE) strain and its descendants indicating that all essential nutrients were provided in satisfactory amounts by yeast extract supplementation.

The results of the titration experiment (section 3.1.1) showed that the method is adequately precise to determine limiting amino acid concentrations that guarantee cAA depletion necessary for ncAA incorporation. A drawback of the method is that the titration has to be performed for every new strain, as well as for each of the 20 cAAs. As well, slightly deviating amino acid compositions of different lots of YE have to be considered.

Up-scaling to $OD_{600} > 4$ in shake flask cultures proved difficult for the B834(DE3) strain due to a rapid drop of the pH below 5. Growth inhibition due to a pH drop by acetate formation was reported previously [70]. However, a buffer system with a higher puffer capacity did not lead to higher densities in shake flask cultures either (data not shown). This points at growth inhibition by another factor than pH (alone), e.g., inhibitory effects of accumulated secondary metabolites, or oxygen transfer limitations at high cell densities.

Compared to the shake flask the protocol could be up-scaled in a batch process by a 10-fold increase of the nutrients. A final OD_{600} of 30 was reached (see Figure 26). Protein expression was successful for shake flask, as well as bioreactor experiments. However, expression levels in the bioreactor seem reduced (see Figure 30) which implies that further optimization of the growth medium is necessary.

All in all it can be concluded that the optimization of the ICDF medium (see Table 21) was successful and can be used for application in different scales. We developed a ICDF to incorporate supplemented Met analogs into target proteins. Nevertheless, the protocol should be expanded to other auxothrophic strains and other ncAA analogs to proof the suitability.

4.2. Synthetic proteins

4.2.1. Production in high cell density shake flask cultures

The established high cell density SPI protocol for shake flask cultures was evaluated with the model enzyme TTL and 3 different cutinases. For all 4 enzymes parent and synthetic variants were expressed as soluble proteins. The amounts of 20-30 mg/L for parent proteins, as well as half the amount for synthetic variants were comparable to previous reports [19, 33] (section 3.1.2.2). In case of Thh_Est 4 hours of expression seemed to be insufficient (see Figure 19). Routine expression for this enzyme is performed with a pET expression system at 20-25 °C over night (internal communication D. Ribitsch). It is possible that individual

adaption of expression conditions can be helpful to increase protein yields. However, the detailed analysis of expression conditions of the cutinases was out of the scope of this study and, therefore, was not further pursued.

An important aspect for SPI experiments is the choice of expression system. The pET system that is routinely used in many labs is applicable only with caution: Expression of heterologous proteins from pET vectors is driven by a T7 phage promoter that requires T7 phage RNA polymerase (T7 RNAP) for full function. *E. coli* strains must be engineered to express T7 RNAP, e.g., on the DE3 lysogen [92]. Most auxotrophic *E. coli* strains do not contain the DE3 lysogen encoding T7 RNA polymerase, i.e., the T7 promoter constructs will not be expressed in those hosts. As T7 RNAP is under the control of the IPTG-inducible *lacUV* promoter on DE3 [92], the ncAA provided for SPI will not only be incorporated into the target protein of choice but also into the simultaneously induced T7 RNAP. Depending on the ncAA, this may lead to the inactivation of T7 RNAP [93]. Nevertheless, pET vectors were successfully used for ncAA incorporation before [19, 33, 39, 94]. In order to avoid the issues mentioned above, pET vectors were excluded from the SPI experiments in this study.

The cutinases were best expressed from the pMS470 vector carrying a *trc* promoter (section 3.1.2.2). This observation points out the importance of the expression system, specifically the promoter, for SPI. This observation also suggests to test several different constructs in order to obtain high yields of soluble protein (upon SPI).

Full Nle labeling was confirmed for all 3 cutinases by mass analysis, although detectable amounts of partially labeled proteins were found, too (see Figure 22). This is most likely caused by incomplete depletion of Met. The masses of the three parent as well as Nle-variant cutinases were found reduced by the molecular weight of Met or Nle, respectively. N-terminal Met excision is very likely if the penultimate amino acid is Ala, Cys, Gly, Pro, or Ser. Nle behaves likewise in this regard [95]. All three cutinases contained an Ala in the penultimate position.

4.2.2. Production in the bioreactor

The high cell density (OD_{600} 30) batch process for SPI of Nle provided in the medium yielded fully labeled TTL (section 3.1.3). This indicates that the necessary Met depletion can be determined simply by observing the growth arrest in late log phase. This confirmed previous observations [96] that incorporation of ncAAs is more a thermodynamically controlled

process depended on K_M values of tRNA^{Met} synthetase for cAA and ncAA than an all or none decision [35]. The batch process was highly reproducible and predictable.

Due to reported toxicity of Nle [19] the increase in OD_{600} and CDM values observed after Nle supplementation was unexpected (section 3.1.3). From the collected data, it cannot unambiguously concluded whether the observed increase in OD_{600} as well as CDM originates from residual growth or another, yet unidentified reason. It has been shown before that Nle can induce reduced but linear growth [35].

However, the isolated amounts of 100 mg pure TTL[Met] and 25 mg pure TTL[Nle] from the bioreactor culture were much lower than expected. The 10-fold increase in biomass compared to the ICDF in the shake flask (OD_{600} 3) did not yield 10-fold more protein, neither of the parent TTL[Met] nor of TTL[Nle]. More complex feeding strategies may adapt the nutrient supply to the elevated levels under ICDF conditions; or prevent accumulation of secondary metabolites that have negative effects on protein expression. The time-resolved expression study in section 3.1.3 showed that sufficient amounts of TTL were produced during 4 h of induction in the bioreactor. The intensity of the TTL[Met] band on the SDS gel (Figure 38, A, lane 1 h-4 h) was comparable to the production in shake flask cultures (Figure 38, A, lane +[Met]). However, the TTL[Nle] band was less prominent (Figure 38, B, lane 1 h-4 h). As already mentioned earlier, lower expression levels for synthetic proteins were observed in previous studies. The group of Budisa observed a ten times higher protein amount when transferring the cells into fresh medium for protein expression with ncAAs [33]. This also calls for a feeding strategy to improve synthetic protein production. Moreover, it has to be taken into account that protein expression efficiency is different for different proteins. Currently, I am producing the Nle variant of another protein in the bioreactor. This protein is excellently expressed with the cAAs.

The calculated yield refers to purified protein. However, this does not necessarily reflect how much is actually produced. Both protein variants were partially insoluble indicating that the expression conditions at high cell densities need further improvement. The down-stream processing, i.e., Ni^{2+} chelate chromatography was used as for standard expression experiments and not further optimized to higher cell densities. The binding capacities of the 5 mL HisTrap columns can be too low to purify a whole batch of enzyme out of a bioreactor. That is the reason why possible losses during purification should be considered. No marked TTL[Met] protein band was visible in the flow through and wash fractions (Figure 32, A).

However, a prominent amount of TTL[Nle] was found in these two fractions. Maybe the increased hydrophobicity of TTL[Nle] changes the binding behavior to the column material. Therefore, noticeably more synthetic than parent protein could have been lost during purification.

The protein concentration determination was always performed by two different optical methods. The results obtained by the colorimetric Biorad assay sometimes deviated for the Nle variant (by less than 20%) from those by the spectrophotometric determination using Nanodrop. This suggests that Nle has an impact on the molar extinction coefficient of the synthetic protein.

Our MS analyses emphasize that the labeling efficiency of the SPI protocol for the bioreactor is fully comparable to that of the shake flask procedure [38]. In both cases, quantitative exchange of the Met residues with Nle was observed (Figure 34).

4.3. Applications

In comparison to the parent protein, the TTL[Nle] variant showed increased activity on short chain esters *para*-nitrophenyl acetate and *para*-nitrophenyl butyrate (section 3.1.2.1) This finding adds to the previous observation that TTL[Nle] is approximately 10-fold more active than TTL[Met] with *para*-nitrophenyl palmitate as the substrate [38]. However, the activity differences between parent and Nle variant were not that pronounced with the short chain esters (1.5-fold higher activity) (Figure 15).

Surprisingly, TTL[Nle] degraded PET twice as efficiently as did TTL[Met]. Thus, TTL[Nle] is not only a very efficient lipase and esterase but also has polyesterase activity.

The polyesterase activity of TTL[Nle] was comparable to that of polyester hydrolases, i.e. cutinases. The spectrum of release products was comparable to that of Thc_Cut1[Met], although the activity was rather low when compared to a known polyesterases.

On long chain esters, TTL[Nle] is most active at 75 °C [38]. This pH optimum is also reflected in its polyesterase activity.

Nle incorporation into cutinases yielded rather different effects. While TTL[Nle] showed improved esterase activity compared to the parent protein, substitution of Met by Nle did not have the same effect in the synthetic cutinases (see Figure 23). With regard to PET degradation, the ratio of the release products TA and MHET was changed from 6:1 for Thc_Cut1[Met] to 1:1 for Thc_Cut1[Nle]. As adverse by-effect, the overall activity of

synthetic Thc_Cut1 was lowered by Nle incorporation. However, Thc_Cut2[Nle] was inactive on PET films. The cutinase model structure [65] may explain the decreased activity of the synthetic cutinase variants: The main-chain NH of Met132 is involved in hydrogen bonding with the substrate [65]. The highly hydrophobic side chain of Nle might twist the main-chain backbone in a way that this interaction is weakened.

A closer look to the postponed degradation mechanism [58] aids in the interpretation of shift in the ratio of the degradation products of Nle variant versus the parent protein: *Endo* activity of PET degrading enzymes produces MHET as a degradation product, which is further cleaved into TA and ethylene glycol. *Exo* cleavage leads to higher TA amounts due to degradation of the termini as well as of soluble MHET. The 1:1 TA/MHET ratio observed with Thc_Cut1[Nle] could hint at improved *endo* activity in comparison to Thc_Cut1[Met] (6:1 TA/MHET). A more detailed analysis will be necessary to elucidate the substrate selectivity of Thc_Cut1[Nle].

The results of the PET adhesion assay (Figure 25) suggest better adherence properties of the synthetic Thc_Cut1 variant in comparison with its parent. Most probably, the incorporation of hydrophobic Nle improves the adhesion of the enzyme to its hydrophobic polymer substrate. It may be speculated that this finding is attributable to the “hydrophobization” of the surface exposed Met residues Met1, Met15 and Met220 (ambiguous) in the enzyme by their substitution with Nle. Nevertheless, further analyses will have to validate this notion.

The Met residues in two enzymes of the same class that is lipases/polyesterases were exchanged by Nle. However, the incorporation provoked markedly different effects in the resulting variant proteins (see above). In part, this may be attributed to the number of Met residues in the proteins: 11 Met residues in TTL vs. only 3, 3 and 4 in the Thc_Cut1, Thc_Cut2 and Thh_Est, respectively. Expectedly, the micro-environment of the Met residues is also very important. The changed properties of synthetic proteins most probably reflect the sum of the impacts of Nle residues on their micro-environments in the protein matrix. In this regard, the substitution of a canonical amino acid by its non-canonical analog has a different quality than classical mutagenesis: The latter is limited to non-isosteric substitutions due to the restricted pool of canonical amino acids (e.g., Met by Ile or Trp by Phe) and often adversely affects protein structure. The first, however, introduces atomic mutations (S in Met to CH₂ in Nle; F instead of H in fluorinated analogs) that provoke rather electronic than structural effects. The elucidation of the effects of ncAA incorporation calls for a systematic

approach that combines comprehensive physico-(bio)chemical analysis of synthetic variant proteins with their 3D structure determination. Matter of factly, it is currently not possible to predict the effects of global amino acid substitution.

4.4. Nle production and amino acid analysis

The strain carrying the gene knockouts $\Delta ilvBN::0$, $\Delta ilvIH::0$ and $\Delta ilvGM::0$ [31] produced gram per liter amounts of Nle and Nva (see section 3.2). Nle production was first verified by a simple TLC analysis (see Figure 40). For the separation of branched chain amino acids in culture supernatants, a HPLC method was then successfully established (Figure 42). The method is useful for the fast analysis of the relevant amino acids Ile, Leu, Nle, Nva and Val. However, Met cannot be separated from Val by this method, and high amounts of Nle suppress the Leu signal. The ncAAs could be reproducibly quantified (see section 3.2) and the method proved valuable for monitoring Nle production.

4.5. Nle biosynthesis and direct incorporation

TTL[Nle] was produced by incorporation of biosynthesized Nle in a bioreactor (see section 3.3).

The designed bioreactor process for Nle biosynthesis in growing cells using BWEC14{pTTL + pLeu*} (details see in Table 26) indicated that growth could be controlled by YE supply as expected (see section 3.3.1).

The experiment on Nle production in resting cells taught us important lessons: The Met-auxotrophic als- strain BWEC14{pTTL + pLeu*} did not restart growth after the resting phase for Nle production, although it was supplemented with all essential amino acids. This observation indicates that an essential nutrient other than an amino acid must be missing although the process was designed appropriately. This nutrient is a component of YE: The same strain readily resumed growth after the resting phase upon the addition of YE. Nevertheless, growth ceased earlier than expected (Met depletion at OD_{600} 13). The strain was most probably lacking one of the branched chain amino acids Ile, Leu or Val, the strain is auxotrophic for (see Figure 50).

Comparison of the amino acid profiles in the culture supernatants of the Met auxotrophic als- strains BWEC14{pTTL} and BWEC14{pTTL + pLeu*} showed that over-expression of the feedback insensitive *leuA*BCD* operon massively boosts Nle productivity (see Figure 49

(BWEC14{pTTL}) and Figure 50 (BWEC14{pTTL + pLeu*}). 3 g/L Nle were produced (Figure 50). This is approximately 30 times more than the amount routinely supplemented in the medium (130 mg/L) for full labeling. However, the productivity in resting cells was extremely low (see Figure 50), which is in contrast to published data [31]. The results obtained out of the process for Nle production in growing cells demonstrated that 300 mg/L Nle were produced during exponential growth of BWEC14{pTTL+pLeu*} (see Figure 45). The amount of Nle produced is still in the range compared to external ncAA feeding experiments. Therefore, a process with Nle production in resting cells is not necessary. This result strongly indicates that simultaneous biosynthesis of Nle and its incorporation into a target protein is feasible.

The mass analysis of the produced TTL[Nle] proteins confirmed the efficiency of the process. The amounts of Nle produced in growing cells (see Figure 45) by BWEC 14{pTTL+PLeu*} were sufficient to obtain fully labeled TTL[Nle] (see Figure 46). In case of the Nle production experiment in resting cells (section 3.3.2) this was not the case. As mentioned above, did the strain BWEC14{pTTL+pLeu*} not reach the expected OD_{600} of 13 after YE supplementation. Most probably, the culture medium still contained Met. This fact led to the production of partially labeled protein. A heterologous protein mixture was produced and in the main species 8 Met residues were exchanged by Nle. Almost no fully labeled protein was produced (see Figure 51).

We have shown for the first time that Nle can be biosynthesized and simultaneously incorporated into a target protein in a bioreactor process. However, protein yields were very low and visible TTL[Nle] bands were just obtained after purification (see Figure 46 and Figure 51). One possibility for improvement can be the supplementation of Ile, Leu and Val at the point of induction. HPLC analysis showed that all 3 of these amino acids are still present at the induction point (see Figure 45 and Figure 50) but in very low amounts.

As well, the process should be repeated with another target protein in order to validate its robustness and efficiency. Further optimization is necessary to improve the yields of synthetic proteins.

5. Conclusions

This study describes ICDF protocols for SPI of Met analogs using auxotrophic *E coli* strains that are suitable for shake flask cultures, as well as fermentation in the bioreactor. The shake flask protocol was validated with several enzymes of the esterase/lipase family. The incorporation of Nle into these biotechnologically relevant enzymes confirmed the suitability of this new protein engineering approach. The combination of metabolic engineering and bioprocess development showed that it is feasible to biosynthesize Nle and to incorporate it into a target protein in the same fermentation process.

6. References

1. J.A. Brannigan and A.J. Wilkinson. *Protein engineering 20 years on*. Nature Reviews Molecular Cell Biology, 2002. **3**(12): 964-970.
2. N. Voloshchuk and J.K. Montclare. *Incorporation of unnatural amino acids for synthetic biology*. Molecular BioSystems, 2010. **6**(1): 65-80.
3. J. Seo and K.J. Lee. *Post-translational modifications and their biological functions: proteomic analysis and systematic approaches*. Journal of Biochemistry and Molecular Biology, 2004. **37**(1): 35-44.
4. F. Wold. *In vivo chemical modification of proteins (post-translational modification)*. Annual Review of Biochemistry, 1981. **50**: 783-814.
5. A. Wang, et al. *Protein Engineering with Non-Natural Amino Acids*, in *Protein Engineering*. 2012, InTech: Manhattan, New York. 253-282.
6. S. Zheng and I. Kwon. *Manipulation of enzyme properties by noncanonical amino acid incorporation*. Biotechnology Journal, 2012. **7**(1): 47-60.
7. M.G. Hoesl and N. Budisa. *Recent advances in genetic code engineering in Escherichia coli*. Current Opinion in Biotechnology, 2012. **23**(5): 751-757.
8. C.C. Liu and P.G. Schultz. *Adding new chemistries to the genetic code*. Annual Review of Biochemistry, 2010. **79**(1): 413-444.
9. S. Hunt. *The non-protein amino acids*, in *Chemistry and biochemistry of the amino acids*, G. Barrett, Editor. 1985, Chapman and Hall: London. 55-137.
10. M.A. Ciufolini and D. Lefranc. *Micrococcin P1: Structure, biology and synthesis*. Natural Product Reports, 2010. **27**(3): 330-342.
11. M.A. Montecalvo. *Ramoplanin: a novel antimicrobial agent with the potential to prevent vancomycin-resistant enterococcal infection in high-risk patients*. The Journal of Antimicrobial Chemotherapy, 2003. **51 Suppl 3**: iii31-iii35.
12. M. Ibba and D. Söll. *Aminoacyl-tRNAs: setting the limits of the genetic code*. Genes & Development, 2004. **18**(7): 731-738.
13. M. Ibba and D. Soll. *Genetic code: introducing pyrrolysine*. Current Biology, 2002. **12**(13): R464-466.
14. A. Bock, et al. *Selenocysteine: the 21st amino acid*. Molecular Microbiology, 1991. **5**(3): 515-520.
15. M.A. Gaston, R. Jiang, and J.A. Krzycki. *Functional context, biosynthesis, and genetic encoding of pyrrolysine*. Current Opinion in Microbiology, 2011. **14**(3): 342-349.
16. R.L. Schmidt and M. Simonovic. *Synthesis and decoding of selenocysteine and human health*. Croatian Medical Journal, 2012. **53**(6): 535-550.
17. A. Ambrogelly, S. Palioura, and D. Soll. *Natural expansion of the genetic code*.

- Nature Chemical Biology, 2007. **3**(1): 29-35.
18. G. Rosenthal. *Plant nonprotein amino and imino acids: biological, biochemical and toxicological properties*. 1982, New York: Academic Press Inc.
 19. M.J. Pine. *Comparative physiological effects of incorporated amino acid analogs in Escherichia coli*. *Antimicrobial Agents and Chemotherapy*, 1978. **13**(4): 676-685.
 20. R. Munier and G.N. Cohen. *Incorporation d'analogues structuraux d'acides aminés dans les protéines bactériennes au cours de leur synthèse in vivo*. *Biochimica et Biophysica Acta*, 1959. **31**(2): 378-391.
 21. J.D. Keasling. *Synthetic biology for synthetic chemistry*. *ACS Chemical Biology*, 2008. **3**(1): 64-76.
 22. K.A. Datsenko and B.L. Wanner. *One-step inactivation of chromosomal genes in Escherichia coli K-12 using PCR products*. *Proceedings of the National Academy of Sciences*, 2000. **97**(12): 6640-6645.
 23. N. Budisa, et al. *Atomic mutations in annexin V--thermodynamic studies of isomorphous protein variants*. *European Journal of Biochemistry*, 1998. **253**(1): 1-9.
 24. S.S. Kerwar and H. Weissbach. *Studies on the ability of norleucine to replace methionine in the initiation of protein synthesis of E. coli*. *Archives of Biochemistry and Biophysics*, 1970. **141**(2): 525-532.
 25. J. Trupin, et al. *Formylation of amino acid analogues of methionine sRNA*. *Biochemical and Biophysical Research Communications*, 1966. **24**(1): 50-55.
 26. D.G. Barker and C.J. Bruton. *The fate of norleucine as a replacement for methionine in protein synthesis*. *Journal of Molecular Biology*, 1979. **133**(2): 217-231.
 27. C.B. Anfinsen and L.G. Corley. *An active variant of staphylococcal nuclease containing norleucine in place of methionine*. *Journal of Biological Chemistry*, 1969. **244**(19): 5149-5152.
 28. P.C. Cirino, et al. *Global incorporation of norleucine in place of methionine in cytochrome P450 BM-3 heme domain increases peroxxygenase activity*. *Biotechnology and Bioengineering*, 2003. **83**(6): 729-734.
 29. C. Wolschner, et al. *Design of anti- and pro-aggregation variants to assess the effects of methionine oxidation in human prion protein*. *Proceedings of the National Academy of Sciences*, 2009. **106**(19): 7756-7761.
 30. G. Bogosian, et al. *Biosynthesis and incorporation into protein of norleucine by Escherichia coli*. *Journal of Biological Chemistry*, 1989. **264**(1): 531-539.
 31. E. Sycheva, et al. *Overproduction of noncanonical amino acids by Escherichia coli cells*. *Microbiology*, 2007. **76**(6): 712-718.
 32. G.N. Cohen and D.B. Cowie. *Total replacement of methionine by selenomethionine in the proteins of Escherichia coli*.

- Comptes Rendus Hebdomadaires des Séances de l'Académie des Sciences, 1957. **244**(5): 680-683.
33. N. Budisa, et al. *High-level biosynthetic substitution of methionine in proteins by its analogs 2-aminohexanoic acid, selenomethionine, telluromethionine and ethionine in Escherichia coli.* European Journal of Biochemistry, 1995. **230**(2): 788-796.
 34. R.S. Mulvey and A.R. Fersht. *Editing mechanisms in aminoacylation of tRNA: ATP consumption and the binding of aminoacyl-tRNA by elongation factor Tu.* Biochemistry, 1977. **16**(21): 4731-4737.
 35. M.H. Richmond. *The effect of amino acid analogues on growth and protein synthesis in microorganisms.* Bacteriological Reviews, 1962. **26**: 398-420.
 36. J.P. Welsh, et al. *Multiply mutated Gaussia luciferases provide prolonged and intense bioluminescence.* Biochemical and Biophysical Research Communications, 2009. **389**(4): 563-568.
 37. J.-D. Pedelacq, et al. *Engineering and characterization of a superfolder green fluorescent protein.* Nature Biotechnology, 2006. **24**(1): 79-88.
 38. M.G. Hoesl, et al. *Lipase Congeners Designed by Genetic Code Engineering.* ChemCatChem, 2011. **3**(1): 213-221.
 39. A.J. Link, M.L. Mock, and D.A. Tirrell. *Non-canonical amino acids in protein engineering.* Current Opinion in Biotechnology, 2003. **14**(6): 603-609.
 40. J. Xie and P.G. Schultz. *Adding amino acids to the genetic repertoire.* Current Opinion in Chemical Biology, 2005. **9**(6): 548-554.
 41. C. Jäckel, P. Kast, and D. Hilvert. *Protein Design by Directed Evolution.* Annual Review of Biophysics, 2008. **37**(1): 153-173.
 42. U.T. Bornscheuer and M. Pohl. *Improved biocatalysts by directed evolution and rational protein design.* Current Opinion in Chemical Biology, 2001. **5**(2): 137-143.
 43. I. Samish, et al. *Theoretical and computational protein design.* Annual Review of Physical Chemistry, 2011. **62**: 129-149.
 44. N. Budisa. *Engineering the Genetic Code: Expanding the Amino Acid Repertoire for the Design of Novel Proteins.* 2006, Weinheim: WILEY-VCH Verlag GmbH & Co. KGaA.
 45. M. Salwiczek, et al. *Fluorinated amino acids: compatibility with native protein structures and effects on protein-protein interactions.* Chemical Society Reviews, 2012. **41**(6): 2135-2171.
 46. M.G. Hoesl, et al. *Azatriptophans as tools to study polarity requirements for folding of green fluorescent protein.* Journal of Peptide Science, 2010. **16**(10): 589-595.
 47. M.D. Crespo and M. Rubini. *Rational design of protein stability: effect of (2S,4R)-4-fluoroproline on the stability and folding pathway of ubiquitin.* PLoS ONE, 2011. **6**(5): e19425.
 48. S. Edwardraja, et al. *Enhancing the thermal stability of a single-chain Fv fragment by in vivo global fluorination of the proline residues.*

- Molecular BioSystems, 2011. **7**(1): 258-265.
49. B. Holzberger, et al. *Structural insights into the potential of 4-fluoroproline to modulate biophysical properties of proteins.*
Chemical Science, 2012. **3**(10): 2924-2931.
 50. T. Steiner, et al. *Synthetic biology of proteins: tuning GFPs folding and stability with fluoroproline.*
PLoS ONE, 2008. **3**(2): e1680.
 51. P.D. Renfrew, et al. *Incorporation of noncanonical amino acids into Rosetta and use in computational protein-peptide interface design.*
Public Library of Science ONE, 2012. **7**(3): e32637.
 52. J.H. Bae, et al. *Expansion of the genetic code enables design of a novel "gold" class of green fluorescent proteins.*
Journal of Molecular Biology, 2003. **328**(5): 1071-1081.
 53. D.H. Jones, et al. *Site-specific labeling of proteins with NMR-active unnatural amino acids.*
Journal of Biomolecular NMR, 2010. **46**(1): 89-100.
 54. J.F. Parsons, et al. *Enzymes harboring unnatural amino acids: mechanistic and structural analysis of the enhanced catalytic activity of a glutathione transferase containing 5-fluorotryptophan.*
Biochemistry, 1998. **37**(18): 6286-6294.
 55. B. Holzberger and A. Marx. *Replacing 32 proline residues by a noncanonical amino acid results in a highly active DNA polymerase.*
Journal of the American Chemical Society, 2010. **132**(44): 15708-15713.
 56. A. Svendsen. *Lipase protein engineering.*
Biochimica et Biophysica Acta, 2000. **1543**(2): 223-238.
 57. J.K. Montclare and D.A. Tirrell. *Evolving proteins of novel composition.*
Angewandte Chemie International Edition, 2006. **45**(27): 4518-4521.
 58. T. Brueckner, et al. *Enzymatic and chemical hydrolysis of poly(ethylene terephthalate) fabrics.*
Journal of Polymer Science Part A: Polymer Chemistry, 2008. **46**(19): 6435-6443.
 59. R.J. Muller, I. Kleeberg, and W.D. Deckwer. *Biodegradation of polyesters containing aromatic constituents.*
Journal of Biotechnology, 2001. **86**(2): 87-95.
 60. R.-J. Müller, et al. *Enzymatic Degradation of Poly(ethylene terephthalate): Rapid Hydrolyse using a Hydrolase from T. fusca.*
Macromolecular Rapid Communications, 2005. **26**(17): 1400-1405.
 61. G.M. Gubitz and A.C. Paulo. *New substrates for reliable enzymes: enzymatic modification of polymers.*
Current Opinion in Biotechnology, 2003. **14**(6): 577-582.
 62. G.M. Guebitz and A. Cavaco-Paulo. *Enzymes go big: surface hydrolysis and functionalization of synthetic polymers.*
Trends in Biotechnology, 2008. **26**(1): 32-38.
 63. I. Kardas, B. Lipp-Symonowicz, and S. Sztajnowski. *The influence of enzymatic treatment on the surface modification of PET fibers.*

- Journal of Applied Polymer Science, 2011. **119**(6): 3117-3126.
64. R.-J. Mueller. *Biological degradation of synthetic polyesters—Enzymes as potential catalysts for polyester recycling*.
Process Biochemistry, 2006. **41**(10): 2124-2128.
 65. E. Herrero Acero, et al. *Enzymatic Surface Hydrolysis of PET: Effect of Structural Diversity on Kinetic Properties of Cutinases from Thermobifida*.
Macromolecules, 2011. **44**(12): 4632-4640.
 66. S.Y. Lee. *High cell-density culture of Escherichia coli*.
Trends in Biotechnology, 1996. **14**(3): 98-105.
 67. J.H. Choi, K.C. Keum, and S.Y. Lee. *Production of recombinant proteins by high cell density culture of Escherichia coli*.
Chemical Engineering Science, 2006. **61**(3): 876-885.
 68. G.N. Vemuri, et al. *Overflow metabolism in Escherichia coli during steady-state growth: transcriptional regulation and effect of the redox ratio*.
Applied and Environmental Microbiology, 2006. **72**(5): 3653-61.
 69. M. De Mey, et al. *Comparison of different strategies to reduce acetate formation in Escherichia coli*.
Biotechnology Progress, 2007. **23**(5): 1053-63.
 70. M.A. Eiteman and E. Altman. *Overcoming acetate in Escherichia coli recombinant protein fermentations*.
Trends in Biotechnology, 2006. **24**(11): 530-536.
 71. Q. Luo, et al. *Optimization of culture on the overproduction of TRAIL in high-cell-density culture by recombinant Escherichia coli*.
Applied Microbiology and Biotechnology, 2006. **71**(2): 184-191.
 72. S.B. Noronha, et al. *Investigation of the TCA cycle and the glyoxylate shunt in Escherichia coli BL21 and JM109 using (13)C-NMR/MS*.
Biotechnology and Bioengineering, 2000. **68**(3): 316-327.
 73. K. Han, J. Hong, and H.C. Lim. *Relieving effects of glycine and methionine from acetic acid inhibition in Escherichia coli fermentation*.
Biotechnology and Bioengineering, 1993. **41**(3): 316-324.
 74. P.F. Stanbury, A. Whitaker, and S.J. Hall. *Principles of Fermentation technology*. 1995, Oxford, U.K.: Butterworth-Heinemann.
 75. G.G. Moulton. *Fed-Batch Fermentation: A Practical Guide to Scalable Recombinant Protein Production in Escherichia Coli*. 2013, Boca Raton, Florida: Crc Press.
 76. H.H. Wong, et al. *Effect of post-induction nutrient feeding strategies on the production of bioadhesive protein in Escherichia coli*.
Biotechnology and Bioengineering, 1998. **60**(3): 271-276.
 77. C.J. Hewitt and A.W. Nienow. *The Scale-Up of Microbial Batch and Fed-Batch Fermentation Processes*.
Advances in Applied Microbiology, 2007. **62**: 105-135.

78. K.J. Jeong and S.Y. Lee. *High-level production of human leptin by fed-batch cultivation of recombinant Escherichia coli and its purification.*
Applied and Environmental Microbiology, 1999. **65**(7): 3027-3032.
79. N. Anderhuber. Biosynthesis of non-canonical amino acids: Metabolic engineering for norleucine production. 2013, diploma thesis, Albert-Ludwigs-Universität Freiburg, Freiburg.
80. C.E. Seidman, et al. *Introduction of plasmid DNA into cells.*
Current Protocols in Molecular Biology, 2001. **Chapter 1**(8): Unit1.8.
81. GeneLink. *Oligo Explorer.* [computer software] [cited 2012; 1.5:][Available from: <http://www.genelink.com/tools/gl-downloads.asp>].
82. J.A. Armstrong and J.R. Schulz. *Agarose gel electrophoresis.*
Current Protocols Essential Laboratory Techniques, 2008.
83. D.G. Gibson, et al. *Enzymatic assembly of DNA molecules up to several hundred kilobases.*
Nature Methods, 2009. **6**(5): 343-345.
84. U.K. Laemmli. *Cleavage of structural proteins during the assembly of the head of bacteriophage T4.*
Nature, 1970. **227**(259): 680-685.
85. J.W. Henderson, et al. *Rapid, Accurate, Sensitive, and Reproducible HPLC Analysis of Amino Acids.*
Agilent technologies - Internal Manuscript, 2000: 1-10.
86. ProIndepServS.r.l. *QtiPlot.* [computer software] [cited 2012; 0.9.8.3-3:][Available from: <http://soft.proindependent.com/qtiplot.html>].
87. F. Rusconi. *massXpert2: a cross-platform software environment for polymer chemistry modelling and simulation/analysis of mass spectrometric data.* [computer software] [cited 2012; 3.1.0.:][Available from: <http://massxpert.org/wiki/Main/HowToCite>].
88. F.W. Studier. *Protein production by auto-induction in high density shaking cultures.*
Protein Expression and Purification, 2005. **41**(1): 207-234.
89. B. Wiltschi. *Expressed protein modifications: Making synthetic proteins.*
Methods in Molecular Biology, 2012. **813**: 211-225.
90. BIOMOL. Guide to Gene Expression in BL21. [Instructor's Manual] 2004, Hamburg. 1-16.
91. M. Kennedy and D. Krouse. *Strategies for improving fermentation medium performance: a review.*
Journal of Industrial Microbiology and Biotechnology, 1999. **23**(6): 456-475.
92. F.W. Studier and B.A. Moffatt. *Use of bacteriophage T7 RNA polymerase to direct selective high-level expression of cloned genes.*
Journal of Molecular Biology, 1986. **189**(1): 113-130.
93. N. Ayyadurai, et al. *Importance of expression system in the production of unnatural recombinant proteins in Escherichia coli.*
Biotechnology and Bioprocess Engineering, 2009. **14**(3): 257-265.
94. A.J. Link and D.A. Tirrell. *Reassignment of sense codons in vivo.*
Methods, 2005. **36**(3): 291-298.
95. F. Frottin, et al. *The Proteomics of N-terminal Methionine Cleavage.*
Molecular & Cellular Proteomics, 2006. **5**(12): 2336-2349.

-
96. A.M. Gilles, et al. *Conservative replacement of methionine by norleucine in Escherichia coli adenylate kinase*.
The Journal of Biological Chemistry, 1988. **263**(17): 8204-8209.

7. Appendix

Table 29 Strains produced in this work with plasmid file names and BT numbers

strain	background	mutation/plasmid	plasmid file name	BT number ¹
BWEC10	BL21(DE3)Gold	$\Delta ilvBN::0$ $\Delta ilvIH::0$ $\Delta ilvGM::0$	-	6900
BWEC14	B834(DE3)	$\Delta ilvBN::0$ $\Delta ilvIH::0$ $\Delta ilvGM::0$ <i>metE</i>	-	6899
BWEC14{pTTL}	BWEC14	pQE80L-TTL-h ₆	pQE80L-TTL-h6	-
BWEC14{pTTL + pleu*}	BWEC14	pQE80L-TTL-h ₆ + pLeuA*BCD	pQE80L-TTL-h6 pBP226_leuA_BCD	-
pQE80L-TTL ²	<i>E.coli</i> Top10F'	pQE80L-TTL-h ₆	pQE80L-TTL-h6	6898
BWEC14{pleu*} ³	BWEC14	pLeuA*BCD	pBP226_leuA_BCD	6901
pQE80L-TTL ⁴	B834(DE3)	<i>metE</i> / pQE80L-TTL	pQE80L-TTL-h6	-
pMS470-Thc_Cut1 ⁴	B834(DE3)	<i>metE</i> / pMS470- Thc_Cut1	pMS470-Thc_cut1	-
pMS470-Thc_Cut2 ⁴	B834(DE3)	<i>metE</i> / pMS470- Thc_Cut2	pMS470-Thc_cut2	-
pMS470-Thh_Est ⁴	B834(DE3)	<i>metE</i> / pMS470- Thh_Est	pMS470-Thh_est	-
pQE80L-Thc_Cut1 ⁴	B834(DE3)	<i>metE</i> / pQE80L- Thc_Cut1	pQE80L-Thc_cut1	-
pQE80L-Thc_Cut2 ⁴	B834(DE3)	<i>metE</i> / pQE80L- Thc_Cut2	pQE80L-Thc_cut2	-
pQE80L-Thh_Est ⁴	B834(DE3)	<i>metE</i> / pQE80L- Thh_Est	pQE80L-Thh_est	-

¹IMBT strain collection number

²This strain was prepared to store the expression plasmid in the strain collection.

³BWEC14 carrying pleu* over-expression plasmid promotes Nle formation.

⁴Expression strains